Perspectives and Integration in SOLAS Science 5

Véronique C. Garçon, Thomas G. Bell, Douglas Wallace, Steve R. Arnold, Alex Baker, Dorothee C.E. Bakker, Hermann W. Bange, Nicholas R. Bates, Laurent Bopp, Jacqueline Boutin, Philip W. Boyd, Astrid Bracher, John P. Burrows, Lucy J. Carpenter, Gerrit de Leeuw, Katja Fennel, Jordi Font, Tobias Friedrich, Christoph S. Garbe, Nicolas Gruber, Lyatt Jaeglé, Arancha Lana, James D. Lee, Peter S. Liss, Lisa A. Miller, Nazli Olgun, Are Olsen, Benjamin Pfeil, Birgit Quack, Katie A. Read, Nicolas Reul, Christian Rödenbeck, Shital S. Rohekar, Alfonso Saiz-Lopez, Eric S. Saltzman, Oliver Schneising, Ute Schuster, Roland Seferian, Tobias Steinhoff, Pierre-Yves Le Traon, and Franziska Ziska

Abstract

Why a chapter on Perspectives and Integration in SOLAS Science in this book? SOLAS science by its nature deals with interactions that occur: across a wide spectrum of time and space scales, involve gases and particles, between the ocean and the atmosphere, across many disciplines including chemistry, biology, optics, physics, mathematics, computing, socio-economics and consequently interactions between many different scientists and across scientific generations. This chapter provides a guide through the remarkable diversity of cross-cutting approaches and tools in the gigantic puzzle of the SOLAS realm.

Here we overview the existing prime components of atmospheric and oceanic observing systems, with the acquisition of ocean–atmosphere observables either from *in situ* or from satellites, the rich hierarchy of models to test our knowledge of Earth System functioning, and the tremendous efforts accomplished over the last decade within the COST Action 735 and SOLAS Integration project frameworks to understand, as best we can, the current physical and biogeochemical state of the atmosphere and ocean commons. A few SOLAS integrative studies illustrate the full meaning of interactions, paving the way for even tighter connections between thematic fields. Ultimately, SOLAS research will also develop with an enhanced consideration of societal demand while preserving fundamental research coherency.

V.C. Garçon (✉)
e-mail: veronique.garcon@legos.obs-mip.fr

T.G. Bell (✉)
e-mail: tbe@pml.ac.uk

D. Wallace (✉)
e-mail: douglas.wallace@dal.ca

P.S. Liss and M.T. Johnson (eds.), *Ocean-Atmosphere Interactions of Gases and Particles*,
Springer Earth System Sciences, DOI 10.1007/978-3-642-25643-1_5, © The Author(s) 2014

The exchange of energy, gases and particles across the air-sea interface is controlled by a variety of biological, chemical and physical processes that operate across broad spatial and temporal scales. These processes influence the composition, biogeochemical and chemical properties of both the oceanic and atmospheric boundary layers and ultimately shape the Earth system response to climate and environmental change, as detailed in the previous four chapters. In this cross-cutting chapter we present some of the SOLAS achievements over the last decade in terms of integration, upscaling observational information from process-oriented studies and expeditionary research with key tools such as remote sensing and modelling.

Here we do not pretend to encompass the *entire* legacy of SOLAS efforts but rather offer a selective view of some of the major integrative SOLAS studies that combined available pieces of the immense jigsaw puzzle. These include, for instance, COST efforts to build up global climatologies of SOLAS relevant parameters such as dimethyl sulphide, interconnection between volcanic ash and ecosystem response in the eastern subarctic North Pacific, optimal strategy to derive basin-scale CO_2 uptake with good precision, or significant reduction of the uncertainties in sea-salt aerosol source functions. Predicting the future trajectory of Earth's climate and habitability is the main task ahead. Some possible routes for the SOLAS scientific community to reach this overarching goal conclude the chapter.

5.1 Perspectives: In Situ Observations, Remote Sensing, Modelling and Synthesis

The scope of SOLAS science depends on multidisciplinary and multi-scale approaches being applied to the complex problems and challenges within the field. Laboratory process studies and in situ lagrangian field experiments make substantial contributions to our understanding of the various biogeochemical processes and their feedbacks. Models are almost the only way to assess what are often complex problems and they rely on input from such studies. To truly represent the domain of SOLAS within Earth System models requires global-scale datasets of accurate measurements of relevant parameters. The most accurate data-based estimates of air-sea exchange processes require as much data as possible at large spatial and temporal scales in order to be able to validate and calibrate both model outputs and satellite data. Maintaining and further expanding existing global arrays of autonomous instrumented platforms, as well as oceanic and atmospheric fixed observatories, is a modern-day challenge. Producing integrated, quality and potential bias-controlled global datasets from the collection of these measurements is our ongoing responsibility. This section of Chap. 5 considers a variety of data collation and synthesis projects relevant to SOLAS science presented in the previous four chapters. The following subsections briefly introduce each project.

5.1.1 In Situ Observations

5.1.1.1 ARGO (T, S, O_2)

In November 2007, the international Argo programme reached its initial target of 3,000 profiling floats (http://www.argo.ucsd.edu/). Every 10 days these floats measure temperature and salinity throughout the global ocean, diving down to 2,000 m and delivering data both in real time for operational users and, after careful scientific quality control, for climate change research and monitoring. Argo results from an outstanding international cooperation. More than 30 countries are involved in the development and maintenance of the array. Argo is the major systematic source of data about the interior of the ocean. Argo aims to maintain a global array of in situ measurements integrated with

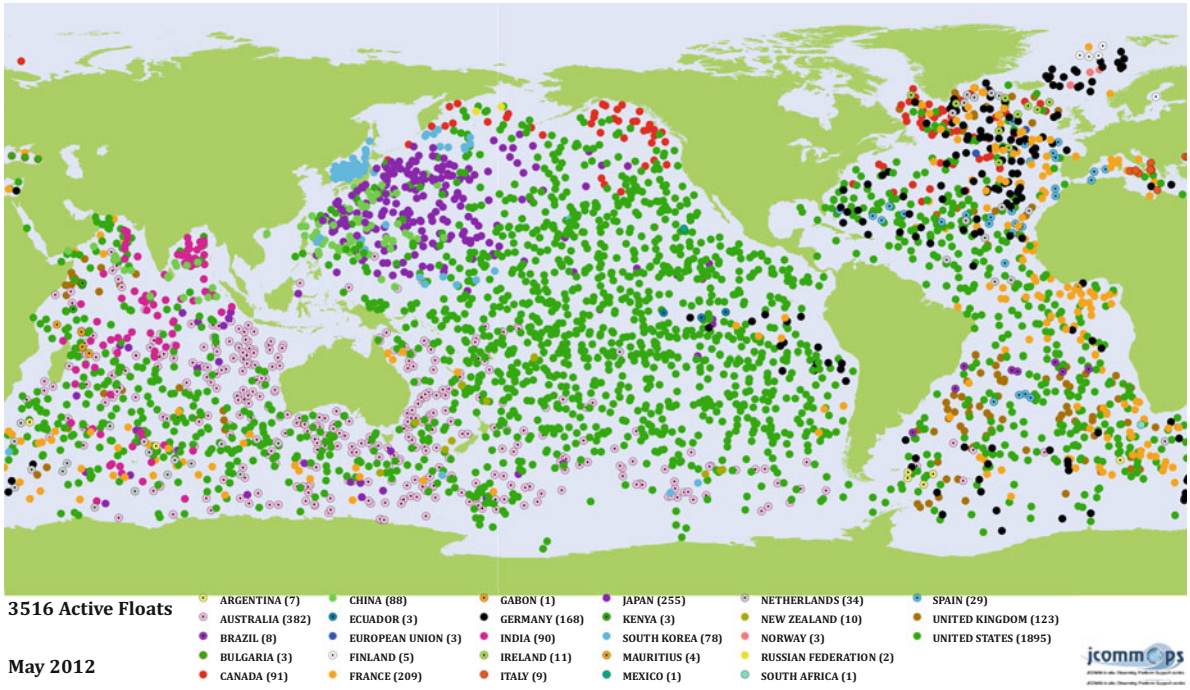

Fig. 5.1 Position of active Argo floats (Figure courtesy of JCOMMOPS, Argo Information Centre, http://argo.jcommops.org)

other elements of the climate observing system (in particular satellite observations) to:

- Detect climate variability from seasonal to decadal scales and provide long-term observations of climate change in the oceans. This includes regional and global changes in temperature and ocean heat content, salinity and freshwater content, steric height and large-scale ocean circulation.
- Provide data to constrain global and regional ocean analysis and forecasting models, to initialise seasonal and decadal forecasting ocean/atmosphere coupled models and to validate climate models.
- Provide information necessary for the calibration and validation of satellite data.

An overview of the achievements of the first decade of Argo is given in Freeland et al. (2010). Argo data (Fig. 5.1) have been used to dramatically improve estimation of heat stored by the ocean, to better understand global sea level rise, to analyse large-scale ocean circulation variations and deep convection areas. Argo has also brought remarkable advances in ocean analysis and forecasting capability. Argo data can be accessed at http://www.nodc.noaa.gov/argo/.

The last OceanObs09 conference discussed the main priorities of the international community for Argo (Roemmich et al. 2009; Freeland et al. 2010; Claustre et al. 2010). Based on the assessment that climate change research requires long-term, sustained, high quality and global observations, the leading priority and challenge for Argo must be to complete and sustain the global array. This requires deploying between 800 and 900 new floats every year. Several developments of the Argo core mission have also been proposed. Minor changes include the extension of the array into seasonal ice zones and marginal seas. Major expansions of Argo will include monitoring the deep ocean below 2,000 m and marine ecosystems. Deeper measurements are needed to constrain the deep ocean property fields for climate monitoring and long-term prediction. Recent technological advances in biogeochemical sensors will permit the acquisition of new observations of the ocean interior (e.g. Claustre et al. 2010; Adornato et al. 2010). The main parameters that are considered for initial implementation are oxygen, nitrate, chlorophyll *a* and particulate carbon. Pilot experiments have already begun, in particular for dissolved oxygen (almost 200 Argo floats are today equipped with an oxygen sensor). Potential systematic errors due to different measurement techniques or sensors need to be analysed and further corrected to

ensure delivery of quality-flagged controlled data sets. These evolutions will require new resources and careful progressive implementation so that the core of Argo is not diminished. If they are managed carefully, however, Argo's second decade will be even more transformative than the first.

5.1.1.2 Ocean Observatories

Ocean observatories provide a view of how the oceans are changing with time and in relation to depth. The spectrum of ocean observations includes data collection from moorings, AUV surveys (e.g. gliders, submersibles), ARGO floats (see Sect. 5.1.1.1) and repeat observations at select time-series sites in the global ocean. The growing network of OceanSites moorings (http://www.whoi.edu/virtual/oceansites/) consists of about 30 surface and 30 subsurface arrays primarily collecting physical data as part of the Global Ocean Observing System. Ocean time-series sites are fewer in number but they allow collection of critically needed data that illustrates temporal variability on ocean–atmosphere exchange and water-column processes over seasonal to multi-decadal timescales. Four of the longest ocean time-series stations include: (1) Hydrostation S, (32°50′N, 64°10′W; 1954-present) located near Bermuda in the NW Atlantic Ocean (Steinberg et al. 2001); (2) BATS (Bermuda Atlantic Time-series Study), located near Bermuda (32°10′N, 64°30′W; 1988 – present) in the NW Atlantic Ocean (Steinberg et al. 2001; Bates 2007); (3) ALOHA (A Long-term Oligotrophic Habitat Assessment) or HOT site, located near Hawaii (22°45′N, 158°W; 1988 – present) in the North Pacific Ocean (Dore et al. 2009); and; (4) ESTOC; European Station for Time-series in the Ocean Canary Islands (29°10′N, 15°,30′W 1994-present) (González-Dávila et al. 2010).

The monthly BATS and biweekly Hydrostation 'S' programmes play a pivotal role in better understanding of the seasonality and long-term changes in ocean–atmosphere exchange of gases and particles. Both sites serve as important frameworks for larger-scale field and modelling studies in the subtropical gyre of the North Atlantic Ocean (or Sargasso Sea). Over the last 50 years, the surface ocean has warmed by ~ 0.3–0.5 °C while salinity has increased by ~ 0.15. The BATS site exhibits strong seasonality in the ocean–atmosphere exchange of gases such as oxygen (e.g. Ono et al. 2001) and carbon dioxide (CO_2 e.g. Bates et al. 1996, 1998; Bates 2001) with the subtropical gyre of the North Atlantic a sink for atmospheric CO_2. The BATS record shows that ocean CO_2 content has kept pace with atmospheric CO_2 changes and demonstrates the change in ocean pH due to ocean acidification (Bates 2007). In the Sargasso Sea, seasonal measurements of oceanic dimethyl sulphide (DMS) and DMSP (dimethylsulphoniopropionate) have provided one of the only long-term time series for DMS in the open ocean (e.g. Dacey et al. 1998; Toole et al. 2008). The observed decoupling of DMS concentration from its precursors (i.e. DMSP) in the Sargasso Sea is the basis for the '*DMS summer paradox*' hypothesis (Simó and Pedrós-Alió 1999).

The challenges that have faced ocean time-series programmes have been both practical and scientific. Sustaining ocean time-series requires the provision of suitable platforms for observation (i.e. research ships, moorings) and creates logistical demands if the continuity of funding and frequency of occupation are to be maintained. Scientific questions include reconciling time-variations within the context of the four dimensional state (space and time) of the ocean, which includes substantial mesoscale and sub-mesoscale variability (e.g. McGillicuddy et al. 1999, 2007). In the future, ocean time-series programmes will be integrated with the Global Ocean Observing System (http://www.ioc-goos.org/), with these sites acting as important nodes for new observing technologies such as gliders and AUV platforms (Dickey et al. 2009). Understanding ocean and climate relevant processes that influence the ocean–atmosphere exchange of gases and particles requires an improved synergy between (sustained) observation and hypothesis testing over a variety of scales, both spatial and temporal.

5.1.1.3 Atmospheric Observatories

The relative homogeneity of marine vs terrestrial air provides an exceptional opportunity to test aspects of surface atmospheric photochemistry. There is a paucity of long-term measurements of reactive trace gases and aerosols in clean marine environments, but the reported studies have revealed important insights into ocean–atmosphere interactions and their consequences for atmospheric composition and climate. Seasonal observations of sulphur-containing gases and aerosols at Cape Grim atmospheric observatory, Tasmania (40.7°S, 144.7°E) showed summer maxima and winter minima in dimethyl sulphide (DMS), methanesulphonic

acid (MSA, a unique product of DMS oxidation), non-sea-salt(nss) sulphate aerosol, and the concentration of cloud condensation nuclei (CCN) (Ayers and Gras 1991; Ayers et al. 1997), supporting proposed mechanisms for DMS oxidation to particulate sulphate. DMS emissions are believed to contribute to a significant fraction of remote marine CCN concentrations, up to 46 % in summer over the Southern Ocean between 30°S and 45°S (Korhonen et al. 2008). Measurements of sea-salt aerosol composition at Cape Grim confirmed that bromine deficits (a decrease of the bromine to sodium ratio of sea- salt aerosol compared to sea water) were linked to the availability of sulphate acidity in the aerosol (Ayers et al. 1992), as proposed by modelling studies which suggest the importance of acid catalysis in the dehalogenation process (Sander and Crutzen 1996; Vogt et al. 1996). This provided experimental evidence for the net transfer of bromine from sea salt aerosol to the gas phase, where it catalyses photochemical ozone destruction and modifies the concentrations of many important tropospheric gases (Sander and Crutzen 1996; Vogt et al. 1996; von Glasow et al. 2004).

Aspects of O_3 photochemistry have also been confirmed by long-term marine observations; at Cape Grim, diurnal cycling of hydrogen peroxide, one of the major products of HO_x radical (OH and HO_2) recombination reactions, is in opposite phase to that of O_3 (Ayers and Gras 1991), as expected in clean low-NO_x air. The observed relationships between free radical levels and the O_3 photolysis rate (jO^1D) change according to NO_x levels, indicating the critical NO concentration required to switch from O_3 destruction to O_3 production (Carpenter et al. 1997). In the northern hemisphere, a longer than 20-year record in baseline O_3 at the coastal Irish station at Mace Head (53.28°N, 9.02°W) showed that mixing ratios rose steadily during the 1980s and 1990s, probably due to increased tropospheric ozone production from methane oxidation in the presence of nitrogen oxides (NO_x), and stabilised during the 2000s (Derwent et al. 2007) with sporadic increases over the period due to boreal biomass burning events. Background O_3 can be an important contributor to the levels experienced in urban regions, which are not declining in developed regions including Europe despite decreasing precursor emissions.

The northern tropical Atlantic ocean is subject to sporadic but significant dust deposition originating in the African Sahara and Sahel regions. Dust emission has immediate impacts on humans, plus widespread influence on the radiative balance and on marine biological production and biogeochemical cycles, and is believed to have increased due to changes in land use practices (Jickells et al. 2005). A wealth of information comes from the long-term record (since 1965) of airborne desert dust measured in Barbados (13.17°N, 59.43°W). At this site, mineral dust concentrations are correlated with rainfall deficits in the sub-Saharan region (Prospero and Nees 1986; Prospero and Lamb 2003), and the net light scattering of dust exceeds that of nss-sulphate aerosol by about a factor of 4 (Li et al. 1996). There are still, however, considerable uncertainties associated with the global radiative forcing of mineral dust, given the high variability of dust loadings and limited knowledge of dust optical properties (Andreae et al. 2002). In the tropical North Atlantic, Saharan dust has been shown to stimulate nitrogen fixation, which is co-limited by iron and phosphorus (Mills et al. 2004 and references therein; Moore et al. 2009; Rijkenberg et al. 2011), and microbial species diversity (Hill et al. 2010, 2012). Recently, Okin et al. (2011) show that atmospheric deposition of iron can potentially contribute considerably to rates of marine productivity in high-nutrient-low-chlorophyll (HNLC) regions, and that iron is likely to be much more important than nitrogen in supporting net primary productivity globally.

5.1.1.4 Monitoring Reactive Trace Species in the Marine Atmosphere: Highlights from the Cape Verde Observatory

The tropics are particularly under-populated with marine reactive gas measurements, and this was a major motivation for setting up the Cape Verde Atmospheric Observatory (CVAO) in 2005. The location of the site (Fig. 5.2) about 800 km off the northwest coast of Africa in the tropical east Atlantic allows the study of clean marine air from diverse origins including North America, the Atlantic, Arctic, Europe and Africa. The station, now part of the global WMO-GAW long-term observing network, has been developed jointly by UK and German scientists at the Universities of York (UK), MPI-Jena (Germany) and IfT-Leipzig (Germany), in collaboration with the Cape Verdean meteorological service (INMG). Atmospheric measurements focus on reactive trace gases, greenhouse gases and aerosols (Fig. 5.3). The CVAO links with a sister oceanographic station, the Cape

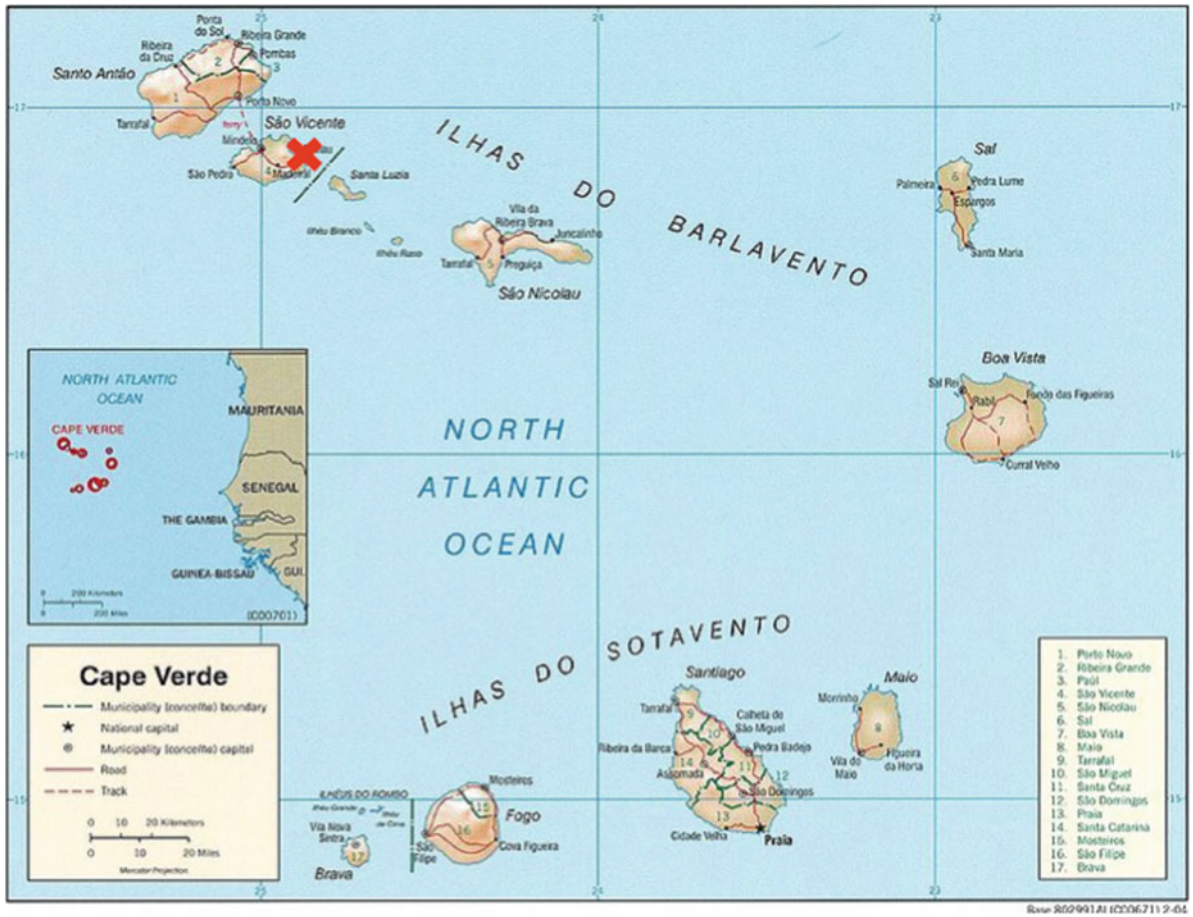

Fig. 5.2 The Cape Verde Islands and location of the CVAO, marked on São Vicente with a *red cross*. Prevailing trade winds are from the north-east (Map from http://commons.wikimedia.org/wiki/File:Cape_Verde_Map.jpg)

Verde Oceanic Observatory, located upwind of the CVAO at 17.59°N, 24.25°W. This was set-up by IFM-Geomar (Germany) in collaboration with the Cape Verde Fisheries Institute (INDP).

Similarly to Barbados, the Cape Verde archipelago is a region subject to very large depositions of dust, originating from the Sahel region, as well as from north-western Saharan sources and as far east as the Bodélé depression in Chad. In this region, dust is deposited mainly by dry deposition, peaking in the winter months when African desert dust is exported across the Atlantic within the lower troposphere. The ionic composition of the aerosol at Cape Verde is dominated by sea salt, but in Saharan dust episodes iron typically constitutes ca. 3.8 % of the total aerosol mass, with aluminium, a tracer of mineral dust, at a slightly higher concentration of ca. 7 % (Trapp et al. 2010; Carpenter et al. 2010). Total iron content reaches up to 33 μg m^{-3} in winter, and the soluble Fe content is between 0.1 % and 15.7 % (Carpenter et al. 2010). Higher solubilities are measured at lower atmospheric dust concentrations, a ubiquitous feature among aerosol solubility datasets.

Although the total aerosol mass is dominated by sea salt, in aerosol particles < 0.14 μm diameter, non-sea-salt components contribute about 80 % of the mass. These components include low-molecular-weight dicarboxylic acids (DCAs) and hydroxylated DCAs, methanesulphonic acid (MSA) and aliphatic amines. A bimodal size distribution for the DCA oxalic acid and coarse mode concentration maxima for the other DCAs are observed, as is typical for marine aerosols. The MSA concentration closely follows that of non-sea-salt-sulphate and the size distribution shows a

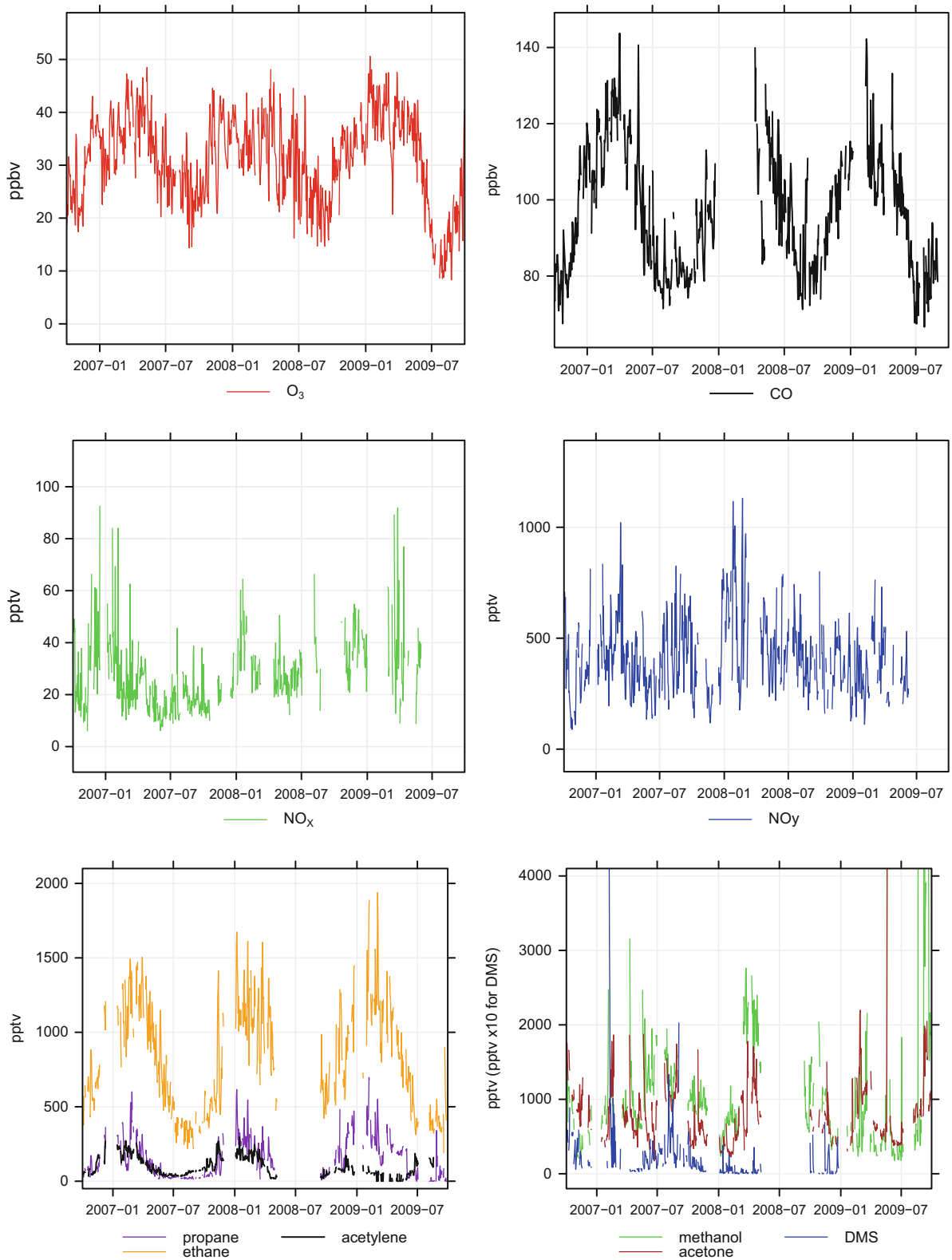

Fig. 5.3 Three-year time series (Oct 2006–Sept 2009) of daily averaged O_3, CO, NO_x, NO_y and VOC (propane, ethane, acetylene, acetone, methanol and DMS) mixing ratios measured at the Cape Verde Atmospheric Observatory (From Carpenter et al. 2010)

maximum mean concentration in the accumulation mode and in sea-salt particles. Aliphatic amines, assumed to be important in the growing process of sulphuric acid clusters, are correlated with phytoplankton activity in the subtropical North Atlantic, especially during an unexpected winter algal bloom (Müller et al. 2009).

The CVAO is one of the few global GAW stations that measures nitrogen oxides (NO_x) (as well as NO_y – both with low pptv detection limits) and VOCs (including oxygenated (O)VOCs). There is very little information on the abundance and distribution of these gases in the marine boundary layer (MBL) in part due to an inability to observe some of these compounds at the very low concentrations characteristic of this environment. Nitrogen oxides act as a catalyst for O_3 production and cycle HO_2 to OH, so are central to determining both the concentration of O_3 and CH_4. Observations show that in this region NO_x levels peak in winter (at 35–45 pptv), when air masses from Africa and Europe prevail (Lee et al. 2009a; Carpenter et al. 2010). This seasonality is attributed mainly to increased NO_x transported from the West African continent from e.g. soils, particularly after rainfall events over the Sahel region during the summer monsoon (Jaeglé et al. 2005; Stewart et al. 2008) or from anthropogenic sources, either directly as NO_x or locally produced from transported reservoir species (e.g. peroxy acetyl nitrate (PAN) or nitric acid (HNO_3)). These reservoir species may undergo decomposition within long-range plumes re-releasing NO_x, particularly for PAN as air masses descend and reach higher temperatures. Averaged NO mixing ratios at Cape Verde (daily averages are between 2 and 8 pptv) are negatively correlated with observed photochemical O_3 destruction; these observations were reproduced using a simple box model and together imply that the presence of 17–34 pptv of NO would be required to turn the tropical North Atlantic from an O_3 destroying to an O_3 producing regime (Lee et al. 2009a). Since NO_x emissions from shipping (e.g. Dalsøren et al. 2010) and African anthropogenic sources (Clarke et al. 2007) are believed to be increasing, future trends of background O_3 in this region could be of major concern for air quality and climate (Lelieveld et al. 2004).

OVOCs are generally present in higher concentrations in the lower atmosphere than non-methane hydrocarbons (NMHC) and have a comparable if not greater effect on oxidising capacity through reaction with hydroxyl radical (OH). Upon photodecomposition, they produce organic radicals that can form organic nitrate compounds such as PAN, sequestering NO_x and transporting it to remote regions of the atmosphere, thus affecting the tropospheric ozone budget and concentrations of OH (Singh et al. 1995; Tie et al. 2003). In the remote marine atmosphere, oceanic sources and sinks are expected to play a significant role in controlling OVOC concentrations, however both the magnitude and direction of OVOC fluxes are a matter of debate (Heikes et al. 2002; Carpenter et al. 2004; Williams et al. 2004; Jacob et al. 2005). Five years of acetone, methanol and acetaldehyde data from the CVAO (October 2006–September 2011) have recently been analysed using the CAM-Chem chemistry-transport model (Read et al. 2012). Observed annual mean mixing ratios of acetone, methanol and acetaldehyde were 763 ± 126 pptv, 1,029 ± 151 pptv and 511 ± 106 pptv, respectively. All three OVOCs show a similar cycle with maxima in spring (March) and autumn (between July and September with particularly high peaks in some years in September), lower levels in summer and generally the lowest levels in winter (Nov-Jan). The model reproduced the acetone concentrations fairly well in magnitude (annual average 670 ± 41 pptv) although underestimating the measured autumn peak, possibly due to underestimation of African biogenic sources. The modeled methanol levels (annual average 355 ± 17 pptv) were almost a factor of 3 lower than the observations, showed considerably less variability, and did not capture the pronounced peaks in spring and in summer – autumn. Possible reasons for the discrepancies include an underestimate by the model of methane concentrations and of terrestrial biogenic sources of methanol, and/or that the tropical North Atlantic is a significant net source of methanol, as suggested by recent data (Beale et al. 2013). Indeed, including estimates of the sea-air flux of methanol based upon these measurements led to an increase in the simulated levels by a factor of ~ 2.5 (new modeled annual average 879 ± 84 pptv) (Read et al. 2012). Of the three OVOCs, the most pronounced model-measured discrepancy was for acetaldehyde, with a model underestimation of over a factor of 10 (modelled annual mean mixing ratio 38 ± 7pptv) and a predicted strong seasonal minimum in summer, contrary to the observations. Acetaldehyde is produced in the ocean through photodegradation of coloured dissolved organic matter and has a strong dependence on sunlight (Kieber and Mopper 1990). Including estimates of the sea-air flux of acetaldehyde from the measurements of Beale et al.

(2013) led to a significant increase in concentrations of acetaldehyde (annual average 139 pptv ± 46). The model thus still falls short of the observations (especially in September through to December – a period of high coastal and continental African influence) for reasons that are currently unknown.

Reactive marine-derived halogens have been proposed to exert a globally significant effect on the concentration and lifetimes of climatically active gases through gas and aerosol phases of the marine boundary layer (Vogt et al. 1996; von Glasow et al. 2002a, b). Bromine and iodine-containing reactive halogen species can influence tropospheric oxidation capacity via a number of reaction cycles including catalytic O_3 destruction, modification of NO_x and HO_x cycles with resulting effects on the lifetimes of other climatically important trace gases (Keene et al. 2009), oxidation of DMS (von Glasow et al. 2004); and oxidation of sulphur(IV) in acidified sea-salt aerosol and cloud droplets (Vogt et al. 1996). Observations of halogen oxide radicals, ozone, and supporting data at Cape Verde made in 2007 provided the first direct experimental evidence for halogen-catalysed tropospheric ozone destruction (Read et al. 2008). More recently, the presence of such halogens at only at a few pptv has been shown to constitute nearly 20 % of the instantaneous sink of HO_2 in this region (Whalley et al. 2010). Iodine monoxide (IO) radicals are believed to be produced mainly via photolysis of iodine-containing halocarbons volatilised from the ocean, yet recent data shows that the sea-air flux of these compounds is sufficient to explain only ~ 20–25 % of the levels of IO observed at Cape Verde (Jones et al. 2010; Mahajan et al. 2010). Recent research (Martino et al. 2009; Jammoul et al. 2009; Carpenter et al. 2013) suggests a role for sea surface chemistry in producing additional halogens, however the significance of such mechanisms remains an open question.

Cape Verde researchers aim to build on these first few years of measurements at the CVAO over the next decade by, for example, quantifying the nitrogen oxides budget, elucidating the nature and magnitude of oceanic iodine emissions, evaluating the influence of dust on the ocean heat budget, understanding oceanic nitrogen fixation, quantifying air-sea exchange fluxes of important gases in the west African upwelling area, and analysing long-term trends in trace gases and aerosols in the context of environmental and climate change. CVAO data can be accessed at http://badc.nerc.ac.uk/data/solas/projects/capeverde.html and http://gosic.org/gcos/GAW-data-access.htm.

5.1.1.5 Conclusions

Oceanic and atmospheric time-series sites started in the 1950s, and their contribution has been invaluable. Some have been in continuous operation without any interruption, some have stopped temporarily and some indefinitely. Since the early 2000s, the launch of the Argo programme with the target of 3,000 floats per year cruising the global ocean has brought a new perspective since it provides a unique and systematic source of information about the interior of the ocean. Only the combination of eulerian and lagrangian observatories in an integrated framework will allow a four dimensional vision of the state of the ocean. One basic key to success of these networks is the constant quest for the best procedures for quality checking, intercomparability and treatment of the data collected. Another key is for the data to be archived in a responsible manner, meaning ensuring proper software developments and addressing management challenges of really huge datasets to secure online delivery and long-term security.

5.1.2 Earth Observation Products

In 1957, the Sputnik was successfully launched and the space age initiated, heralding the evolution of Earth Observation, i.e. the scientific study of the Earth's surface and atmospheric composition from space. Since the early 1970s, satellite oceanography has made huge progress and global satellite observations are now crucial elements of the global climate observing systems (GCOS). Remotely sensed data are also basic ingredients of any oceanic and atmospheric process study. Sea surface temperature, sea level, wave height, winds, sea surface salinity, sea ice and ocean colour are ocean–atmosphere observables monitored with near global coverage on a daily to monthly basis. Satellite measurements of concentrations of trace gases and long lived greenhouse gases, when combined appropriately with atmospheric chemistry models, have over the past 30 years provided a continuously improving picture of the distribution of the surface fluxes of these gases at the air-sea interface. Satellite observations are instrumental tools of SOLAS science to address seasonal to multi-decadal time scale variability in the ocean–atmosphere

exchange of gases and aerosol-borne chemicals. In situ observations, both oceanic and atmospheric, presented in Sect. 5.1.1, provide groundtruthing for the calibration algorithms necessary for deriving these oceanographic and atmospheric properties from space. Remotely sensed data provide global-scale data sets at an unprecedented spatio-temporal resolution. One major challenge ahead is to avoid any discontinuity of operating satellites for the long-term archive and to minimise calibration drift for performing proper climate studies. Earth observations represent a unique observational capability to detect changes in the ocean–atmosphere system and to better understand how planet Earth functions as a complex adaptive system. The following subsections briefly introduce each type of ocean–atmosphere observation.

5.1.2.1 Altimetry, SST, Winds, Sea State

The advent of **satellite altimetry** has given oceanographers a unique tool for studying oceanic circulation and its changes with time. From the vantage point of space, a radar altimeter is able to measure the shape of the sea surface globally and frequently. Due to three decades of international effort, satellite altimetry has benefited from a series of missions, leading to an improvement in measurement accuracy by three orders of magnitude, from tens of meters to a few centimeters (Fu and Cazenave 2001). The evolution from Seasat (1978), Geosat (1985–1989), ERS-1/2 (1991–2011), TOPEX/POSEIDON (1992–2008), Jason1 (2001 to present), OSTM/Jason2 (2008 to present), ENVISAT (2000–2012) to Cryosat-2 (2010 to present) has produced and will produce a wealth of data of progressively improving quality (http://www.aviso.oceanobs.com/, http://sealevel.jpl.nasa.gov). The Saral/Altikal mission, launched in 2012, will ensure, in association with Jason-2, the continuity of the service currently provided by the altimeters onboard Envisat and Jason-1, and will contribute to building a global ocean observing system. The Surface Water and Ocean Topography (SWOT, http://swot.jpl.nasa.gov/mission) mission to be launched in 2020 will revolutionise our conceptual view of ocean dynamics since it will characterise mesoscale and submesoscale circulation with a 10 km space resolution or better. In order to meet the long wavelength calibration accuracy requirements, topography profile measurements will be available with an accuracy equal to or better than the Jason series of altimeters and radiometers (see

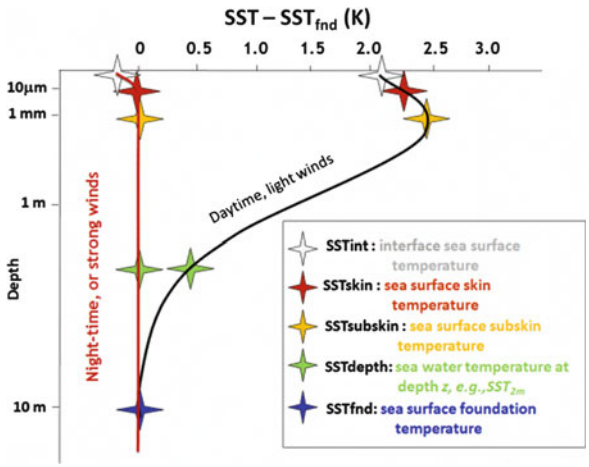

Fig. 5.4 The hypothetical vertical profiles of temperature for the upper 10 m of the ocean surface in high wind speed conditions or during the night (*red*) and for low wind speed during the day (*black*) (https://www.ghrsst.org/ghrsst-science/sst-definitions) (© American Meteorological Society. From Donlon et al. 2007. Used with permission)

SWOT Science Requirements Document, Version 1.1, 2012). Satellite altimetry observations, often assimilated by global ocean circulation and coupled numerical models, constitute the first global synoptic data sets for the study of the following topics: large scale circulation, mesoscale eddies, boundary currents, tropical circulation, large-scale variability on time scales from intraseasonal to interannual in relation to forcing mechanisms, El Niño and La Niña, planetary wave dynamics, eddy dynamics, to list a small sample of topics.

Sea Surface Temperature (SST) is a difficult parameter to define exactly because the upper ocean (~ 10 m) has a complex and variable vertical temperature structure that is related to ocean turbulence and the air-sea fluxes of heat, moisture and momentum. Figure 5.4 presents a schematic diagram that summarises the definition of SST in the upper 10 m of the ocean. The skin temperature (SSTskin) is defined as the temperature measured by an infrared radiometer typically operating at wavelengths 3.7–12 μm (chosen for consistency with the majority of infrared satellite measurements) that represents the temperature within the conductive diffusion-dominated sub-layer at a depth of ~ 10–20 μm. Merging measurements of SST made by different satellite and in situ instruments on drifting or moored buoys requires a proper framework to understand the information content and relationships between these measurements.

The latest reprocessing (Pathfinder Version 5.2) is a new reanalysis of the Advanced Very High Resolution Radiometer (AVHRR) data stream developed by the University of Miami RSMAS and the NOAA National Oceanographic Data Center. It uses an improved version of the Pathfinder algorithm and processing steps to produce twice-daily SST and related parameters dating back to 1981, at an areal resolution of approximately 4 km, the highest possible for a global AVHRR (see http://www.nodc.noaa.gov/SatelliteData/pathfinder4km/). The through-cloud capabilities of microwave radiometers (AMSR-E, TMI) provide a global daily SST map without missing data due to orbital gaps or environmental conditions precluding SST retrieval. Microwave optimally-interpolated products have been proposed at ¼° resolution, and by blending with infrared SSTs from MODIS at 0.09° resolution.

Under the Global Ocean Data Assimilation Experiment (GODAE) umbrella, the *Group for High Resolution SST* (GHRSST) aims at providing the best quality sea surface temperature data, without missing data, for applications in short, medium and decadal/climate time scales in the most cost effective and efficient manner. Each day the *GHRSST Multi-product Ensemble (GMPE)* experiment produces a median *SST* map and associated standard deviation map using *SST* analysis data collected over the previous 24 h period (i.e. yesterday). Thus, the nominal analysis time for the *GMPE* median ensemble *SST* is 12:00 for the previous day (i.e. T-1). The *GMPE* median ensemble *SST* is computed as a median average using a variety of *GHRSST L4* analysis products after their differing analysis grids have been homogenised by area averaging onto a standard ½° latitude longitude grid (https://www.ghrsst.org/data/todays-global-sst/). The median-ensemble *SST* coverage is restricted by the use of the *OSTIA* analysis land mask. The *GMPE* median ensemble *SST* is currently derived using the following inputs: the Met Office *OSTIA SST* analysis http://ghrsst-pp.metoffice.com/pages/latest_analysis/ostia.html, the *NCEP RTG_SST_HR SST* analysis http://polar.ncep.noaa.gov/sst/, the *NAVOCEANO NAVO K10 SST* observations https://www.navo.navy.mil/ops.htm, JMA *MGDSST SST* analysis http://goos.kishou.go.jp/rrtdb-cgi/jma-analysis/jmaanalysis.cgi, the RSS *MW Fusion SST* and MW + IR Fusion SST analyses mentioned above http://www.remss.com/sst/microwave_oi_sst_browse.html, the *FNMOC GHRSST-PP SST* analysis http://www.usgodae.org/cgi-bin/datalist.pl?summary=Go&dset=fnmoc_ghrsst, the MERSEA *ODYSSEA SST* analysis http://www.mersea.eu.org/Satellite/sst_validation.html, the *NOAA AVHRR OI* (Reynolds) http://www.ncdc.noaa.gov/oa/climate/research/sst/oi-daily.php, the *Meteorological Service of Canada (CMC) 1/3° SST analysis* http://www.msc-smc.ec.gc.ca/contents_e.html, and the BMRC *GAMSSA SST* analysis http://podaac.jpl.nasa.gov/dataset/ABOM-L4LRfnd-GLOB-GAMSSA_28km.

As an example central to ocean–atmosphere interactions at the heart of SOLAS science, Fig. 5.5 presents the *GMPE ensemble SST anomaly map* for January 18, 2012 showing clearly that La Niña conditions are present across the Equatorial Pacific. SSTs are at least 0.5 °C below average across much of the central and eastern equatorial Pacific ocean. A horseshoe pattern of above-average SSTs extends from the Maritime Continent into the mid-latitudes of the Pacific Ocean. The sea surface height anomalies from Jason-2 for January 20, 2012 confirm that La Niña is peaking in intensity in the equatorial Pacific (Fig. 5.6). This image is based on the average of 10 days of data centered on January 20, 2012. It depicts places where the Pacific sea surface height is higher than normal (due to warm water), and where the sea surface is lower than normal (due to cool water). Green colour indicates near-normal conditions. The La Niña episode changes global weather patterns and is associated with less moisture in the air over cooler ocean waters. This results in less rain along the coasts of North and South America and along the equator, and more rain in the far Western Pacific.

Ocean surface winds are needed to estimate momentum transfer (surface stress) and gas transfer velocity between the atmosphere and the ocean, and are instrumental for determining large-scale ocean circulation and transport. Accurate wind speeds are essential for ensuring reliable computations of air-sea heat and mass fluxes making surface winds critically important for budgeting energy, moisture, gases and particles (Fairall et al. 2010). Several reviews of space-based wind measurements and applications have been published (i.e. Liu 2002; Liu et al. 2008; Bourassa et al. 2010). The challenge is to continuously improve the present ocean wind system by means of better bias removal and calibration for low and very high wind speeds, increased temporal sampling using a constellation of instruments, finer spatial resolution and improved methods of fusing observations from multiple platforms.

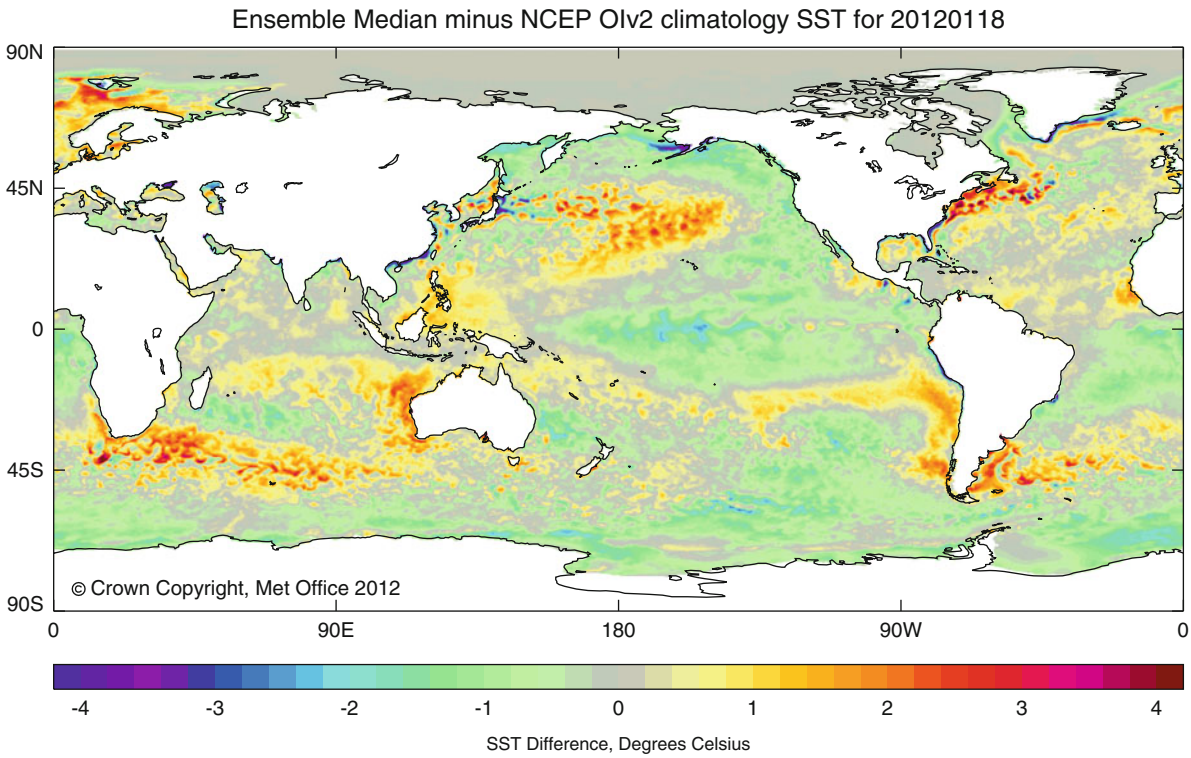

Fig. 5.5 GMPE ensemble SST anomaly map for January 18, 2012; climatology is derived from NCEP/NOAA between 1985 and 2001 (https://www.ghrsst.org/data/todays-global-sst/; Martin et al. 2012) (Figure provided by J. Roberts-Jones, Met Office UK, Crown Copyright)

Instruments that are routinely used to measure vector winds (speed and direction or two vector components) include scatterometers, passive polarimetric sensors and Synthetic Aperture Radar (SAR), and those measuring scalar winds (speed only) include passive microwave radiometers and altimeters. The SeaWinds scatterometer on the QuikSCAT satellite measures surface winds with a resolution of ~ 25 km across a swath width of ~ 1,600 km. The temporal sampling is a function of the orbit and the swath width. The main weaknesses of scatterometers are rain contamination for some rain conditions and lack of data near land (~ 15 km for QuikSCAT) (Weissman et al. 2002; Draper and Long 2004; Nie and Long 2008). Fusion of data from multiple scatterometers significantly improves the temporal coverage (Liu et al. 2008). The assimilation of scatterometer winds in Numerical Weather Prediction (NWP) models has improved the quality of forecasts of tropical cyclones (e.g. in wave forecasting and hurricane force warnings for nowcasting applications). High winds play a large role in Earth's climate, dramatically enhancing gas exchange of greenhouse and trace gases and marine aerosols. However, validation under high winds is difficult due to the scarcity of such events and their tendency to occur in high latitude regions, together with uncertainty in data from buoys and/or ships in rough seas due to wave sheltering.

The root mean square (rms) difference between remotely sensed and buoy wind speeds is generally less than 1 m s^{-1} in non-rainy regions, provided that atmospheric stability and surface currents are taken into account as satellite measurements are physically more related to wind stress than to atmospheric wind speed. The sensitivity of satellite microwave (synthetic aperture radar, scatterometer, altimeter and microwave radiometer) measurements to the **sea state** varies according to the instrument type and to its operating frequencies.

In the future, the combination of multi-frequency, multi-angular and multi-sensor measurements should improve the characterisation of the sea state and

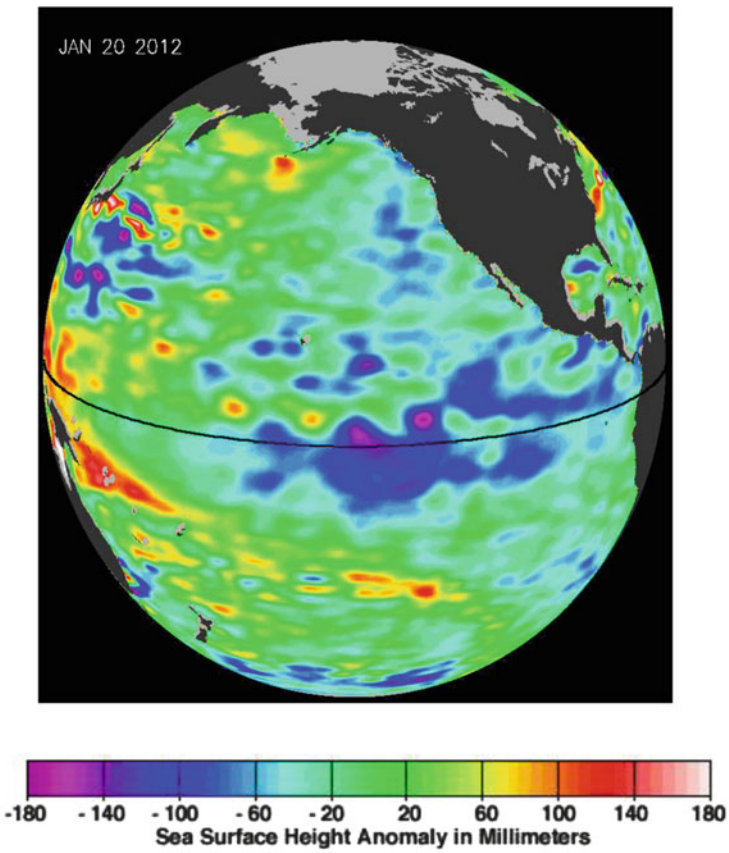

Fig. 5.6 Jason-2 Sea surface height anomalies centered on January 20th, 2012 (Figure courtesy of NASA/JPL-Caltech)

spatial resolution, especially in rainy cases and in very strong wind speed cases. Recent studies show that the retrieval of wind speed in rainy regions, with a degraded precision, is now possible using WindSat radiometric measurements (Meissner and Wentz 2009), that ocean satellite altimetry can retrieve wind speeds from the radar backscatter in gale to storm conditions (Quilfen et al. 2011) and that the new L-band radiometer measurements, much less affected by rain than at higher frequencies, allow measurements of winds in a cyclone up to 50 m s^{-1} (Reul et al. 2012b). Apart from wind speed, the combination of existing and future instruments should also help to retrieve wave parameters.

Altimeters enable the measurement of wave height and mean square slope (mss) in various wavelength ranges depending on the altimeter frequency. Until now, altimeters (e.g. Jason, ENVISAT) have operated at three frequencies (S, C, Ku bands), corresponding to wavelengths of 2.2, 5.6 and 9.3 cm. The future Saral/Altika altimeter operating in the Ka band (wavelength of 8 mm) will complement existing measurements. First retrievals of mean square slope using Global Navigation Satellite System-Reflectometry (GNSS-R) are encouraging (e.g. Clarizia et al. 2009).

Among the new planned missions, the French-Chinese CFOSAT mission (see http://smsc.cnes.fr/CFOSAT/index.htm) will, in addition to wind speed, provide the directional wave spectrum.

Scatterometer observations together with microwave observations of SST have facilitated the collection of data that couple air-sea processes at scales smaller than the regional, typically at the mesoscale. Indeed Chelton et al. (2004) and Small et al. (2008) have identified an intimate link between modification of the dynamics of the atmospheric boundary layer by the SST and the feedback of this modification on the ocean through wind surface stress and heat flux. This link has been observed between sharp SST gradients and surface winds – the so called 'Chelton effect', where winds tend to accelerate over warm and decelerate over cold waters in the frontal zone, resulting in a

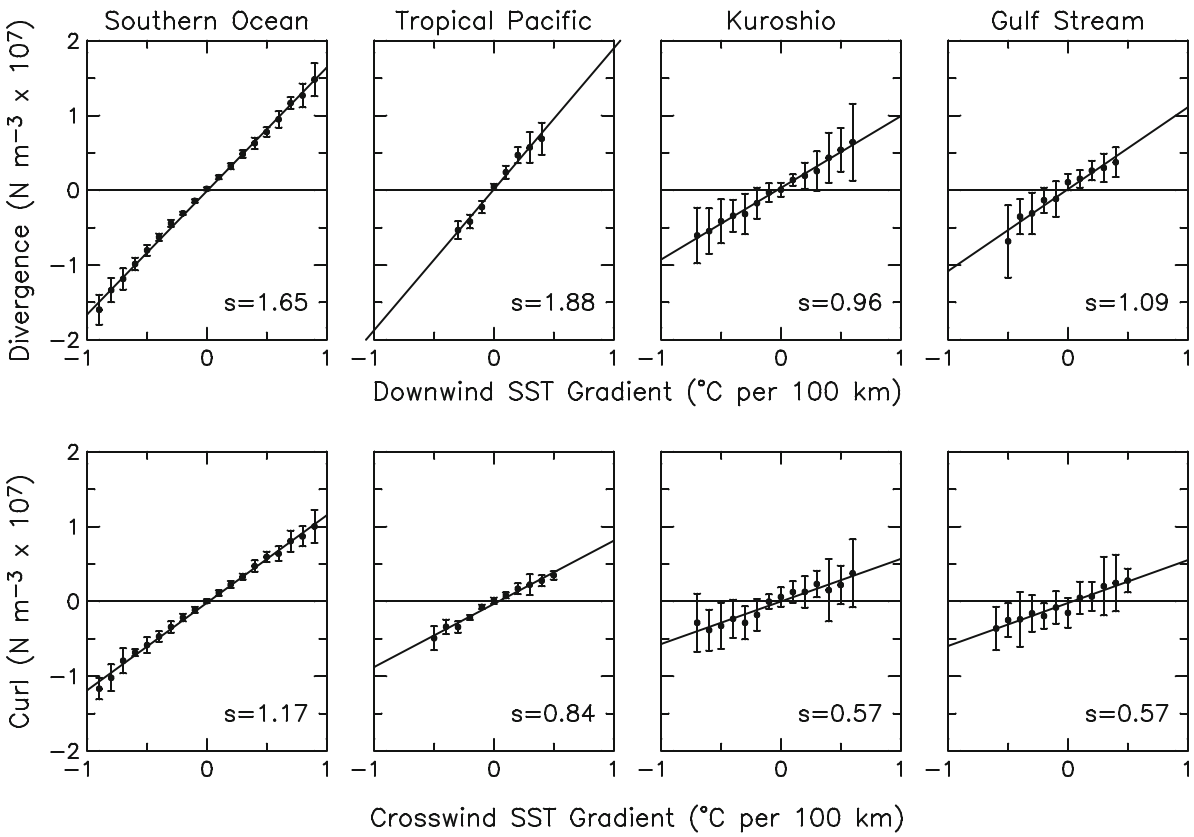

Fig. 5.7 Frontal-scale SST effects on wind stress divergence and curl. Shown are binned scatter plots of spatial high-pass filtered fields of the wind stress divergence as a function of the downwind SST gradient (*top row*) and the wind stress curl as a function of the crosswind SST gradient (*bottom row*) for four geographical regions: the Southern Ocean, the eastern tropical Pacific, the Kuroshio Extension and the Gulf Stream. The points in each panel are the means within each bin computed from 12 overlapping 6-week averages, and the error bars are ± 1 standard deviation over the 12 samples in each bin. The wind stress divergence and curl are multiplied by 10^7 and the units are Nm^{-3} (From Chelton et al. 2004)

quasi-linear relationship between the curl (divergence) of the wind and the SST gradient according to a perpendicular (parallel) direction to the wind (Fig. 5.7). The remarkable 10-year QuikSCAT data record has given some insight into the nature of this variability and the dynamic and thermodynamic impacts of this atmosphere–ocean coupling on ocean circulation and atmospheric weather patterns. However, the intricacy of interaction between the atmospheric and oceanic boundary layers through the 'Chelton effect' has yet to be merged with the still unresolved biogeochemical impact of mesoscale eddies (Siegel et al. 2011).

5.1.2.2 Sea Surface Salinity

While sea surface temperature, sea level, sea ice and sea state are relatively well monitored as an intrinsic part of the global climate observing system (GCOS 2009), until 2009 **sea surface salinity** (SSS) was not measured from space. Salinity is recognised as an essential climate variable (GCOS 2010) and satellite SSS is expected to be highly complementary to existing in situ salinity measurements (Lagerloef et al. 2010).

The feasibility of measuring SSS from space was first demonstrated in the frame of the Skylab mission launched in 1973. However, at L-band frequencies around 1.4 GHz, the sensitivity of radiometric measurements to salinity is low and the radiometric resolution of the instruments remained an obstacle to the development of new satellite missions until the 1990s. Since then, the development of new technologies (Lagerloef et al. 1995) has contributed to two satellite missions accepted by space agencies: the Soil Moisture and Ocean Salinity (SMOS) mission of the European Space Agency and the Aquarius/SAC-D

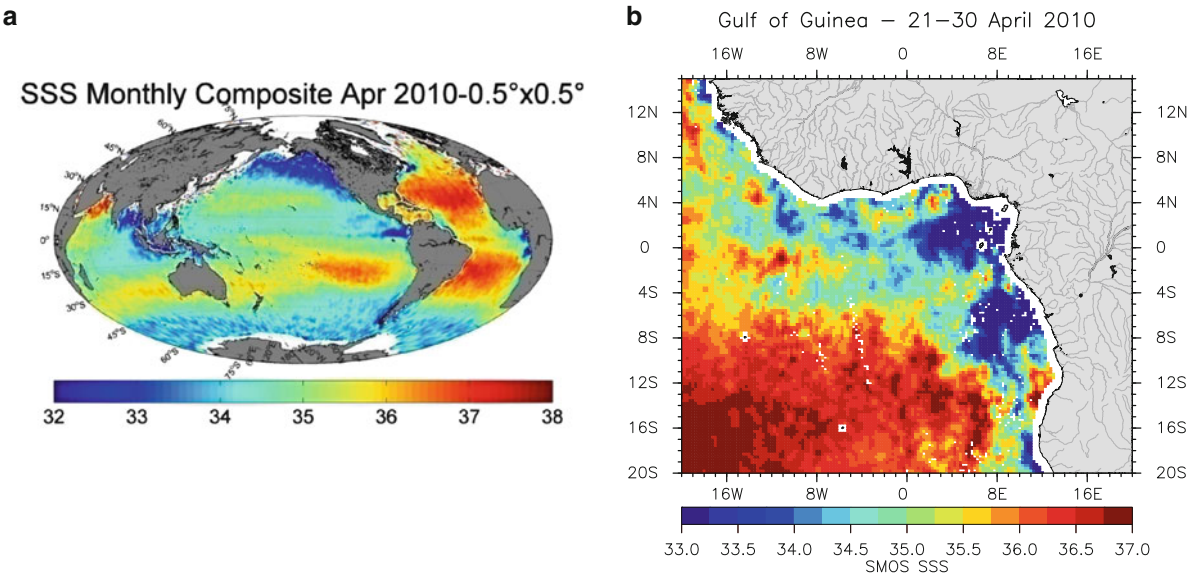

Fig. 5.8 SMOS SSS maps derived at (CATDS-CEC-OS), after applying a thorough filtering of the outliers. (**a**) global map in April 2010; (**b**) in the Gulf of Guinea from 21 to 30 April 2010 (See http://www.catds.fr/ for CATDS processing activities; N. Reul and J. Tenerelly, SMOS Level 3 SSS Research products -Algorithm Theoretical Breadboard Document, 2011, available on http://www.ifremer.fr/naiad/salinityremotesensing.ifremer.fr/CATDS_CECOS_SMOS_Level3Products_ATBD.pdf)

mission of the NASA/CONAE agencies. SMOS uses a new antenna concept (synthetic aperture) for spaceborne radiometry applications and was launched in November 2009; Aquarius uses a large size real aperture antenna and was launched in June 2011. The goal of these two missions is to achieve SSS accuracy of ~ 0.2 or better when averaged over 150–200 km and a monthly timescale.

An overview of the first retrievals of SMOS SSS is given in Font et al. (2012) and is detailed in papers submitted to the IEEE TGRS SMOS special issue (May 2012). Recently, numerous improvements have been made; below we present examples obtained from recently reprocessed data (Fig. 5.8).

Data for the entire year 2010 has been reprocessed at the Centre Aval de Traitement des Données SMOS (CATDS-CEC-OS). In order to remove outliers linked to radio-frequency interferences (RFI), consistency checks based on yearly SMOS data have been performed before retrieving SMOS SSS. When comparing monthly 1° SMOS SSS with in situ SSS data from ships, ARGO and moorings at a global scale, the error standard deviation is 0.6 globally and 0.4 in the tropics (Reul et al. 2012a).

SSS derived in July 2010 with Version v5 of the ESA processors (v5 will be used for the whole mission reprocessing until the end of 2011), led to a precision of 0.2 for SSS averaged over 10 days and 100 km in the subtropical Atlantic. In the rainy tropical Pacific Ocean between 5°N and 5°S, the SMOS-ARGO SSS scattering is greater due to the SSS vertical gradient: SMOS exhibits a mean freshening of 0.1 in the surface water with respect to 5 m depth (Fig. 5.9 Boutin et al. 2012).

The new SMOS data processing demonstrates the capability of retrieving SSS from satellites with a precision of about 0.3 or even better in warm areas. The combination of experience from the SMOS and Aquarius missions is expected to improve this precision.

New satellite SSS will be a key tool for studying air-sea interactions, e.g. the spread of fresh river water into the open ocean, rain surface freshening and the detection of fronts (see BEC processings on http://www.smos-bec.icm.csic.es/).

5.1.2.3 Marine Carbon Observations from Satellite Data: Ocean Color/PIC/POC

Phytoplankton are the basis of marine food webs and contribute up to about 50 % of global primary production. Phytoplankton play a role in the budgets of both organic trace gases and aerosols as a marine source: for example, dimethylsulphide production by

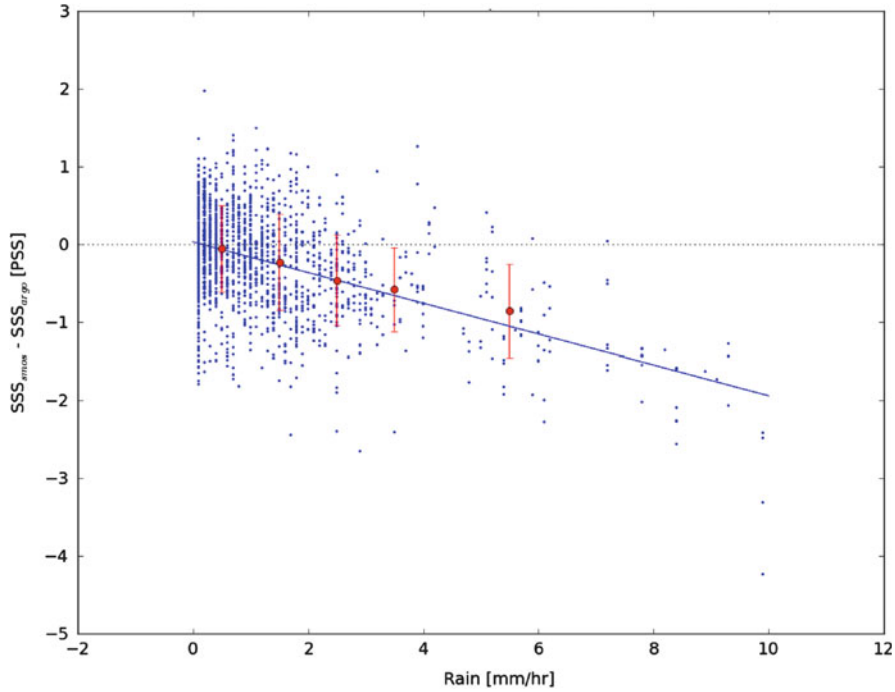

Fig. 5.9 SMOS SSS at 1 cm depth minus ARGO SSS at 5 m depth in the tropical Pacific Ocean (5–15°N; 180–110°W) versus SSMI Rain Rate (Boutin et al. 2012) (More details about along-track SMOS ESA processing is available on www.argans.co.uk/smos/ and about LOCEAN/IPSL SMOS Cal/Val activities on www.locean-ipsl.upmc.fr/smos)

oceanic phytoplankton, leading to the formation of sulphate aerosol and cloud condensation nuclei formation/growth in the marine atmosphere has been studied extensively (e.g. Liss et al. 1997). A link between oceanic chlorophyll *a* content (chl *a*), the indicator of phytoplankton biomass, and cloud droplet numbers over the Southern Ocean (Plass-Dülmer et al. 1995) has been observed, as well as enhanced organic mass in marine aerosols during periods of enhanced ocean biological activity (Singh et al. 2003; O'Dowd et al. 2004). Bromoform observations in the tropical eastern Atlantic Ocean (Quack et al. 2004, 2007) have revealed a pronounced subsurface maximum at the depth of the subsurface chl *a* maximum, suggesting a phytoplanktonic source of bromoform. Ocean-emitted volatile organic compounds also appear to be related to phytoplankton activity (e.g. Gantt et al. 2009; Yassaa et al. 2008). An improved quantification of the dependence of atmospheric composition on marine biological activity is important for studying the ocean–atmosphere interactions of gases and particles and understanding the Earth's climate system and its response to anthropogenic influence. In order to study the dynamics of phytoplankton distribution over longer timescales, optical remote sensing of ocean phytoplankton (ocean colour) provides data on phytoplankton distribution and related parameters with near global coverage on a daily to monthly time resolution. Using relationships derived from in situ oceanic and atmospheric data at or just above the sea surface, ocean colour data products can then be used to infer emission rates of trace gases on longer time scales with reasonable temporal and spatial resolution (down to 1 km), e.g. Arnold et al. (2009, 2010).

Ocean colour has been focused since the 1980s on the detection of chl *a*, due to its strong absorption properties. Merged chl *a* and reflectance satellite data products are available from the SeaWiFS, MODIS and MERIS sensors (1997 until present), through NASA and ESA efforts to produce essential climate variables (Maritorena et al. 2010). However, chl *a* concentration changes with species composition and physiological state and cannot be converted directly into carbon biomass, which is the currency used in ocean carbon models. Therefore, recent advances in ocean colour have focused on the quantification of carbon pools, such as particulate organic carbon (POC), particulate inorganic carbon (PIC) and dissolved organic carbon (DOC), as well as on the assessment of different phytoplankton functional types (PFTs). Different PFTs have distinct impacts on the marine food web and biogeochemical cycling, e.g. variable relationships of

different PFTs to isoprene production have been observed in laboratory experiments (Bonsang et al. 2010). Ocean colour satellite observation is restricted to the near-surface layer, which varies from meters to about 60 m thick depending on the presence of optically-significant water constituents and the wavelength considered (Smith and Baker 1978). Products derived from ocean colour satellite data are integrated over the first penetration depth.

POC algorithms are based on empirically-derived relationships of POC to either inherent optical properties (particle backscattering or attenuation coefficients), which are related to reflectances, measured by remote sensing at several wavelengths (Stramski 1999, Loisel et al. 2001, 2002; Gardner et al. 2006), or to the blue-to-green reflectance ratio (Stramski et al. 2008). The latter algorithm seems less sensitive to regional variability, but is closely related to chl *a* as it uses the same input parameters (the blue to green reflectance ratio). For biogeochemical studies, satellite near-surface POC data are insufficient because they correspond to the first attenuation layer only and deep chl *a* maxima often exist. Moreover, biogenic detrital particles, heterotrophic bacteria and viruses also contribute to POC in variable proportions throughout the entire water column. Stramski et al. (2008) provided quantitative estimates of the POC reservoir in three oceanic layers: the attenuation, the mixed-layer (MLD) and the 200 m layer depth. In oligotrophic waters, this approach may underestimate the POC reservoir where high POC accompanies deep chl *a* maxima, because it assumes that POC is uniform throughout the MLD and equals the near-surface POC concentration. This work has been improved by the empirical algorithm of Duforêt-Gaurier et al. (2010) who derive integrated euphotic zone POC from the entire SeaWiFS satellite data set.

The PIC ocean colour product represents biogenic particles composed of calcium carbonate which is produced by several phytoplankton groups, mainly coccolithophores. These create massive blooms in the ocean, and their PIC, being white, strongly reflects light, which imparts a turquoise-blue-white colour to the ocean. The blooms are easily observed in the pseudo-true-colour images from satellites and can be monitored using ocean colour (Brown and Yoder 1994). Algorithms have been elaborated to quantitatively retrieve PIC at regional and global scales (Gordon et al. 2001; Balch et al. 2005) and the most recent have been used to process the whole SeaWiFS and MODIS data set. An important constraint of these algorithms is that, at typical non-bloom concentrations, the PIC scattering represents only a few percent of the total scattering. Thus, to maximise the signal to noise ratio, satellite pixels must be aggregated in space and time, in order to define accurate mean concentrations. Currently, more verification with PIC field measurements is underway to optimise the use of PIC ocean-colour data in models (Balch et al. 2011). PIC is also produced by certain zooplanktonic organisms but these particles are too large to be detected by ocean colour (Balch et al. 1996).

Different bio-optical and ecological methods have been established that use ocean colour data to identify and differentiate between PFTs or phytoplankton size classes (PSCs) in the surface ocean. These can be summarised into four main types: spectral-response methods which are based on differences in the shape of the light reflectance/absorption spectrum for different PFTs/PSCs (Sathyendranath et al. 2004; Alvain et al. 2005, 2008; Ciotti and Bricaud 2006; Bracher et al. 2009; Sadeghi et al. 2011; Brewin et al. 2010a; Devred et al. 2011), methods which use information on the magnitude of chlorophyll *a* biomass or light absorption to distinguish between PFTs or PSCs (Devred et al. 2006; Uitz et al. 2006; Hirata et al. 2008; Brewin et al. 2010b; Hirata et al. 2011; Mouw and Yoder 2010), methods that retrieve the particle size distribution from satellite-derived backscattering signal and derive PSCs (Kostadinov et al. 2010), and ecological-based approaches which use information on environmental factors, such as temperature and wind stress, to supplement the bio-optical data for investigating PFTs (Raitsos et al. 2008). All methods derive dominant phytoplankton groups, while Uitz et al. (2006), Bracher et al. (2009, improved by Sadeghi et al. 2011) and Hirata et al. (2011) also give chl *a* for the different PFTs. Nearly all the PFT methods mentioned use information from the multi-spectral ocean colour sensors SeaWiFS, MERIS or MODIS and are based on the parameterisation of a large global or regional in situ data set in order to yield PFTs from satellite chl *a* or normalised water leaving radiances. Unexpected changes in the relationships between these parameters resulting from a regional or temporal sampling bias leads to a bias in the

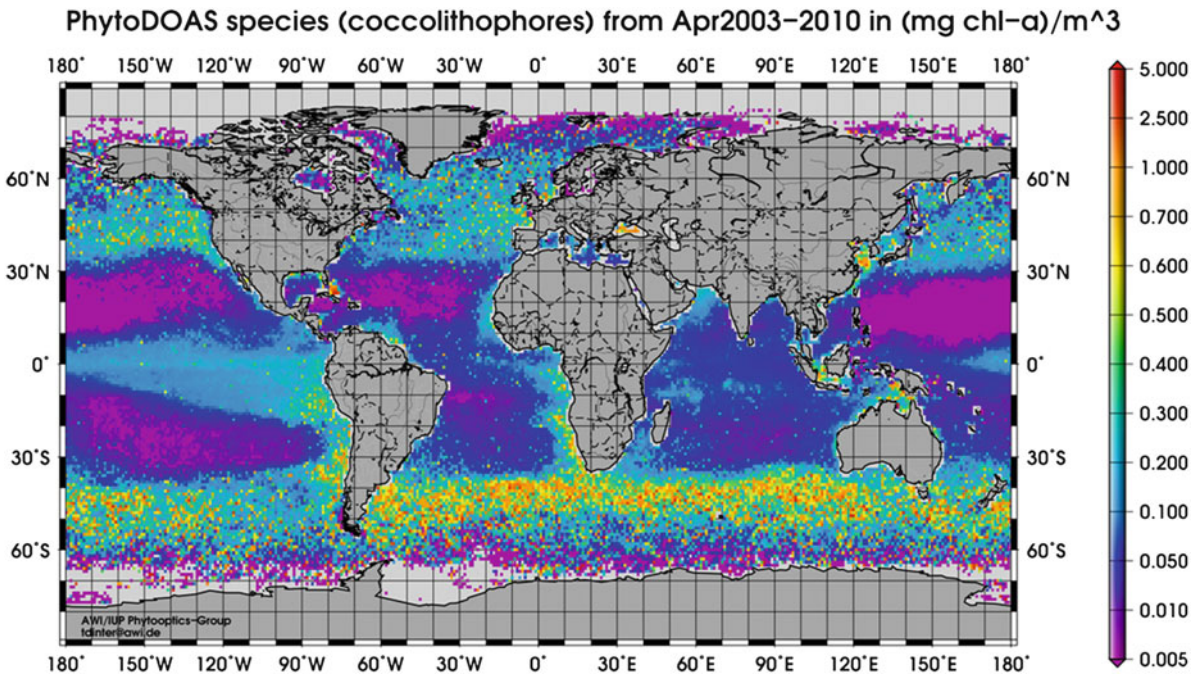

Fig. 5.10 Global climatology for April of coccolithophore biomass (given as chlorophyll *a* concentration) derived from the average of all SCIAMACHY data retrieved via PhytoDOAS multitarget-fitting (according to Sadeghi et al. 2011, 2012) (Source: T. Dinter, A. Bracher, Phytooptics, AWI-IUP)

detection of PFTs. In contrast, the PhytoDOAS method of Bracher et al. (2009, improved by Sadeghi et al. 2011) exploits the whole spectrum by using hyperspectral data of the satellite sensor SCIAMACHY and discriminates different PFTs by their characteristic absorption. Diatoms, cyanobacteria, dinoflagellates and coccolithophores are quantified (example in Fig. 5.10) without assuming empirical relationships as in the case of other PFT methods. Recent PFT algorithm intercomparison studies show the robustness of the abundance-based approaches at detecting dominant PSCs (Brewin et al. 2011). A new PFT algorithm intercomparison has been initiated where the quantitative assessment of PFT distributions will be compared. PFT monthly resolved products are available for the whole SeaWiFS or SCIAMACHY missions, using the methods of Alvain et al. (2008) and Hirata et al. (2011) covering 1998–2009 for the first data sets and the PhytoDOAS method covering 2002–2011.

5.1.2.4 Sea Ice

Methods for studying sea ice, including Earth observation products, have recently been thoroughly reviewed by Eicken et al. (2009), which includes a comprehensive reference list. Here we provide a brief summary of the approaches most relevant to the science of surface ocean-lower atmosphere exchanges.

In addition to satellite-borne remote sensing tools (e.g. Massom 2009), automated in situ systems (see Perovich 2009), mainly mounted on buoys, are proving to be a critical component of the global sea-ice observing network. In contrast to open water, sea ice is a very complex and variable surface, complicating calibration of remote sensing signals, and information from multiple sources is generally required to resolve measurements. Therefore, both multiple satellite sensors and widely distributed automatic measurement stations (also called ice-based observatories) remain critical to interpreting Earth observation data on sea ice (see Massom 2009 for a detailed discussion).

Sea ice distribution and motion are fundamental parameters needed for research on air-sea exchange in polar oceans. Passive microwave data (e.g. from the SSM/I series satellites) may be the most valuable tool available for tracking sea ice. Not only does microwave radiation provide information in the dark and through clouds, but in the Arctic, where summer brine

flushing is common, it can also distinguish between first- and multi-year ice. While the relatively low resolution of passive microwave data precludes their use for studying landfast ice, synthetic aperture radar (SAR; aboard, for example, the ERS series and RADARSAT satellites) provides very high resolution data, to as good as 1 m, which is adequate not only for fast ice, but also for detailed ice edge information. Visible and infrared sensors (e.g. MODIS and AVHRR) also provide data on ice distribution, although only far-infrared sensors are useful during winter. Deriving ice motion from time series of satellite images carries a high uncertainty, and data from drifting ice buoy arrays are a vital component of accurate ice motion estimates.

Beyond the simple presence or absence of sea ice, ice thickness and the rates of freezing or melting strongly impact air-ice-ocean exchanges. To date, ice mass balance buoys (e.g. Metocean) and moored sonar have been the most accurate tools available to determine sea ice thickness over distributed areas. Kwok (2010) reviewed satellite remote sensing of sea-ice thickness and concluded that at least in the Arctic, ice thickness from radar and lidar altimetry is maturing and its shortcomings are relatively well understood. In contrast, Southern Ocean ice cover, in which flooding and snow-ice formation cause substantial density variations and where there are fewer observations to help address processing deficiencies, sea-ice thickness retrieval has not achieved the same level of accuracy as in the Arctic. The CryoSat-2-satellite, launched in 2010, was designed to use SAR to measure ice thickness very precisely, and appears to be meeting expectations.

While visible-IR sensors can provide surface skin temperatures, sea ice is often covered by a snow layer of variable thickness, and the temperature at the ice-snow interface is an important parameter in determining ice-atmosphere exchanges. Passive microwave has shown potential for providing information on both the snow thickness and snow-ice interface temperatures, but these applications are still in development. The impurity content of the snow (i.e. its salinity) can be derived from visible-IR imagery, and the salinity of sea ice substantially influences its radar transparency, providing a potential tool for remotely sensing sea ice bulk salinity that has not yet been fully developed. Frost flowers, which form on the surface of new ice under very cold and still conditions, appear to play an important role in transferring sea-ice salts, organohalides, and other organic matter to the atmosphere and can be identified with synthetic aperture radar or with a combination of active and passive microwave sensors (Kaleschke and Heygster 2004).

Regardless of which sensor data are used, classification of ice types, including leads or polynias, from remote sensing involves refined analytical tools (e.g. Soh et al. 2004; Qin and Clausi 2010). Most are formulated in Bayesian frameworks, which require substantial ground truth data to train the analytical classifier. To help meet this need, Clausi et al. (2010) developed a tool for generating high-resolution (pixel-based) maps for SAR images. They provide estimates of ice concentrations, types, and floe sizes derived from manually classified ice charts of low spatial resolution, such as those produced by the Canadian Ice Service. Similarly, Röhrs et al. (2012) used manual observation of visible satellite images to test and validate an algorithm for identifying leads in passive microwave imagery. Note that although these approaches provide a lot of data for training classification algorithms, the data are not truly ground-truthed, which requires instruments at the surface.

The autonomous O-buoys developed by the Ocean–Atmosphere-Sea Ice-Snow (OASIS) programme during IPY (Fig. 5.11) have successfully measured both ozone and CO_2 over sea ice for at least 3 months during the winter-spring transition (Knepp et al. 2010). As these buoys are further developed and more are deployed, they will provide valuable ground-truthing data to supplement those from satellite-borne absorption spectrometers (see Sects. 5.1.2.5 and 5.1.2.6) measuring aerosol and trace gas emissions from sea ice.

As yet, surface waters below the ice are inaccessible to satellites except through openings in the ice, such as leads and polynias. Therefore, the only available tools that potentially could provide operational information on ice-sea water exchanges are ice buoys, such as the Autonomous Ocean Flux Buoys (AOFB), and ice-tethered profilers (Krishfield et al. 2008). Gliders also have the potential to provide surface-ocean information at higher temporal and spatial resolution than ship-borne measurements, but their use at shallow depths under sea ice can be complicated by ice keels.

As noted before, interpreting remotely sensed data on sea ice requires synthesising information from

Fig. 5.11 O-buoy OB-5 shortly after deployment on August 5, 2011, at 78° 0.4′ N, 139° 55.5′ W in the Beaufort Sea (Photo: John W. Halfacre)

numerous tools, including different satellite sensors and buoy arrays. Recent initiatives to coordinate observations in ice-covered seas should substantially improve the utility of Earth observation products for sea ice research. Notably, the International Polar Year programme on integrated Arctic Ocean Observing Systems initiated basin-wide research coordination in the Arctic Ocean, including deployments of ice buoys and ice-tethered profilers (e.g. Dickson 2009; Perovich et al. 2012, IAOOS: Ice-Atmosphere- Arctic Ocean Observing System see http://www.iaoos-equipex.upmc.fr/en/index.html). A similar initiative in the Southern Ocean (SOOS, the Southern Ocean Observing System) is also now underway (Rintoul et al. 2012).

5.1.2.5 Aerosols

Properties of aerosols in the marine atmosphere are extensively described in Chap. 4 of this book (see also Sects. 5.1.1.3 and 5.1.1.4), including the use of satellite remote sensing for the determination of the organic mass fraction in sea spray aerosol. In this section we further elaborate on the use of satellite remote sensing for the determination of aerosol properties, which started some three decades ago with the retrieval of the aerosol optical depth (AOD, often also called aerosol optical thickness or AOT) over the ocean. The retrieval of aerosol properties over the oceans can be achieved due to the relatively small reflection of solar radiation by the ocean surface, as compared to the reflection by aerosol particles, at wavelengths in the visible and near infrared part of the electromagnetic spectrum. Over land the surface reflection at these wavelengths is much larger and over bright surfaces this overwhelms the aerosol signal.

A brief description of the history of aerosol observations from space was presented by Lee et al. (2009b) and Kokhanovsky and de Leeuw (2009), including an overview of instruments used for this purpose (see also de Leeuw et al. 2011a). Currently, AOD observations are available from several instruments, including operational products such as MODIS, which provides AOD with a validated accuracy over the ocean of $\pm$ (0.03 + 0.05AOD) (Remer et al. 2008). Other examples of instruments providing aerosol products are: MISR, PARASOL, AATSR, MERIS, OMI, SCIAMACHY, GOME-2, MSG and CALIOP. These products include a variety of parameters, in addition to AOD at one or more wavelengths, such as fine mode fraction, absorption aerosol index (AAI) and an indication of aerosol chemical composition. Products, accuracy and spatial and temporal coverage depend on the instrument characteristics. The results are validated by comparison with independent ground-based sun photometer data.

Results from a comparison of MISR and MODIS aerosol products by Kahn et al. (2009) show good correlations between the AOD products (correlation coefficient 0.9 over ocean and 0.7 over land) and the Ångström exponent (correlation coefficient 0.67 over ocean when MISR AOD values > 0.2 are considered). Kahn et al. emphasise the necessity for proper interpretation of the satellite products. In particular

data-quality statements should be followed to ensure proper interpretation and use of the satellite aerosol products. Other intercomparisons of satellite products also reveal significant discrepancies between AOD (order of 0.1) from different instruments, even over the ocean (Myhre et al. 2004, 2005).

The AOD is important for the measurement-based assessment of aerosol effects on climate and chemical processes in the atmosphere. Satellite data also show the spatial distribution of aerosols over the ocean which reveals, e.g. transport patterns of dust, biomass burning aerosols and anthropogenic pollution, all of which play a role in the atmospheric input of nutrients into the ocean and their biogeochemical effects (see Chap. 4 for a description of current knowledge on this subject).

Measurements of AOD over the ocean clearly show the effect of wind speed on SSA production, as reported by e.g. Mulcahy et al. (2008); O'Dowd et al. (2010), both using local sun photometer and wind speed measurements at Mace Head, Glantz et al. (2009) using SeaWifs data and ECMWF wind speeds, Lehahn et al. (2010) using MODIS AOD and QuickSCAT, AMSR-E and SSM/I data, Huang et al. (2010) using AATSR AOD and ECMWF wind speed data, Kiliyanpilakkil and Meskhidze (2011) using CALIOP and AMSR-E data and Smirnov et al. (2011) using data from the Marine Aerosol Network (MAN, Smirnov et al. 2011). Smirnov et al. (2012) compare various AOD versus wind speed relationships showing large differences in the AOD at the same wind speed. Most of these relationships show a similar change in AOD over the wind speed range of 0–10 ms^{-1}, with the exception of the relations of Mulcahy et al. (2008) and O'Dowd et al. (2010). The latter relations show exponential dependence of AOD on wind speed whereas Smirnov et al. (2012) found a linear dependence.

AOD has been used by several authors to evaluate or improve their model results. Sofiev et al. (2011) used MODIS AOD data to evaluate their model results over the ocean. Jaeglé et al. (2011) used AOD observations to include the effect of SST on the production flux of coarse mode sea-salt aerosol in their model through a correction to the sea salt aerosol source function (see Chap. 4 and Sect. 5.2.4). Lapina et al. (2011) used MODIS and MAN AOD data for comparison with GEOS-Chem model results that use the Jaeglé et al. (2011) correction for coarse mode sea-salt aerosol production fluxes as well as an emission scheme for organic matter (see Chap. 4). These authors found that the model AOD is lower than the mean MODIS AOD value but agrees well with MAN AOD for the studied regions. Lapina et al. (2011) argue that this may be partially explained by uncertainties in the satellite retrieval and that uncertainties in the marine OM emission scheme cannot account for the AOD estimate. They conclude that only a sea spray aerosol emission parameterisation resulting in a very different spatial distribution of sea salt could resolve this discrepancy, which may suggest that either some additional marine source of aerosol has not been accounted for or that observations used in the study are insufficient to close the marine aerosol budget.

Sea spray aerosol is principally produced from waves breaking under the action of the wind. The area of the ocean covered with whitecaps is expressed in the whitecap fraction. The retrieval of whitecap fraction using satellite data was explored by Anguelova and Webster (2006). A review of this subject can be found in Lewis and Schwartz (2004), see de Leeuw et al. (2011b) for the current status in this area and a comparison of different methods.

5.1.2.6 Satellite Measurements of Trace Gases Over the Oceans

Carbon dioxide (CO_2) and methane (CH_4,) are the two most important greenhouse gases (GHG) being modified directly by anthropogenic activity, primarily fossil fuel combustion, biomass burning and land use change. In 1957, during the International Geophysical Year, IGY, accurate measurements of the mixing ratio of CO_2 at the Mauna Loa Observatory, led by C.D. Keeling, were initiated. These revealed the growth of CO_2, attributed to fossil fuel combustion, and the annual biogeochemical seasonal cycling of CO_2. Measurements were extended to other sites and to include CH_4 and other relevant gases, resulting in a global but sparse network. However global measurements at high spatial resolution are needed to identify and assess the local and regional response of CO_2 and CH_4 surface fluxes in a warming world and for the verification of national inventories of GHG.

During the 1980s, the retrieval of the total dry atmospheric columns of CO_2 and CH_4 from space was proposed as part of the SCIAMACHY (SCanning Imaging Absorption spectroMeter for Atmospheric CartograpHY, Burrows et al. 1995 and Bovensmann et al. 1999) mission. This is achieved by the remote

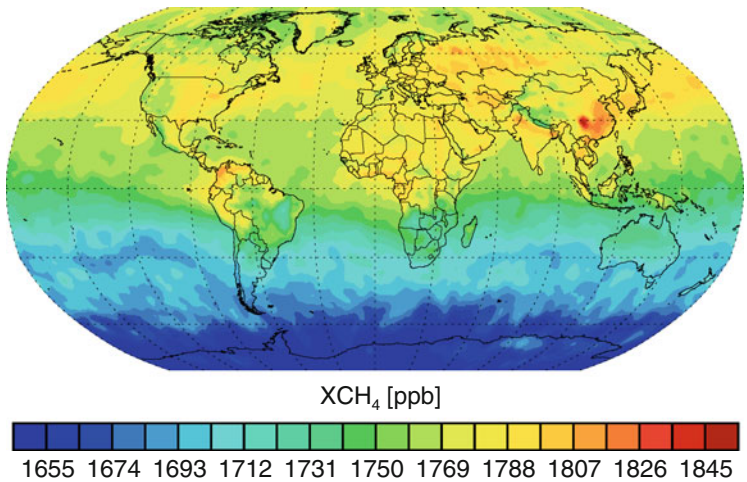

Fig. 5.12 The average global distribution of the dry column of methane retrieved from SCIAMACHY, showing the source regions such as natural wetlands and rice paddies and the hemispheric gradient

sounding in the short wave infrared spectral region and the retrieved CO_2/CH_4 data products, provided they have been adequately sampled with sufficient accuracy and are coupled with models, constrain local and regional surface fluxes. SCIAMACHY was selected in 1989, as a national contribution by Germany to the ESA ENVISAT, with The Netherlands and Belgium joining the funding consortium in Phase A and B, respectively. ENVISAT flies in a sun-synchronous orbit in descending node, having an equator crossing time of 10.00 a.m. and was launched on the 28th of February 2002. SCIAMACHY measures contiguously in eight channels scattering, reflecting and transmitting solar electromagnetic radiation upwelling from the earth's atmosphere between 214 and 2,380 nm at a channel dependent spectral resolution between 0.2 and 1.4 nm. Measurements are made alternately in limb and nadir viewing geometry and for solar and lunar occultation. Mathematical inversion of the nadir measurements of the absorptions of CO_2, CH_4 around 1.6 μ and molecular oxygen, O_2 around 0.76 μ, yields the total dry columns of CO_2 and CH_4.

The map of the average dry total column of methane is shown in Fig. 5.12. The source regions in the northern hemisphere, such as natural wetlands, rice paddies and anthropogenic regions are readily identified along with the hemispheric gradients. In Fig. 5.13 the dry column of CO_2 and CH_4 are plotted against time and sin(latitude) to show the latitudinal distribution of increase from 2003 to 2012. Combining these measurements appropriately with atmospheric models yields and constrains the surface fluxes of CH_4 and CO_2. There is now a growing body of literature combining these data and an accurate network of measurements with which to assess our understanding of surface flux distributions. SCIAMACHY has demonstrated the feasibility, but higher spatial resolution measurements and improved sampling are needed to unambiguously measure point sources and sinks of CO_2 and CH_4.

The GOSAT (Greenhouse gases Observing SATellite) was launched on 23rd of January 2009. The instrument TANSO-FTS (Thermal And Near infrared Sensor for carbon Observations - Fourier Transform Spectrometer) has now made over four years of measurements in space (Hamazaki et al. 2004). The measurements have higher spectral resolution and contain potentially more information than those of SCIAMACHY but have poorer sampling. The OCO (Orbiting Carbon Observatory) was selected by NASA but the OCO-1 launch vehicle failed in February 2009 (Crisp et al. 2004). OCO aims to make high spatial resolution measurements of the dry column of CO_2 and OCO-2 is now planned for launch in 2014. Based on the success of SCIAMACHY, the MaMap instrument was developed in 2006 to demonstrate that high spatially resolved measurements, e.g. 50 m, and high signal to noise of the total dry mole fraction of CO_2 and CH_4 are feasible from aircraft (Gerilowski et al. 2011). The results of MaMap have been used to retrieve surface fluxes of CO_2 and CH_4 from point sources. This demonstration was an essential prerequisite for the development of the CarbonSat and CarbonSat Constellation concepts. A single CarbonSat was proposed for the ESA earth explorer opportunity mission 8, and selected in November 2010 by ESA for Phase A, B1 studies,

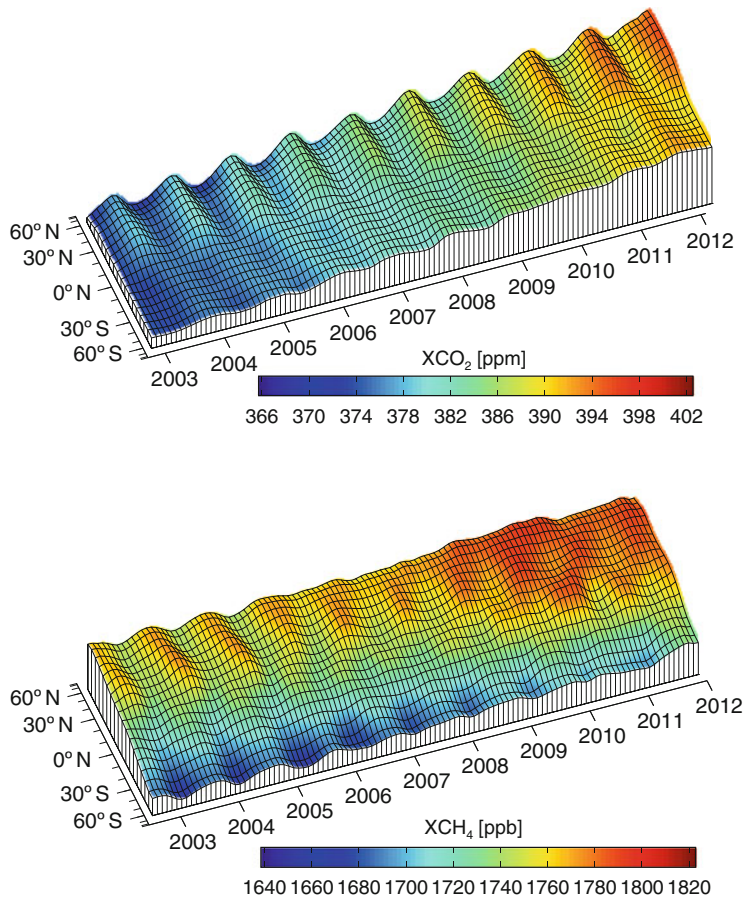

Fig. 5.13 Plots of the dry mole fraction of CO_2 and CH_4 versus sin (latitude) from 2003 to 2012 retrieved from SCIAMACHY. These show the latitudinal increase of CO_2 and the changes in CH_4. The rate of increase accelerates in 2008 and is not yet unambiguously explained (Figures courtesy of O. Schneising, M. Buchwitz and J. P. Burrows University of Bremen)

yielding 5 day global coverage. A constellation yields the daily measurements at high spatial resolution measurements required for the verification of CO_2 and CH_4 emissions in the post Kyoto era and the observation of the response of the ecosystem in a warming world.

The background concentration of most trace gases in the lower marine atmosphere is difficult to quantify from space, mainly due to low atmospheric concentrations and the low reflectance of the ocean surface. This is particularly true for ozone as its concentration in the lower troposphere is considerably lower than that throughout the rest of the ozone column. However, emissions from volcanic eruptions (e.g. SO_2), shipping routes (NO_2) and long-range transport plumes can be monitored over the oceans.

International shipping routes are a significant source of pollution in the marine boundary layer. Emissions of traces gases such as NO_2 have been measured from different satellite instruments (e.g. Richter et al. 2004; Beirle et al. 2004). For instance, Franke et al. (2009) compared modelled and satellite-observed NO_2 for the shipping lane between India and Indonesia using GOME, SCIAMACHY, OMI and GOME-2 data, finding indications of an upward trend in shipping emissions over recent years.

The background concentration of SO_2 is difficult to measure by instruments onboard satellites, although volcanic eruptions and their emission plumes can be monitored over several days. The first observation of a volcanic eruption from satellite SO_2 measurements was made using data from the Total Ozone Mapping Spectrometer (TOMS) during the El Chichón eruption in 1982 by Krueger (1983). Since then, several authors have reported satellite SO_2 observations from volcanic ash plumes across the world (e.g. Heue et al. 2010; Nowlan et al. 2011).

Reactive halogen species, such as BrO and IO, lead to ozone destruction in the lower atmosphere,

especially during the polar spring. Measurements from satellite instruments such as GOME, GOME-2, SCIAMACHY and OMI have delivered detailed maps of BrO (e.g. Chance 1998; Wagner and Platt 1998; Richter et al. 1998). The detection of IO over Antarctica has also been demonstrated using SCIAMACHY data (Saiz-Lopez et al. 2007; Schönhardt et al. 2008).

Oxygenated volatile organic compounds such as HCHO and $(CHO)_2$ are key intermediate species produced during the oxidation of precursor hydrocarbons. Their short lifetime of a few hours in the lower troposphere links them to emission sources and makes them useful tracers of photochemical activity. Vrekoussis et al. (2009) and Lerot et al. (2010) observed high values of glyoxal over the oceans, mainly in the tropics close to the upwelling areas and regions having significant amounts of phytoplankton, implying oceanic biogenic activity as a possible source of glyoxal precursors. Marbach et al. (2009) have reported the detection and quantification of HCHO linked to shipping emissions from GOME data.

5.1.2.7 Conclusions

The success of integration of Earth Observations products in SOLAS Science depends on the efforts of the international atmospheric and marine science communities. They need to maintain a continuous series of sensors on satellite missions, without interruption, with a constant aim to optimise the quality of the retrieved observables. This required quality implies continuous and rigorous calibration with in situ measurements in the atmosphere and in the ocean including coastal regions. The European Space Agency has launched in 2011 a Support to Science Element Project on SOLAS Science entitled Oceanflux (http://due.esrin.esa.int/stse/projects.php) comprising three themes: Upwellings, Sea spray aerosols and Greenhouse Gases to foster the use of EO data in addressing these SOLAS science questions. Ultimately, it is up to SOLAS scientists together with Earth Observation experts to imagine and develop novel sensors, products, algorithms and methodologies to provide the long duration records of all relevant parameters of the ocean–atmosphere coupled system. Together with models, Earth Observation products constitute the key sentinels for predicting the future trajectory of Earth's climate.

5.1.3 Modelling

Modeling has emerged as a critical and successful method to answer scientific questions, to test hypotheses and to make predictions (Gruber and Doney 2008). Models range from conceptual (essentially ideas about the functioning of a system or process) to complex realistic models that push the boundaries of computational capabilities. We restrict our discussion here to mathematical models and their numerical implementations unless explicitly stated. But in all cases, models are designed for a particular purpose and therefore their transferability is often strongly limited.

Modeling has become the third pillar of the scientific method. In particular, the development of models can be thought of as an iterative process in that observations and experiments stimulate the formulation of conceptual models and hypotheses, which are then translated into mathematical models. The models can then produce predictions, which when confronted with new observations permit the developer to evaluate the models and to either corroborate their underlying hypotheses or to reject them. This leads to an iterative process of modification and improvement. The predictions do not necessarily have to lie in the future (*forecast* mode), since models can also make "predictions" for the past, i.e. when the models are run in *hindcast* mode. Finally, models can also be run in *assimilation* mode, where the model's parameters or its initial or boundary conditions are modified in order to optimally fit a given set of observations.

Physical models of oceanic and atmospheric circulation are used routinely and several mature coupled climate modelling systems exist (e.g. Gent et al. 2012; Roeckner et al. 2006; Collins et al. 2006). Ocean biogeochemical models, obtained by coupling ocean circulation models with mathematical representations of biogeochemical processes, are less mature partly because the quantitative understanding of biogeochemical processes is relatively patchy and mostly empirically-based. This is aggravated by the relative lack of critical biological and chemical observations. As a result, ocean biogeochemical/ecological models differ widely in terms of their complexity (e.g. number of functional plankton groups/state variables) and process parameterisations used (see e.g. Le Quéré et al. 2005). Arguably this is less due to differences in scientific objectives and more to the fact that an

optimal compromise between realism and feasibility has not yet emerged (Anderson 2005). Also, biogeochemical predictions depend on many parameterisations and parameter choices that are not well constrained – a direct reflection of the relative paucity of biogeochemical observations and experiments.

Ocean and atmospheric models are often run independently of each other, where atmospheric model output is used as boundary information for ocean models (e.g. atmospheric temperature, humidity and carbon dioxide concentration) and vice versa. An interactive coupling between ocean and atmosphere is needed when feedbacks are of interest that lead to changes in the oceanic or atmospheric mean state, e.g. in climate models and Earth System models such as those used in the IPCC assessments. Global models are constantly being pushed to finer spatial resolutions. However, for reasons of computational efficiency and convenience models are often run at regional and local scales (as three-dimensional or one-dimensional, vertical models). Regional models allow for higher spatial resolution and more complex representation of biogeochemical processes than global models. They can thus be targeted to better resolve, for example, the scales of open ocean process studies or processes in coastal regions and on continental shelves (e.g. Gruber et al. 2011). These regional models require boundary information either from climatological observations or larger scale models.

Model simulation results are always approximations of reality. They come with uncertainties resulting from inadequacies in process resolution and parameterisations, numerical approximations and imperfections in initial and boundary information. Some of these uncertainties are not well understood or quantified. Data assimilation and inverse modeling, which encompass a variety of statistically based techniques for blending observations and models, are a way to reduce uncertainty in model simulations. Data assimilation has been used routinely for many years in numerical weather prediction for short-term forecasting and, more recently, for ocean models that are run operationally (in forecast mode) or for improving state estimates in hindcasts (e.g. Wunsch and Heimbach 2007; Brasseur et al. 2009).

For model development and validation in general and data assimilation and inverse modeling in particular, the availability of high-quality observations is essential. For example, the Argo array has led to remarkable improvements in our ability to characterise the physical state of the ocean (see Sect. 5.1.1.1). Expansion of this initiative aimed at including chemical and bio-optical measurements will likely lead to tremendous improvements in our ability to characterise the biogeochemical state of the ocean (Johnson et al. 2009; Brasseur et al. 2009).

Perhaps the most pressing modeling challenge is to provide estimates of how the mean physical and biogeochemical state of ocean and atmosphere and variations around this mean will change in the future on time scales of a century or longer. Such simulations are referred to as projections. An obvious difficulty is that these future states are outside the envelope of historical observations against which models can be validated. One strategy is to run climate models for periods in the geological past, where some information is available from palaeo-oceanographic proxies, although this solution is imperfect in that no direct and well-understood analogue to the future exists and that palaeo-proxies provide only an incomplete characterisation of the coupled ocean–atmosphere system. In IPCC assessments, attempts are made to address uncertainty in future projections by using multi-model ensembles. Experience has shown that the means of such ensembles frequently perform better than any single model (e.g. Tebaldi and Knutti 2007).

In summary, modeling is an integral part of SOLAS science. Different modeling approaches and techniques are used for different purposes depending on the scientific objective. Key examples are given in the following sections.

5.1.3.1 Global Perspective, Prognostic IPCC and Hindcast

Over the past two centuries, the ocean has taken up about 30 % of total anthropogenic CO_2 emissions, which include the emissions from the burning of fossil fuel and from land use change (Sabine et al. 2004). Although this uptake came at the cost of ocean acidification, it helped considerably to mitigate the accumulation of this anthropogenic CO_2 in the atmosphere. It is thus of great importance to determine whether the ocean will continue to provide this service to mankind, or whether feedbacks between global climate change and the ocean carbon cycle will reduce the uptake of CO_2 from the atmosphere (Sarmiento et al. 1998; Joos et al. 1999; Gruber et al. 2004). Increases in ocean

stratification and marine oxygen levels can also lead to the enhanced production of marine N_2O, which would further accelerate global warming (see Chap. 3).

Global prognostic models are the only means to provide answers to such questions. In order to assess all aspects of such climate-ocean-biogeochemical feedbacks, coupled Earth system models need to be employed. In such models, all components of the system, i.e. atmosphere, ocean, land surface and sea-ice are fully prognostic, and include not only descriptions of how energy, momentum, and water are cycled between these reservoirs, but also how carbon and other important biogeochemical constituents, such as nitrogen, are transported and transformed. In the last 10 years, several such models have been developed, and they have formed an important contribution to the 4th assessment report of IPCC (Denman et al. 2007). Such models are typically forced with a prescribed set of CO_2 emission scenarios, and the model itself then determines what fraction of the emitted CO_2 stays in the atmosphere, and what amount of warming corresponds to the resulting increase in this greenhouse gas (Friedlingstein et al. 2006).

Roy et al. (2011) recently conducted an intercomparison of four such Earth system models and investigated how the net ocean CO_2 uptake was altered in response to increases in atmospheric CO_2 and global warming. Specifically, a linear sensitivity analysis was performed, where they represented the net oceanic CO_2 uptake as a sum of a CO_2-driven part, and of a temperature-driven part, i.e.,

$$\mathrm{Int}\left(F_{as}{}^{net}\right) dt = \gamma^* \Delta T + \beta^* \Delta CO_2$$

where $F_{as}{}^{net}$ is the net ocean CO_2 uptake, ΔT is the change in global mean temperature and ΔCO_2 is the change in atmospheric CO_2, and where γ is the temperature sensitivity and β that for CO_2 (Friedlingstein et al. 2006). Figure 5.14 reveals that all values of β are negative, i.e. that the oceanic CO_2 uptake increases as atmospheric CO_2 increases. Small differences in the responses are related to differences in the buffer factor and differences in the age structure of the water that resides at the surface (Gruber et al. 2009; Roy et al. 2011). Regions where waters upwell that have not been in contact with the atmosphere for several decades and more have a large relative deficit with regard to anthropogenic CO_2 and hence have a high tendency to take it up from the atmosphere. Figure 5.14 also shows that most regions have a positive γ, i.e. that climate change decreases the uptake of atmospheric CO_2. An important exception are the high-latitude oceans, especially the Southern Ocean and the Arctic, where global warming tends to increase the uptake. These differential patterns are a result of the complex interactions occurring between ocean physics (primarily warming and vertical stratification) and ocean biology working primarily on the natural carbon cycle. Although these results represent multi-model means, the robustness of the details in these results is not yet well established. Nevertheless, the general tendency is clear. Climate change will tend to make the ocean carbon sink weaker (Gruber et al. 2004; Denman et al. 2007).

5.1.3.2 Regional Perspectives from High-Resolution Modeling

A disproportionate fraction of the air-sea fluxes of climatically relevant gases (e.g. CO_2, N_2O) is thought to occur in coastal and continental shelf regions even though they cover only about 7 % of the global ocean surface area. However, processes on continental shelves are not well described by global and basin-wide models, primarily because these models do not resolve the smaller scales relevant for shelf and coastal processes. Instead high-resolution regional models are nested within larger scale, state-of-the-art operational models such as MERCATOR (Bahurel et al. 2006) and HYCOM (Chassignet et al. 2007) and are used to quantify air-sea fluxes in these regions and to improve our understanding of the underlying mechanisms. For example, drivers of air-sea CO_2 fluxes for the wide, passive-margin shelves of the western North Atlantic were studied by Fennel et al. (2008), Fennel and Wilkin (2009) and Previdi et al. (2009) and for the semi-enclosed North Sea, a marginal sea in the eastern North Atlantic, by Prowe et al. (2009) and Kühn et al. (2010). Lachkar and Gruber (2013) recently investigated the air-sea CO_2 fluxes in the Canary and California Current Systems.

On the western North Atlantic shelves, where exchange between shelf and open ocean waters is restricted by a pronounced shelf-break front, coupling between biogeochemical processes in sediments and in the overlying water column was found to be highly relevant for air-sea fluxes of CO_2 (snapshots of the air-sea gradient in partial pressure are shown in Fig. 5.15). For example, sediment denitrification (the anaerobic remineralisation of organic matter which produces

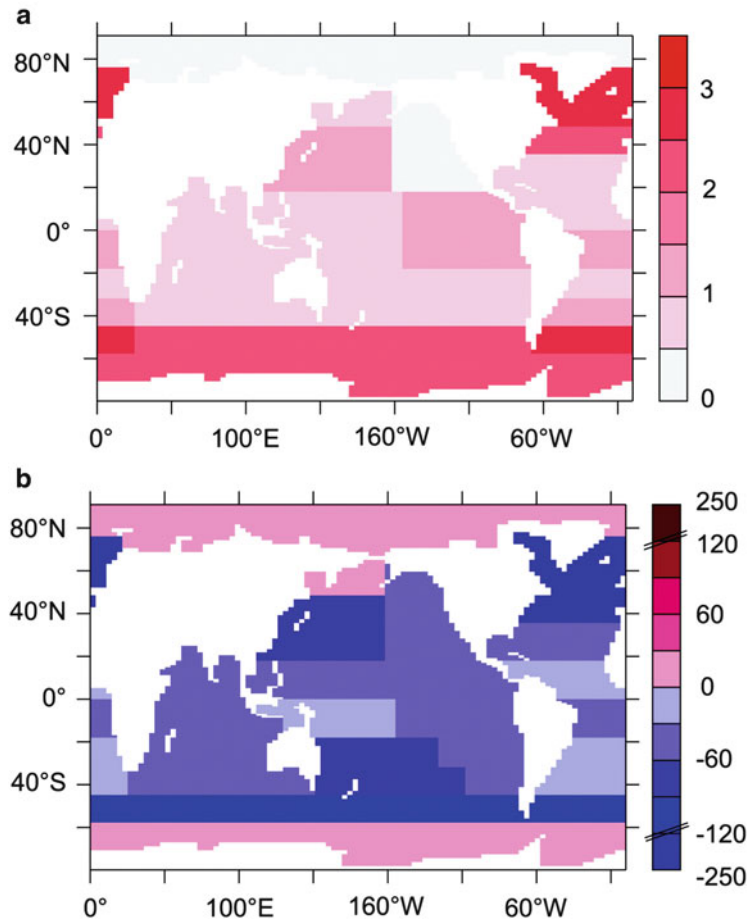

Fig. 5.14 Separation of the regional response of integrated air-sea CO_2 fluxes into a CO_2 (**a**) and a temperature (**b**) driven component. Data are for the period from 2010 until 2100 and represent the multi-model mean (From Roy et al. (2011) © American Meteorological Society. Used with permission)

nitrogen gas, N_2) leads to decreases in primary production and increases in alkalinity, both of which alter air-sea fluxes of CO_2 (Fennel et al. 2008). Furthermore, the restricted exchange of shelf water with the open ocean prevents an efficient export of shelf-generated organic carbon to the deep ocean (Fennel and Wilkin 2009). Previdi et al. (2009) investigated interannual variations in air-sea fluxes of CO_2 and found differences in the Middle Atlantic Bight to be driven mostly by changes in wind stress while differences in the Gulf of Maine were due to changes in sea surface temperature and new production.

In the North Sea, which is seasonally stratified in its northern part and year-round tidally mixed in its southern part, pronounced spatial differences exist in terms of air-sea fluxes of CO_2. In the stratified northern part there appears to be net uptake of CO_2 from the atmosphere driven in large part by biological processes including the overflow production of semi-labile dissolved organic matter in summer. In contrast, the tidally mixed southern part is a weak source of CO_2 to the atmosphere (Prowe et al. 2009). Interannual variability of air-sea CO_2 fluxes in the North Sea appears to be driven by variability in atmospheric forcing and river inputs (Kühn et al. 2010).

Continental shelf regions are heterogeneous with respect to air-sea fluxes and regional differences result from a diversity of characteristics and mechanisms. This makes it hard to scale up from individual regions to global estimates. Since coastal regions are of most direct relevance for human activities and most directly subjected to many human perturbations (e.g. riverine and atmospheric inputs of nitrogen), regional modeling studies will continue to play an important role.

In eastern boundary upwelling regions, the net air-sea CO_2 exchange is governed by a zone of intense outgassing in the nearshore region, and a region of marginal outgassing to actual uptake further offshore,

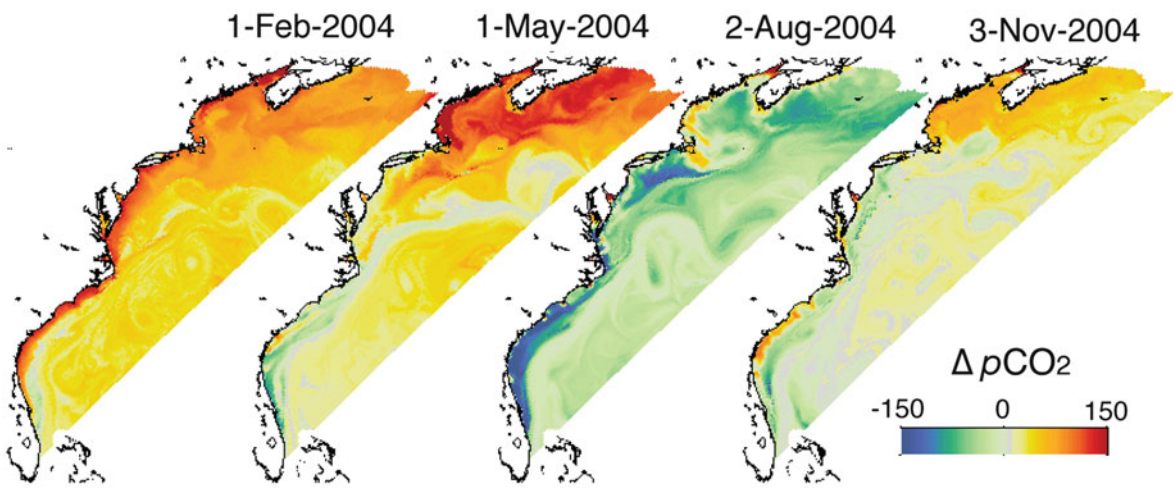

Fig. 5.15 Snapshots of simulated pCO_2 difference between atmosphere and surface ocean (positive values indicate uptake of atmospheric CO_2) for the western North American shelves (Reproduced from Fennel and Wilkin 2009 by permission of the American Geophysical Union)

making the entire region a small sink to a small source (Lachkar and Gruber 2013; Turi et al. 2013). The zone of intense outgassing is a consequence of the nearshore upwelling of waters rich in respired CO_2, creating strongly supersaturated conditions when these waters reach the surface. As these waters are rich in nutrients as well, the upwelling stimulates a strong growth by phytoplankton, creating a strong drawdown of DIC and consequently also of CO_2. Overall there appears to be a balance between upwelling-driven outgassing and biologically driven uptake, with preformed concentrations also playing a role (Hales et al. 2005).

5.1.3.3 Inverse Modelling

The aim of inverse modelling is to estimate the air-sea exchange fluxes of CO_2 (or other trace gases) on the basis of suitable data sets. This requires some model to quantitatively link the measured quantity and the CO_2 fluxes. Then, state variables or parameters of the model can be fit to the data by 'inverse methods'.

A prototypical example uses measurements of tracer abundance within the ocean or the atmosphere, respectively. This 'transport inversion' method is based on the fact that the spatial and temporal patterns of air-sea exchange, being transported and mixed away, lead to spatial gradients and temporal changes in the oceanic/atmospheric tracer field. Air-sea fluxes can thus be estimated from the condition that their corresponding tracer field, as simulated by a numerical or empirical model of oceanic/atmospheric transport, matches as closely as possible the tracer observations. Mathematically, the match is most often quantified by a 'least squares' cost function minimisation.

The oceanic transport inversion was introduced by Gloor et al. (2001) and Gruber et al. (2001). Based on inorganic carbon observations from throughout the ocean, the first set of CO_2 fluxes was estimated by Gloor et al. (2003). As inorganic carbon is not only changed by air-sea exchange but also by marine photosynthesis and remineralisation, nutrient data are needed to remove these biological influences from the data (C* method, based on Redfield ratios between biological carbon and nutrient changes). Moreover, the portion of carbon recently injected into the ocean following the anthropogenic CO_2 rise can be split off from the data (e.g. using the ΔC^* technique, Gruber et al. 1996), allowing separate estimates of natural and anthropogenic air-sea CO_2 exchange.

As oceanic transport proceeds on long time scales, the ocean inversion can estimate the mean spatial pattern of air-sea exchange, but not its seasonal or interannual variability. Results are also affected by errors in the modelled transport, though this can partially be taken into account by considering ensembles of transport models (Mikaloff Fletcher et al. 2006, 2007; Gruber et al. 2009).

The atmospheric transport inversion was pioneered by Bolin and Keeling (1963), and later formalised by

Newsam and Enting (1988). Presently, more than 100 atmospheric measurement stations have been operated by many institutions, providing weekly or even hourly CO_2 mixing ratio time series, some of which extend for several decades. These data have been used to estimate the spatial patterns of CO_2 exchange (e.g. Gurney et al. 2002) or their seasonal and interannual variability (e.g. Bousquet et al. 2000; Rödenbeck et al. 2003; Baker et al. 2006, and many others).

However, the atmospheric CO_2 mixing ratios do not only reflect ocean–atmosphere exchanges, but also terrestrial and anthropogenic fluxes. Due to the diffusive nature of the atmospheric flow, the CO_2 data from the relatively few locations do not provide enough information to fully separate land and ocean fluxes. The dominance of the terrestrial signals in the atmospheric records thus largely obstructs the estimation of ocean–atmosphere exchange. Several studies therefore rely on Bayesian prior estimates of ocean fluxes, most often based on the flux climatology of Takahashi et al. (2009) calculated from measurements of CO_2 partial pressure (pCO_2) and a gas exchange parameterisation. In some cases, Bayesian priors are derived from results of ocean transport inversions; Jacobson et al. (2007) formalised this into a joint ocean–atmosphere inversion. In all these cases, however, air-sea fluxes are mainly constrained by the oceanic data from most of the globe. An exception is the Southern Ocean, where multi-decadal trends in the ocean–atmosphere CO_2 exchange have tentatively been detected from atmospheric data (Le Quéré et al. 2007).

Besides oceanic or atmospheric transport inversions, recent studies use measurements of CO_2 partial pressure (pCO_2) in an inverse context. Valsala and Maksyutov (2010) employed a tracer transport and biogeochemical model, and inversely adjusted the inorganic carbon concentration to match the pCO_2 observations. Ongoing studies involve neural networks, using inverse methods to 'learn' the relationships between pCO_2 and oceanic state variables available from ocean reanalysis projects; these relationships can then be applied to calculate the pCO_2 field at any location and time. Other ongoing studies employ simple diagnostic models of the biogeochemistry in the oceanic mixed layer, estimating ocean-internal carbon sources and sinks.

A common challenge of all these pCO_2-based studies is the need to parameterise air-sea gas exchange, involving substantial uncertainties in its formulation as well as in the driving wind fields (see Chap. 2). This problem may be solved by combining the pCO_2 approach with transport inversions, which do not depend on gas exchange parameterisations.

Further information on air-sea CO_2 fluxes may be obtained from measurements of other tracer species that share source and sink processes. For example, biological processes do not only involve uptake or release of carbon, but also of oxygen. Measurements of the small changes in the atmospheric oxygen content have been used in an atmospheric transport inversion (Rödenbeck et al. 2008) to infer interannual variations in the biogeochemistry of the tropical oceans. Also remote-sensing data offer potential to constrain air-sea CO_2 fluxes. On the one hand, measurements of the atmospheric CO_2 column mixing ratios (see Sect. 5.1.2.6) with much higher spatial density (albeit lower precision) than the surface stations, may allow atmospheric transport inversions to better separate land and ocean fluxes. Satellite observations of ocean surface properties, such as ocean colour (see Sect. 5.1.2.3) reflecting chlorophyll *a* content, can also constrain inverse models of ocean productivity as part of the CO_2 exchange.

5.1.3.4 Conclusions

The scope and ambition of modeling is rapidly expanding. For example, exponentially increasing computational power now permits scientists to simulate global and regional models at ever increasing resolution and over longer periods. The complexity of the models and of their coupling is rapidly increasing as well. While these two developments provide many fascinating new opportunities, they also come with certain risks. Our level of understanding of the results of high-resolution complex models tends to develop less rapidly, creating increasing gaps between our ability to model a system and our ability to fully decipher why a particular model produces a particular result (e.g. Anderson 2005). A second risk is that the observations and experiments that challenge the models are also not increasing as rapidly as the model development is being pushed forward. This requires sustained efforts, also in the interests of the modeling community, to maintain and expand oceanographic observations.

5.1.4 SOLAS/COST Data Synthesis Efforts

The very nature of data collection at sea leads to relatively small-scale cruises of necessarily limited spatial/temporal scope. At an international level, the elevated resource requirements and organisational difficulties associated with large-scale research campaigns further impede coordinated data collection efforts. Considering this, it is unsurprising that oceanic data coverage is fragmentary. As set out within the *Memorandum of Understanding* for COST Action 735 and the aims of SOLAS Project Integration, a major Earth System Science challenge is to translate the findings of these research campaigns into large scale datasets and climatologies that help improve our understanding of global concentrations and air/sea fluxes. Data paucity calls for centralising all concentration measurements of relevant SOLAS parameters into one common database to secure their longevity. The tasks seemed dantean because of two major issues, central to the usability of a database, to be solved as a pre-requisite. One is intercomparing measurements originating from different cruises/instruments/scientists, and another is establishing rigorous quality control and flagging of the data. To get global concentration fields, methods to inter/extrapolate in space and time are used introducing uncertainties in the resulting concentrations. Including the uncertainty in gas exchange velocity parameterisation will yield substantial uncertainties in air/sea flux calculations. Any progress in the future in this velocity parameterisation will allow recomputation of fluxes from the existing global concentrations data sets.

This section presents some specific initiatives carried out within the COST Action 735 and SOLAS Project Integration framework trying to highlight in each case the difficulties encountered, the solutions found and the recommendations proposed.

5.1.4.1 MEMENTO (MarinE MethanE and NiTrous Oxide) Database

The assessments of radiative forcing from long-lived greenhouse gases such as nitrous oxide (N_2O) and methane (CH_4) depend on an accurate synthesis of the global distribution and magnitudes of N_2O and CH_4 sources and sinks (see Chap. 3 of this book). Atmospheric dry mole fractions of N_2O and CH_4 have been routinely available since the late 1970s and they benefit from a highly coordinated global monitoring network (see e.g. Prinn et al. 2000). In stark contrast, although measurements of marine N_2O and CH_4 date back over almost four decades, they lack the temporal continuity and spatial coverage of their atmospheric counterparts. This is because almost all of them relate to single cruises or at best coordinated cruise programmes of rather limited scope. In large part this reflects the high costs and organisational difficulties of mounting large coordinated oceanographic expeditions, especially at the international level. Not surprisingly, oceanic data coverage remains fragmentary.

Seasonal and interannual variability, spatial heterogeneity in coastal areas and gradients between coastal and open ocean areas all impact the quality of marine emission estimates for N_2O and CH_4, compounded by the limited overall data coverage (Bange et al. 2009). A cost effective way of using all existing N_2O and CH_4 measurements, despite the data limitations, is to establish a global database to improve the value of marine emissions estimates. To this end the MEMENTO (MarinE MethanE and NiTrous Oxide) database has been launched as a joint initiative between SOLAS and COST Action 735. MEMENTO's major aims are to:

- Collect available N_2O and CH_4 data (i.e. underway and depth profile data) from the global ocean including coastal areas. To date 129,012 N_2O and 21,003 CH_4 measurements have been collated;
- Archive the data in a database with open access for the scientific community;
- Compute global fields of dissolved N_2O/CH_4 concentrations as well as air-sea fluxes in both the open and coastal ocean, and;
- Publish the database and the derived flux data.

Once all existing datasets have been incorporated into MEMENTO it will rapidly become a valuable tool for identifying regions of the world ocean that should be targeted in future work to improve the quality of the emissions estimates. The locations of the data archived so far in MEMENTO are shown in Fig. 5.16. Further information on MEMENTO can be obtained from https://memento.ifm-geomar.de/.

5.1.4.2 HalOcAt (Halocarbons in the Ocean and Atmosphere)

Compilation of existing air and seawater measurements of halogenated hydrocarbons into the project HalOcAt (https://halocat.geomar.de/) was

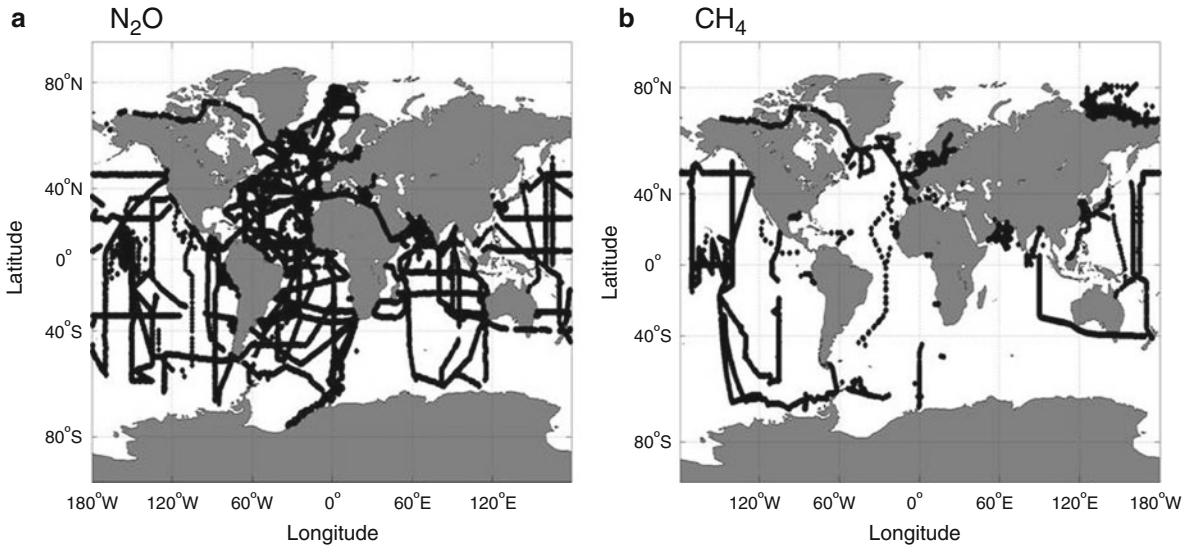

Fig. 5.16 Locations of N_2O (**a**) and CH_4 (**b**) measurements archived in MEMENTO (Version as of October 2012)

initiated through SOLAS/COST Action 735 in May 2009 and is still ongoing. Global oceanic and atmospheric halocarbon data with an emphasis on short-lived brominated and iodinated trace gases from the surface ocean and lower atmosphere have been collated in order to obtain concentration fields and air-sea fluxes. At the time of writing, the database contains 191 contributions, comprising roughly 55,400 oceanic and 476,000 atmospheric data points from depth profiles in the surface ocean and a range of heights in the lower atmosphere. Although predominantly bromoform measurements, these data represent 19 different halocarbon compounds and were collected between 1989 and 2011 during research cruises, aircraft missions and coastal studies from all over the globe. The database stems from active submission of data, literature review and publicly available data.

Quality checks as well as precision and error estimates were often missing from the contributions, coinciding with a large range in reported concentrations. Based on the current available scientific knowledge it is unfortunately not possible to retrospectively identify which data is 'correct' or 'incorrect'. Especially for oceanic data, recalibration is highly unlikely and the database is too small to perform a statistical evaluation of the data quality or to take advantage of utilising datasets that physically crossed paths for inter-calibration. There is some hope that it might be possible to check the consistency of atmospheric data from time series stations, and the community is already assessing inter-calibrations for some compounds (Jones et al. 2011). This information will be incorporated into the HalOcAt data analysis.

In spite of the challenges described above and the paucity of data on a global scale it has been possible to construct meaningful global concentration fields on a $1° \times 1°$ grid. Data interpolation, statistical regression, analysis of published distributions and information about coastal and biological sources including relation to physical and biogeochemical constraints has enabled the calculation of plausible compound distributions (Ziska et al. 2013). From these data, global climatological air-sea fluxes have been calculated for certain halocarbons such as $CHBr_3$ (see Fig. 5.17) and these fall within the published ranges of top down and bottom up emission approaches (Montzka and Reimann 2011). This novel data set now facilitates the use of more realistic data based emission fields to drive atmospheric chemistry models and enables the community to revise current emission scenarios.

Future work on and with the database will focus on its further enlargement, quality control and publication of the data products (database and climatologies of concentrations and ocean/atmosphere exchange). Although simple correlations between oceanic halocarbon concentrations and biological, physical and chemical parameters have not yielded noteworthy

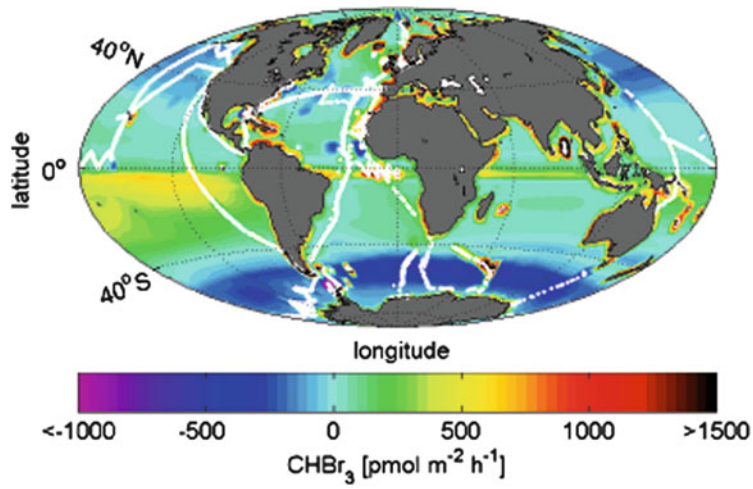

Fig. 5.17 Global air-sea flux climatology of bromoform in pmol m^{-2} h^{-1} including surface oceanic bromoform data points (*white points*) extracted from the HalOcAt database

results to date, the construction and evaluation of proxies and parameterisations for concentrations and fluxes will continue to be explored.

5.1.4.3 DMS-GO (DMS in the Global Ocean)

In 1999 Jamie Kettle and Meinrat Andreae (Kettle et al. 1999) initiated a collation of available seawater DMS measurements into a global database and subsequently created a climatology of surface ocean concentrations based on the data available. However, this important contribution to the literature (over 285 citations to date) was limited by the number of data points (15,617) of surface seawater DMS concentration and the large areas of the global ocean that lacked data, requiring crude estimates to be made. In the years since, many more DMS measurements have been made and in 2010 the DMS-GO (DMS in the Global Ocean) team initiated a call to update the database and climatology. In April 2010 the DMS database had grown to approximately 47,000 data points (Fig. 5.18), and these were used to construct an updated surface ocean DMS concentration climatology.

The construction of the climatology involved data mapping, extrapolation and interpolation onto biogeochemical provinces, smoothing, and data re-assimilation (see Lana et al. 2011 for details). The first step was the transformation of DMS concentration data into a mean value using a delineation of $1^\circ \times 1^\circ$ grid squares. The second step was also based exclusively on the DMS measurements – a background DMS field was created using biogeochemical ocean provinces (Longhurst 2007), which have been defined using spatial similarities in the chemistry, physics and biology of the world ocean. The background field was created for each province for each month using an average DMS concentration. If there was a temporal paucity of data, the gaps were filled by applying an interpolation to the time series of the province, or in some cases by substituting with a scaled pattern of another province with similar biogeochemical characteristics. After these two steps, the construction of the climatology was based on the combination of $1^\circ \times 1^\circ$ pixels and the background field. The new DMS climatology along with an estimate of the uncertainty (upper and lower concentration bounds) is available online for free download on the SOLAS-BODC server (http://www.bodc.ac.uk/solas_integration/implementation_products/group1/dms/).

The global sea-to-air DMS flux estimate (between 17.6 and 34.4 Tg S $year^{-1}$) using the new climatology has improved understanding of ocean–atmosphere DMS emissions in the global sulphur cycle and suggests an approximate 17 % increase in flux c.f. the previous climatology, mainly due to the inclusion of data from new areas of the ocean (e.g. the Indian Ocean). The updated distribution of global DMS measurements and the new DMS climatology will be useful for the validation of future ocean biogeochemical models. In addition, the continuous climatological surface ocean DMS field will likely be used as an input variable for atmospheric chemistry models. However, the updated DMS database has also highlighted areas of the global ocean that require more measurements and this is powerful information in the context of recent developments in automatic and semi-automatic DMS analysis systems. As new

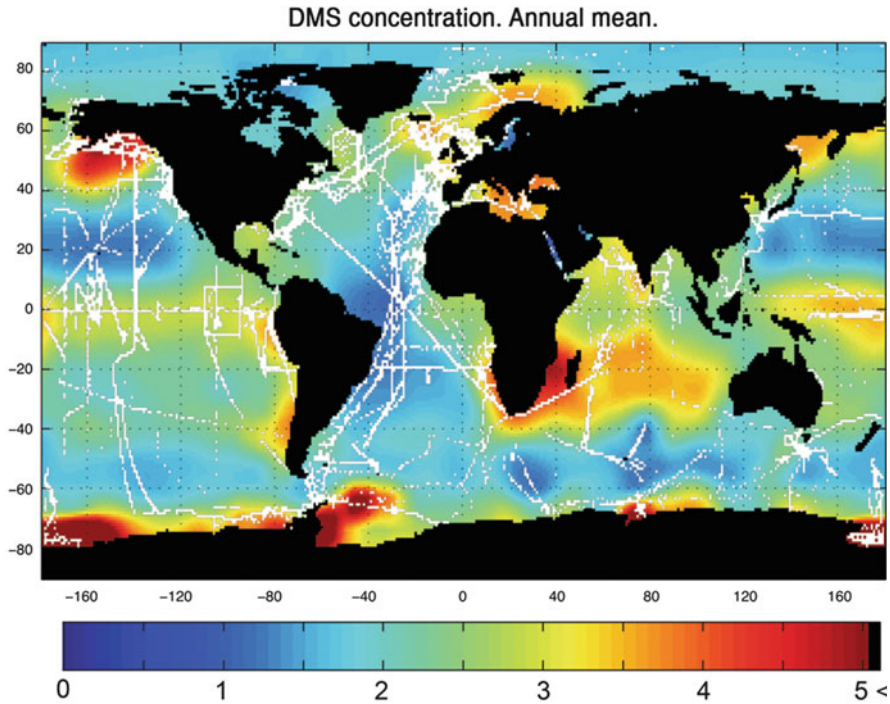

Fig. 5.18 Locations of global surface ocean DMS measurements (approx. 47,000 as of April 2010) for all months of the year (*white*) plotted over the mean climatological DMS concentration (in nM) from the same data (Data is available for download at http://saga.pmel.noaa.gov/dms/)

techniques become more widely-used the challenge will be ensuring data inter-comparability as the database swells in size (see Bell et al. 2011).

5.1.4.4 The Surface Ocean CO_2 ATlas (SOCAT)

The Surface Ocean CO_2 ATlas (SOCAT) is a global synthesis of surface ocean carbon dioxide (CO_2) measurements collected on research vessels, voluntary observing ships and moored as well as drifting platforms (http://www.socat.info/). The first public release of SOCAT (version 1.5) took place at UNESCO in September 2011. Version 1.5 consists of 6.3 million quality controlled, uniform format and recalculated surface water fCO_2 (fugacity of CO_2) data from 1851 voyages in the global ocean between 1968 and 2007 (Fig. 5.19).

SOCAT was initiated at the Surface Ocean CO_2 Variability and Vulnerabilities (SOCOVV) workshop in 2007 (IOCCP 2007). At that time surface ocean CO_2 data were archived in a wide range of formats and at numerous sites around the world, each with its own rules for access, and documentation of the data was frequently poor. This made it virtually impossible to generate comprehensive data synthesis products for large scale or long-term studies. To alleviate this situation the international ocean carbon community decided to initiate the Surface Ocean CO_2 Atlas as a community driven effort to assemble, harmonise, quality control and document the surface ocean CO_2 data into one open access database. While the outlook of the SOCAT products in version 1.5 has closely followed this original vision, as documented in the 2007 meeting report, the community underestimated the amount of work involved in the first release of SOCAT. It took 4 years of hard work by marine carbon scientists around the world to assemble and quality control the first version of SOCAT.

Two SOCAT products are available:

1. A global data set of recalculated surface water fCO_2 values in a uniform format, which has undergone 2nd level quality control;
2. A global, gridded product of monthly mean surface water fCO_2, with no temporal or spatial interpolation.

The above SOCAT products can be accessed at the Carbon Dioxide Information Analysis Center (CDIAC, http://cdiac.ornl.gov/oceans/) on a global and basin wide level. In addition to the concatenated data, products are all recalculated and available at the ICSU World Data Centre PANGAEA – Data Publisher for Earth & Environmental Science (http://www.pangaea.de/) as individual cruise files. Those files

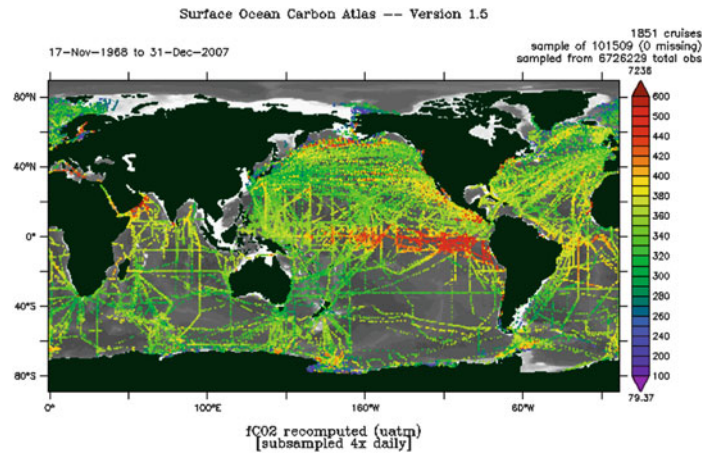

Fig. 5.19 Spatial distribution of recalculated fCO_2 measurements of SOCAT Version 1.5 (Courtesy of NOAA/PMEL), http://www.socat.info/

are in a uniform format and give access to the detailed metadata, input data and recalculated fCO_2 values. SOCAT tools include an online data visualisation and analysis tool (PMEL's Live Access Server) and desktop tools like an Ocean Data View Collection. All can be accessed via http://www.socat.info/.

The methods in SOCAT are fully documented (Pfeil et al. 2013; Sabine et al. 2013). The products and individual cruises are citable through Digital Object Identifiers (DOI-s). Cruises in SOCAT have an Expocode (a code containing Cruise ID, Year, Month and Day of Cruise), a DOI and detailed information on the data, so-called metadata (e.g. investigator name, vessel, methods, calibrations). Every data point in SOCAT has a link to its cruise file as archived at PANGAEA via the DOI string in the data file.

Preparations for the second version of SOCAT are underway. Regular releases of SOCAT are planned, e.g. every 1–2 years from the 3rd release onwards. Data can be submitted to CDIAC (http://cdiac.ornl.gov/oceans/submit.html) for inclusion in future SOCAT releases. Prompt data and metadata submission as well as citation of SOCAT in publications are deemed essential for the future existence of SOCAT. Automation of data and metadata submission and quality control as well as inclusion of additional variables (e.g. atmospheric CO_2 and calculated fCO_2 from discrete measurements) is currently being discussed.

SOCAT meets the needs of the global carbon community by making high quality surface water fCO_2 data available for addressing major scientific questions in the field of global change. The large number of visitors to the SOCAT website (> 1,000 hits/month) demonstrates the intense interest in these carbon synthesis products. It is anticipated that SOCAT will be used in high profile scientific analyses informing policy decisions by governments and intergovernmental organisations. We kindly ask colleagues to inform SOCAT (submit@socat.info) of recommendations for and publications that use SOCAT data products. Updates on SOCAT will be posted on http://www.socat.info/.

5.1.4.5 Aerosol and Rainwater Chemistry Database

The development of the aerosol and rainwater chemistry database is motivated by the desire to provide a repository for datasets collected from ships at sea because there had previously been no facility for collecting such data, while databases for land-based measurements are already well established (e.g. the World Data Centre for Aerosols; http://wdca.jrc.it/data/parameters/data_chem.html). The database has a deliberately broad focus in terms of the chemical species accepted, with nutrients, trace metals and organics being primary targets, but other data equally welcome. So, for instance, iron data may be a key interest for the database, but submitters of iron data are encouraged to also supply any other chemical data associated with those measurements. This ancillary data may be of use to the iron community as well as in other, unrelated research fields.

Data has been collated at BODC since 2007 and a data portal was added to the site in 2011 (http://www.bodc.ac.uk/solas_integration/implementation_products/group1/aerosol_rain/). At the time of writing the database has ~ 1,300 aerosol and ~ 80 rainfall data points, most directly downloadable from the website

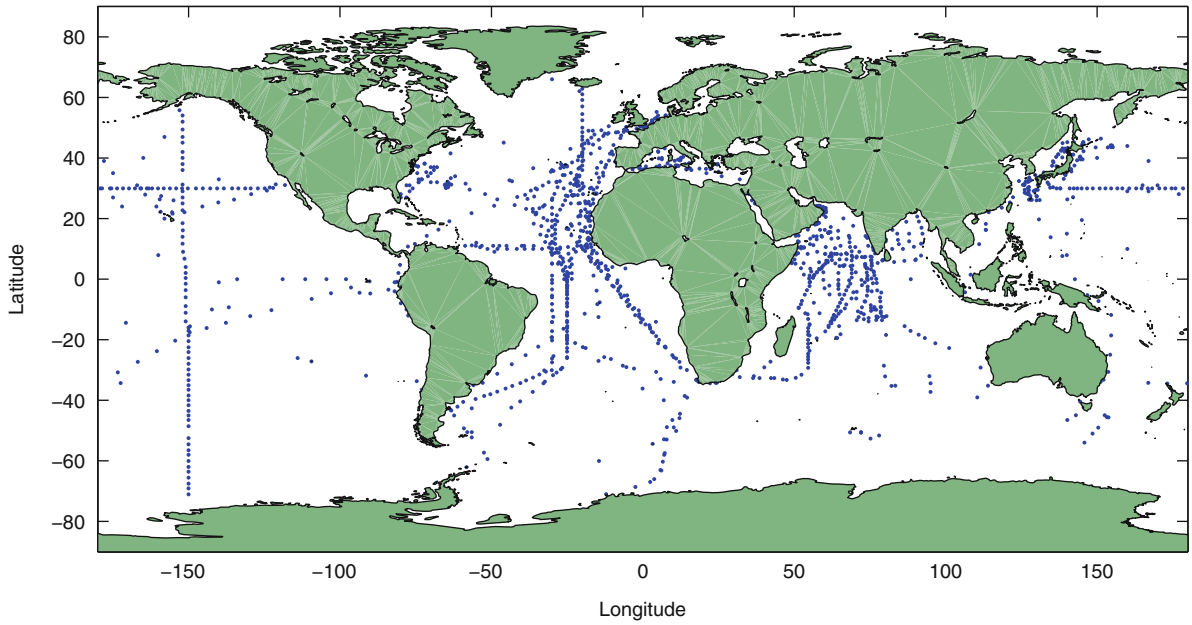

Fig. 5.20 Distribution of aerosol sample locations contained in the database as of November 2011

(Fig. 5.20). The site also contains links to other on-line databases holding related data and seven datasets of aerosol chemistry obtained from island sites which are not housed in any other publicly available database.

Baker et al.'s study (2010) is a good example of the potential benefits attainable from large ship-based datasets. Aerosol and rain data obtained during 12 cruises was used to estimate atmospheric nitrogen inputs to the Atlantic Ocean. This was achieved partly through a process of classifying the aerosol samples in their database according to which source regions they had recently passed over, and marrying these classifications, and their chemical characteristics, to an air mass climatology for the Atlantic basin. The applicability of this approach is strongly determined by the availability of data, and its spatial and seasonal distribution, as well as the seasonal variation in atmospheric source strength. For example, a subtly different approach has been required for recent attempts to estimate atmospheric iron inputs to the Atlantic (Powell et al. in preparation).

To date, the COST Action 735 database contains only chemical and very limited metadata such as sample positions, but no other potentially valuable resources such as air mass back trajectories. All of the studies discussed above used data obtained from only one research group. Similar efforts using data from multiple sources will encounter problems associated with lack of inter-comparability, particularly in 'historical' datasets. The marine aerosol community is only just starting to address these problems through an inter-comparison exercise led by the GEOTRACES programme, with active participation from within SOLAS (see http://www.geotraces.org/ for more information).

5.1.4.6 A Data Compilation of Iron Addition Experiments

In the last 3 years datasets from ten mesoscale iron enrichment experiments have been brought together through a SCOR working group (WG 131) entitled 'The Legacy of mesoscale ocean enrichment experiments'. This data collation has then been transformed into a relational database (the *Iron Synthesis Database*) by the database management team (Cyndy Chandler & Steve Gegg at BCO-DMO) based at Woods Hole Oceanographic Institution (WHOI) in the USA (http://bcodmo.org/data). The database has been structured using project and data directories, metadata, the status of data rescue for each project, and tools that are available to discover and download data of interest (see Fig. 5.21).

Datasets from the following experiments reside at the BCO-DMO site: IronEX I, IronEX II,

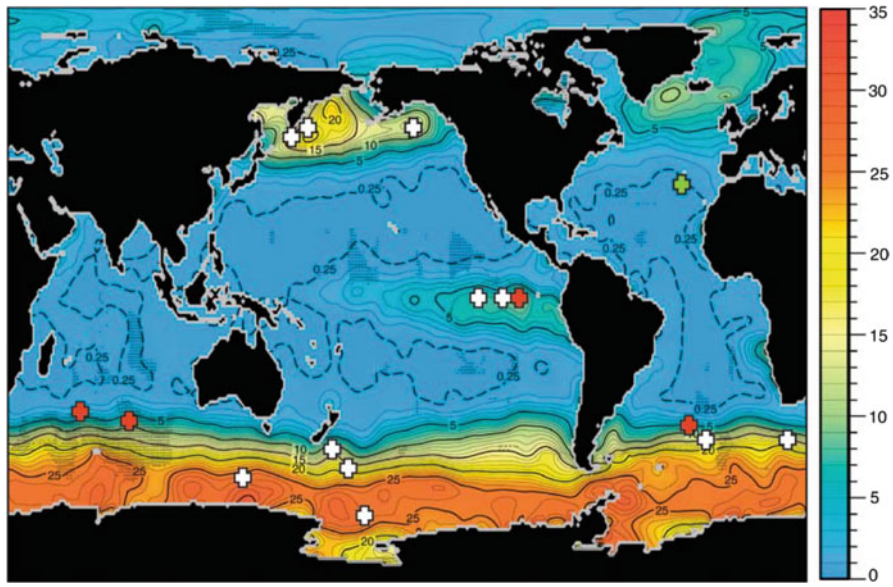

Fig. 5.21 Annual surface mixed-layer nitrate concentrations in units of μmol liter^{-1} with approximate site locations of iron addition experiments. Fe addition experiments: *white crosses*, Fe natural enrichment experiments: *red crosses*, and joint Fe and P enrichment study of the subtropical LNLC Atlantic Ocean: *green cross* (Figure reproduced with kind permission from *Science*. See Boyd et al (2007) for full details)

SOIREE, SAGE, SEEDS, SEEDS II, SOFEX North, SOFEX South and SERIES. The dataset from the Eisenex Southern Ocean study is held at the German PANGEA database (http://www.pangaea.de/). No comprehensive datasets are presently available from the EifEX Southern Ocean experiment, although some papers have been published (e.g. Hoffmann et al. 2006). The datasets within the relational database consist of physical (e.g. mixed layer depth), chemical (e.g. dissolved iron concentrations), biological (e.g. net primary production rates), optical (e.g. incident irradiance) and in some cases meteorological (e.g. wind speed) parameters.

The ten experiments all straddle High Nitrate Low Chlorophyll (HNLC) regions from polar to tropical HNLC waters and hence provide a robust test for modeling studies and comprehensive details for synthetic studies. For example, datasets concerning the production of DMSP and its subsequent transformation to DMS are available for multiple experiments including SOIREE and SERIES. Such datasets can be readily related to a wide range of environmental properties such as mixed layer depth, incident irradiance, and microbial rate processes. The interplay of these factors has been proposed as important in setting DMS concentrations following iron enrichment (Le Clainche et al. 2006). Data are also available concerning changes in the concentration of other biogenic gases following iron enrichment, and in some cases their efflux and fate.

The main challenge in setting up this relational database was obtaining datasets from some of the first in situ experiments – such as IronEX I and II – and from some of the more recent experiments. In the case of the early studies from almost two decades ago, some of the data was on very old laptops. Alternatively, for the most recent experiments, manuscripts are still being written and published and at this point there was an understandable reluctance to contribute to the public domain.

So what is the future for large-scale Fe addition experiments and what else would we really wish to better understand? Some scientists have called for larger experiments (100 km length scale) to overcome some of the artefacts such as dilution with surrounding HNLC waters, but these bring enormous logistical challenges with them. In the conventional 10 km length scale experiments conducted so far, it takes one ship 24 h to add the iron and SF_6 (tracer) to the 100 km^2 area of ocean in a manner that results in a coherent patch of tracer/iron. So how many ships would be required to enrich 10,000 km^2? Using planes to 'top-dress' the ocean would be equally problematic (Boyd 2008). The most promising research areas for the future are the study of naturally high iron regions where phytoplankton blooms occur, such as around the Crozet Islands in the Southern Ocean, and conducting medium scale in situ enrichments, or using mesocosms, in the generally quiescent oligotrophic waters of the lower-latitude

ocean to study the environmental controls on different groups of diazotrophs.

5.1.4.7 Conclusions

The initiatives discussed in this section represent the spectrum of integration activity within SOLAS. MEMENTO and the aerosol and rainwater chemistry databases are still in relative infancy, just beginning to collate data. In contrast, the relatively mature DMS database has recently been substantially updated, tripling the number of data points and re-estimating the climatological DMS flux to the atmosphere (Lana et al. 2011). Ultimately, the SOCAT project is leading the field, with a lot of data points collated from the global ocean and well established procedures for treating the data and archiving it in a responsible manner. Its progress and willingness to continue pushing forward the boundaries of data collation and synthesis are admirable. Meanwhile, the synthesis of data and information from the various large-scale iron addition experiments has been invaluable.

Past experience suggests that such data collation exercises often prove their worth many times over, informing the scientific community in ways that were previously unforeseen. For example, the original DMS database attempted to find correlations between in situ concentrations and other ancillary parameters such as chlorophyll *a* (Kettle et al. 1999). Despite a relative lack of success at the time, understanding of the reduced sulphur cycle has benefitted enormously from this database – much of the work carried out *after* the initial data collation period has arguably proven to be much more fruitful. Without attempting to predict the future, a similar scenario appears to exist with the HalOcAt database, with initial examinations of the data suggesting no obvious correlating factors; only time will tell...

What challenges remain for the integration of SOLAS data? Success depends in part on the scope of the project. Based on the projects outlined within this chapter, data collation initiatives must overcome the following issues common to many of the databases:

Community engagement. The number of scientists willing to be a part of any initiative and who actively engage with the process can have a significant impact on the scale of data collation and the degree of community involvement. Engaging the community to deliver to data bases is an extremely time consuming effort which requires strong motivation and determination.

Support for the project. This can take the form of a website, advice on data management and/or project personnel, often data managers. Existing projects that have had resources for a data manager have benefitted enormously from this. Data management should be an intrinsic part of any project.

Approaches to data paucity. Whether extrapolating to biogeochemical provinces (e.g. DMS-GO), performing deep ocean cross over checks (e.g. SOCAT) or using aerosol chemical composition data to characterise different air masses within an Atlantic-scale dataset, these techniques are very important for 'filling' data gaps and estimating global fluxes. The techniques need to be adequately described stating clearly the assumptions being made and resulting uncertainties.

Data intercomparability. Arguably, this is one of *the* major challenges facing many datasets within SOLAS science. Collating a large-scale dataset is almost useless if the data are subsequently shown to be incomparable. An obvious way forward is to carry out regularly, at the international level, measurement intercalibration exercises. Some work has begun on the halocarbons (e.g. Butler et al. 2010; Jones et al. 2011) and for DMS (Bell et al. 2011), while GEOTRACES has plans to address this important issue for trace metal aerosol and rainwater chemical composition. SOCAT in particular has spent a lot of time on such issues, and it was noteworthy that in their 2007 meeting report the community recognised that they had probably underestimated the amount of work involved for the first release of SOCAT.

Data legacy. Managing large data sets is a challenging task. It takes dedicated efforts to set up efficient online processed data delivery (e.g. metadata added and formatted in an internationally recognised format), to mount them on an open access portal, to provide archiving and data enhancement (e.g. post processing, climatology enhancement), and to provide a data portal for archived data. International and national data centres should be the natural repositories to ensure long-term security of our community efforts.

The success of SOLAS Integration and the production of global databases depends on a concerted effort from the international atmospheric and marine science communities to not only collect data through extensive

field campaigns, but also to engage with and support projects such as those outlined above.

5.2 Examples of SOLAS Integrative Studies

This section of the chapter offers a selection of SOLAS integrative studies. Integration implies a synergistic use of cross-cutting tools and eclectic data in both the atmosphere and ocean to address specific SOLAS science questions. These studies all contribute to an improved understanding of biogeochemical cycling, the establishment of present-day climatologies or the closure of global budgets.

5.2.1 DMS Ocean Climatology and DMS Marine Modelling

5.2.1.1 Global Climatologies Based on Observations

The need for a global climatology of DMS sea-surface concentrations was identified more than a decade ago. The first global database of DMS measurements was put together by Kettle et al. (1999) and Kettle and Andreae (2000). At the time, the database compiled of the order of 15,000 data points, unevenly distributed in time and space. Since then, the original database has been growing extensively and has now reached more than 45,000 data points (see: http://saga.pmel.noaa.gov/dms/). This on-going extension has been made possible thanks to the scientific community feeding the database with new measurements, but also thanks to the DMS-GO initiative (see Sect. 5.1.4.3) and SOLAS integration (Surface Ocean Lower Atmosphere Study, http://www.bodc.ac.uk/solas_integration/).

As discussed in Sect. 5.1.4.3, Lana et al. (2011) have used this updated database to obtain a new global climatology of sea surface DMS concentrations following a modified interpolation approach to the one used by Kettle et al. (1999) (Fig. 5.22). They obtained a global annual sea-to-air DMS flux, estimated at 28.1 Tg S $year^{-1}$ (17.6–34.4), which represents a global emission increase of 17 % with respect to previous calculations. Regionally, annually-averaged concentrations show rather homogeneous values, most of them between 1 and 5 nM. The characteristics of the seasonal cycle, already shown by Kettle et al. (1999), are mostly confirmed: maximum concentrations (up to 15–20 nM) are obtained in summer at high latitudes, in phase with chlorophyll *a*. Between 40°S and 40°N, however, DMS and chlorophyll *a* do not seem to be in phase, with high summer DMS concentrations associated with low chlorophyll *a* levels, a part of the DMS cycle which has been referred to as the "summer paradox".

5.2.1.2 Diagnostic Approaches: Based on Empirical Correlations

In addition to the climatology described above, several other approaches have been proposed to estimate DMS concentrations (Anderson et al. 2001; Simó and Dachs 2002; Belviso et al. 2004a). These diagnostic approaches are based on empirical relationships between DMS sea-surface concentrations and some other variables (e.g. SST, chl *a*, MLD), derived at a local scale, and then extrapolated to the global scale. Anderson et al. (2001) generated monthly global DMS fields using a relationship between DMS and the product of chlorophyll *a*, light and nutrient concentration. Simó and Dachs (2002) proposed a double-equation algorithm in which chlorophyll *a* and mixed layer depth are used to derive DMS sea-surface concentration. Belviso et al. (2004a) subsequently proposed a non-linear parameterisation to relate DMS concentration to chlorophyll *a* and an index of the community structure of marine phytoplankton.

These approaches offer some additional advantages compared to the use of DMS climatologies solely derived from in situ DMS measurements. They make use of additional information (ocean physics and biogeochemistry) in regions where no DMS measurements are available. They can be used to study the variability in time (e.g. interannual variability) of DMS sea-surface concentrations and emissions if information on ocean physics and biogeochemistry are available. These approaches have been compared in Belviso et al. (2004b) and their use in Earth System Models in the context of anthropogenic climate change has been described in Halloran et al. (2010).

5.2.1.3 Prognostic Modelling: From 1D to 3D

In addition to the diagnostic approaches described above, a number of prognostic DMS models have been developed in the last decade. Contrary to diagnostic approaches, these models include an explicit

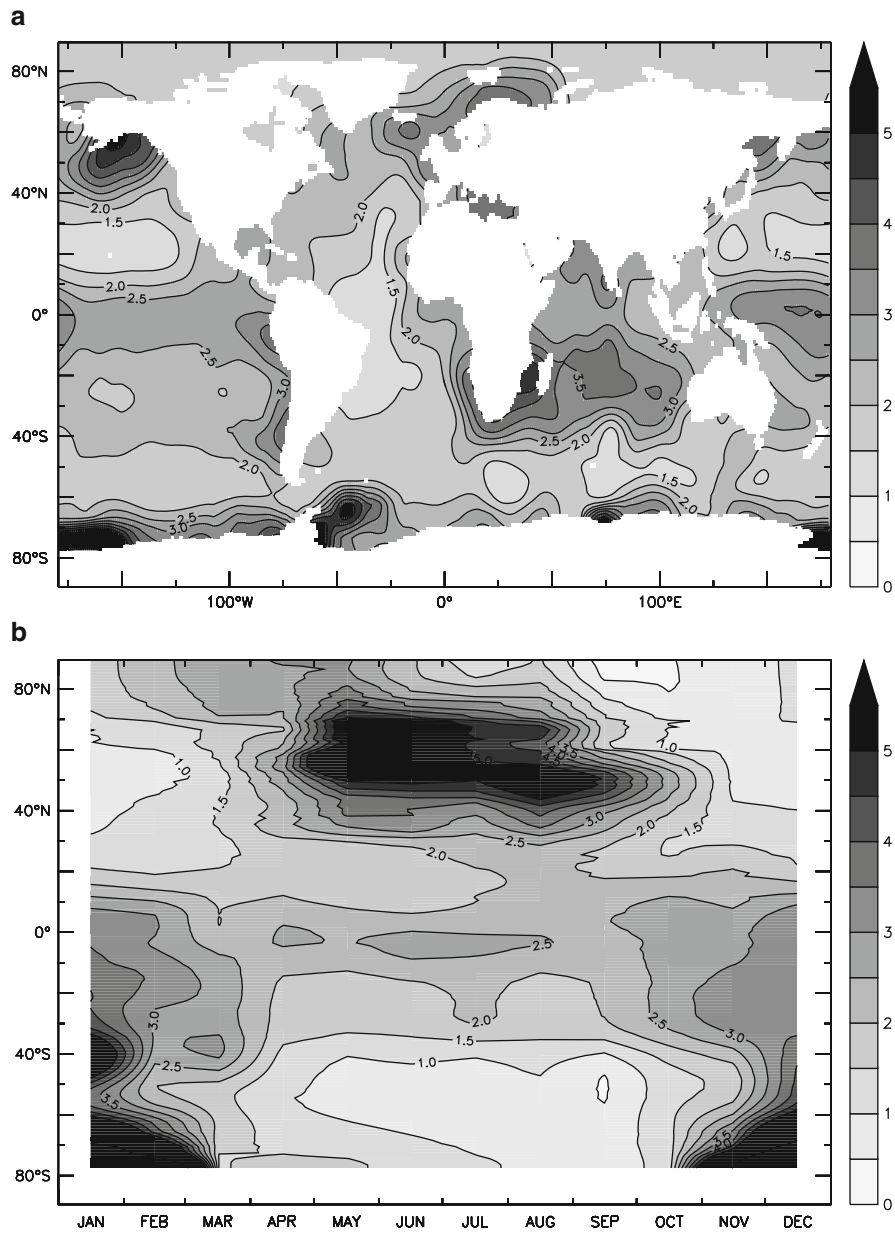

Fig. 5.22 (**a**) Annually-averaged DMS concentrations (nM), and (**b**) latitude-time (Hovmoller) diagram of DMS concentrations (nM) (Modified from Lana et al. (2011))

description of processes leading to DMS production and emission.

These models are coupled to marine biogeochemical models that represent plankton ecosystem dynamics. They have been applied at specific one-dimensional vertical column sites (1-D), but also at the global scale coupled to Ocean General Circulation Models (3-D OGCM).

Le Clainche et al. (2010) conducted a model inter-comparison exercise, CODiM, which stands for Comparison of Ocean Dimethylsulfide Models, in the frame of the SOLAS science plan and implementation strategy. They compared nine process-based models, both local one-dimensional (1-D) or global three-dimensional (3-D). From that comparison, their major point is the divergence among models related to their (in)ability to reproduce the summer peak in DMS concentrations usually observed at low- to mid- latitudes. This deficiency in simulating the summer mismatch between chl

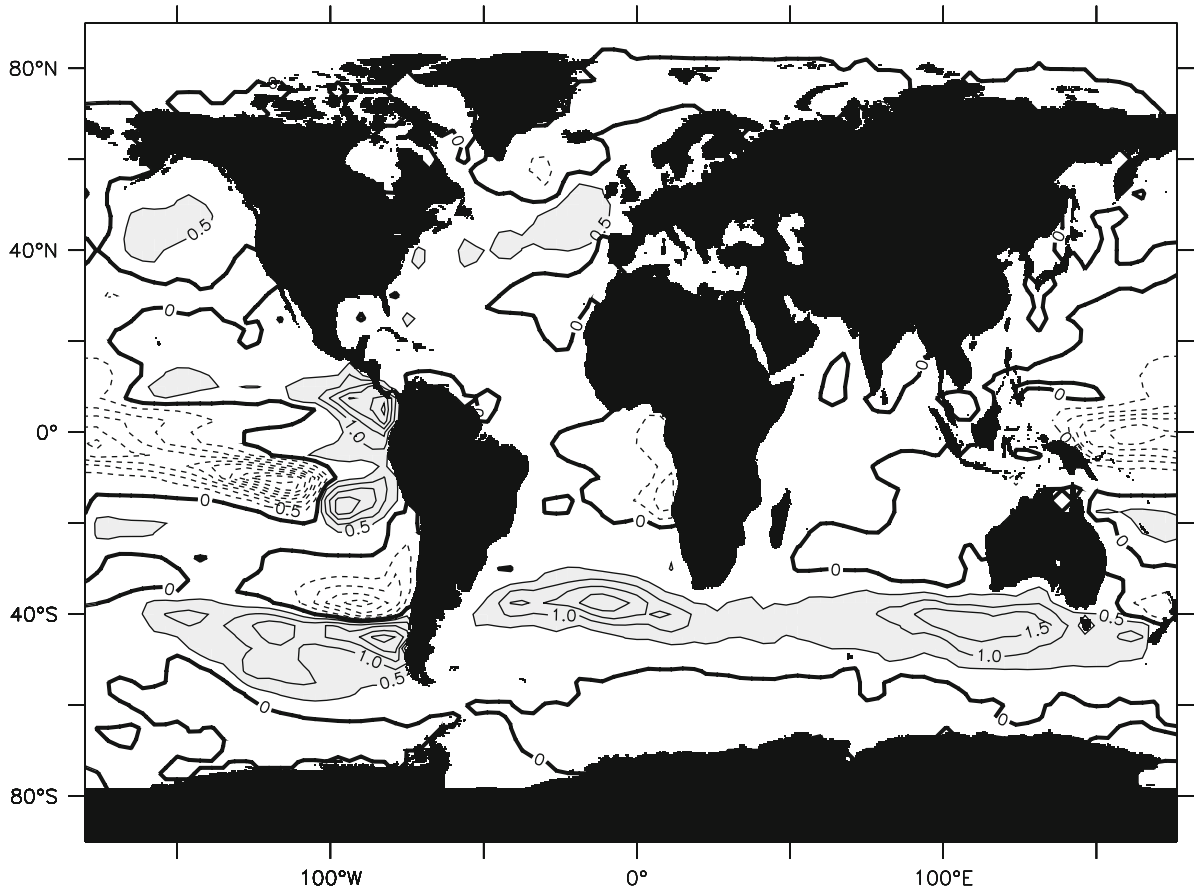

Fig. 5.23 Changes in DMS emissions at 2 × CO_2 (in micromol m^{-2} d^{-1}) as simulated by a coupled climate – ocean DMS model (Adapted from Bopp et al. 2003)

a and DMS at low- to mid-latitudes could have significant implications by reducing simulated global DMS emissions by up to 15 %. They point towards processes related to particulate DMSP production and release as critical pathways not well represented in prognostic DMS models, e.g. increased DMSP synthesis in phytoplankton, increased DMS release from phytoplankton under stress conditions, light-dependent DMSP to DMS conversion by bacteria.

5.2.1.4 Examples of Applications

Climate Change

Several diagnostic (Bopp et al. 2003; Gabric et al. 2004) and prognostic (Kloster et al. 2007) DMS models have been coupled to climate models to predict future DMS emissions and/or sea-surface concentrations. Due to the large variety of approaches used to model DMS emissions, there is still no consensus among the different models, even for the sign of evolution of DMS emissions with anthropogenic climate change: in summary, models tend to simulate either a slight increase or a slight decrease in global DMS emissions in a warming world. Gabric et al. (2004) for example predict an increase of DMS emissions of 14 % for a tripling of pre-industrial atmospheric CO_2. Models agree however in projecting large spatial heterogeneities in future DMS emissions. Bopp et al. (2003) for example predict an increase in the sea-to-air DMS flux of 3 % for doubled atmospheric CO_2 (Fig. 5.23), but with large spatial heterogeneities (up to + 30 % in the Southern mid-latitudes).

Iron Fertilisation

Large increases (of up to 400 %) in DMS concentrations have been documented in some

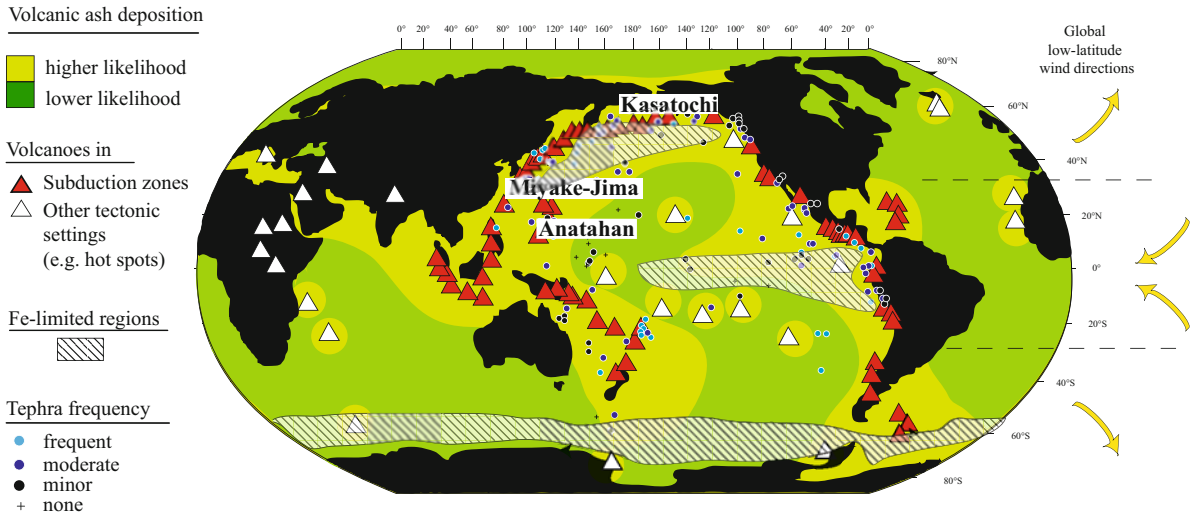

Fig. 5.24 World-map illustrating the distribution of subaerial (Holocene-) active volcanoes indicated as *triangles* (highlighted are the volcanoes cited in the text). Oceanic regions with higher likelihood of volcanic ash deposition are shown as *yellow* regions (Olgun et al. 2011), based on marine sediment core data, the frequency of tephra layers found in the ocean sediments (*coloured circles*) and global wind directions. Volcanic ash deposition can affect marine primary production in much of the Fe-limited areas that are found in the Subarctic Pacific, the Eastern Equatorial Pacific and the Southern Ocean (shown as areas with *oblique lines*)

Southern Ocean artificial iron addition experiments (Turner et al. 2004). These results have been used to suggest that iron fertilisation of the Southern Ocean could act to increase DMS fluxes from the ocean and hence amplify the potential cooling due to increased uptake of carbon (Wingenter et al 2007). Bopp et al. (2008) used a global biogeochemical model including a DMS process-based scheme. They showed that whereas patchy iron fertilisation may stimulate a short-term increase in DMS due to the initial increase in productivity, a long-term and large-scale iron fertilisation could indeed lead to reduced DMS sea-surface concentrations and emissions because of an increase in bacterial consumption rates of DMS.

5.2.2 North Pacific Volcanic Ash and Ecosystem Response

The Pacific Ocean, the largest of the ocean basins, is encircled by a ring of numerous explosive volcanoes (the *Pacific Ring of Fire*) and hosts several hot spot volcanic islands (e.g. Hawaii) (Fig. 5.24). The North Pacific is one of the most active volcanic belts in the Pacific, surrounded by more than 150 active volcanoes in Kamchatka, the Aleutians and mainland Alaska (Fig. 5.24), which create at least ten explosive volcanic eruptions each year (http://www.volcano.si.edu/). Recent geochemical and bio-incubation experiments have shown that volcanic ash rapidly releases sufficient amounts of nutrients into seawater that are potentially bio-available for phytoplankton production and growth (Frogner et al. 2001; Duggen et al. 2007; Jones and Gislason 2008; Hamme et al. 2010; Langmann et al. 2010; Lin et al. 2011; Olgun et al. 2011). Atmospheric impacts of other volcanic products such as the sulphate aerosols are discussed in Sect. 4.2.3.5 of Chap. 4.

The North Pacific, especially the subarctic region, is a high-nutrient, low-chlorophyll (HNLC) ocean region where phytoplankton growth is known to be limited by iron (Martin and Fitzwater 1988; Boyd et al. 1996; Boyd and Harrison 1999) and sporadically by silicate (Wong and Matear 1999; Whitney et al. 2005). Episodic increases of Asian mineral dust input have been observed to increase primary production in the North Pacific (Young et al. 1991). The causal connection between aeolian iron input and diatom production over longer time-scales (e.g. Quaternary) was also indicated by sediment core studies (McDonald and Pedersen 1999). In the North Pacific, volcanic ash is one of the major iron sources, due to the high flux of ash

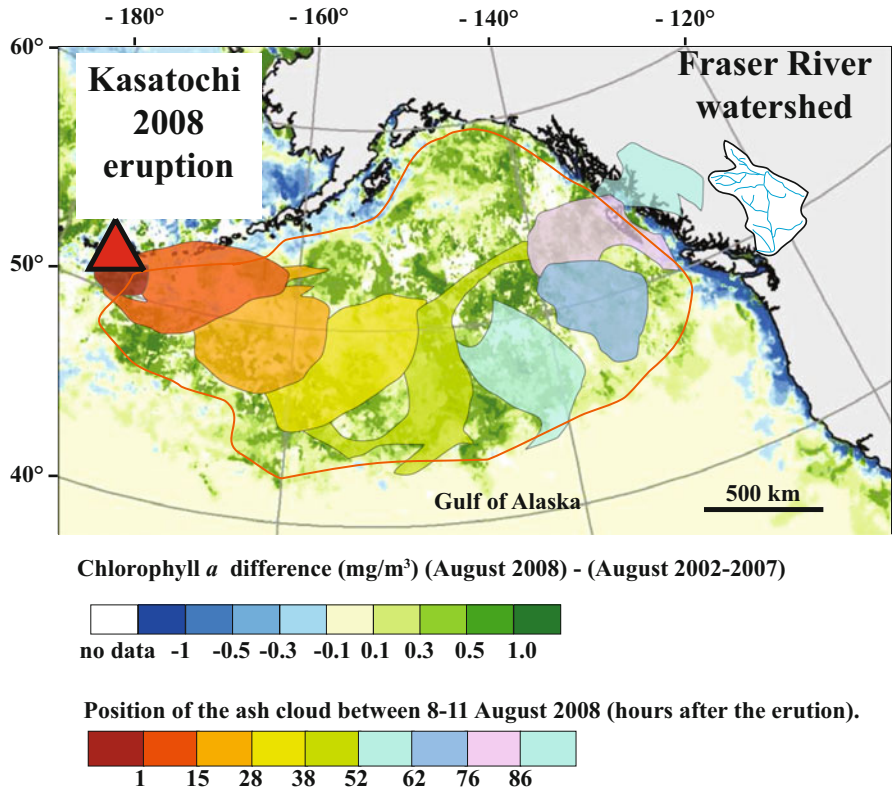

Fig. 5.25 MODIS-Aqua image showing the diatom bloom that has been related to the volcanic ash-fall during the Kasatochi eruption on 7th and 8th of August 2008, with the volcanic ash plume that has been transported over the Gulf of Alaska (*coloured areas* show the position of the plume) (Langmann et al. 2010). The relative increases in chlorophyll *a* concentrations in August 2008 are based on monthly mean August 2008 minus the monthly mean in the years between August 2002 and 2007 (Langmann et al. 2010). Also shown is the location of the Fraser River watershed area related to the discussion of increased salmon populations that are likely to have been positively affected by ocean fertilisation by the Kasatochi eruption during summer 2008

released by active volcanism in the region (Olgun et al. 2011). Deposition of volcanic ash during explosive eruptions can therefore impact phytoplankton and marine foodwebs in the North Pacific by releasing especially iron and other nutrients into seawater.

The first evidence of volcanic enhancement of marine primary production was related to the eruption of Miyake-Jima volcano (Japan, Fig. 5.24) in 2000 (Uematsu et al. 2004). The powerful Miyake-Jima 2000 eruption spread out a volcanic plume that formed ammonium-sulphate aerosols, more than 200 km away in the oligotrophic western North Pacific, resulting in an increase in chlorophyll *a* levels (Uematsu et al. 2004). Similarly, the eruption of Anahatan Volcano (in the Mariana Islands, Fig. 5.24) in 2003, produced a bloom-like patch in the western North Pacific a week after the eruption, evidenced by the MODIS images (Lin et al. 2011).

Volcanic ash fall during a recent eruption of Kasatochi volcano (a remote Aleution island, Fig. 5.25) in August 2008, has also been speculated to generate a massive diatom bloom in the Fe-limited eastern subarctic North Pacific (Fig. 5.25). The unusual phytoplankton bloom in the Gulf of Alaska started a few days after the eruption (Hamme et al. 2010; Langmann et al. 2010). Geochemical experiments also confirmed that iron released from the Kasatochi volcanic ash is sufficient to iron-fertilise the surface North Pacific (Olgun et al. 2013). The bloom area in the eastern subarctic North Pacific (Fig. 5.25) was dominated by large diatoms, and a notably high abundance of large copepods (Hamme et al. 2010), providing a good-quality food-source for the young salmon in the ocean. Lindenthal (2011) provided another source of evidence for the fertilisation of the NE Pacific Ocean by volcanic ash fertilisation from the eruption of the Kasatochi volcano. Indeed, by using an ocean biogeochemical model study and this iron source, he found a good agreement between model outputs and measured chlorophyll *a*, nutrient concentrations, pH and surface ocean pCO_2.

Volcanic eruptions are likely to have impacted the marine foodweb in the North Pacific many times in Earth's recent history (Duggen et al. 2010). The 1980 eruption of Mount St. Helens, for example, was suggested to have fertilised rivers and lakes and

led to an increase in populations of golden algae (chrysophytes) and diatoms (Smith and White 1985). Notably, the Kasatochi 2008 eruption has gained further public attention because of its potential impact on fish populations (Jones 2010; Parsons and Whitney 2012; Olgun et al. 2013).

In late summer 2010, record numbers of sockeye salmon (estimated 35 million fish) returned back to Fraser River (Fig. 5.25) 2 years after the large Kasatochi eruption (Jones 2010). It has been speculated that the Kasatochi eruption provided rich food conditions (zooplankton) by enhancing marine primary production (Hamme et al. 2010; Langmann et al. 2010), and increased the marine survival of sockeye during their most critical marine life stage – the first months after they migrate into the ocean (July-October) (Parsons and Whitney 2012; Olgun et al. 2013).

Similarly, one of the largest salmon runs in 1958 followed the large eruption of Bensiammny volcano in Kamchatka. The eruption in 1912 of the Katmai volcano (Alaska) was also suggested to have fertilised the neighbouring lakes by input of phosphorus (Eicher and Rousefell 1957). High ash-loads during Katmai eruption, however, caused initial mortality of pre-smolts due to gill damage (Eicher and Rousefell 1957; Duggen et al. 2010). Despite the smaller number of spawners after the Katmai eruption, the numbers that returned in the following 4 years were as large as the pre-eruption, indicating a rapid recovery and favourable survival conditions in the ocean (Eicher and Rousefell 1957).

Further surveys of the Kasatochi 2008 eruption suggest that the local wildlife was also (directly or indirectly) affected by the eruption (del Moral 2010; Drew et al. 2010; Williams et al. 2010). The largest direct impact was probably the mortality of about 20,000–40,000 young birds (Williams et al. 2010). Most of the seabirds were displaced and the terrestrial birds did not return in 2009 (Williams et al. 2010). Marine mammals (e.g. seals) probably suffered less, but there was a clear disruption or loss of breeding habitat on the land due to meter-scale ash layers on the island (Drew et al. 2010).

In summary, the long-term response (months to years) of the ecology after major eruptions may provide new insights into how marine ecosystems are affected. Recent observations indicate that ocean fertilisation by volcanic eruptions may affect marine biomass within the ash-fall and neighbouring areas.

5.2.3 CO_2 in the North Atlantic

The North Atlantic Ocean is a major sink for atmospheric carbon dioxide (CO_2), and is therefore significant in slowing the global increase of atmospheric CO_2 caused by human activity. Until 1994, the North Atlantic stored approximately 23 % of anthropogenic carbon whilst covering only about 15 % of the world's ocean surface area (Sabine et al. 2004). Due to its significance, the North Atlantic uptake of CO_2 is continuing to be studied intensively, in order to determine the long-term trends of the uptake and its variability.

In the North Atlantic, the high-latitudes are a net sink of atmospheric CO_2 whilst the low-latitudes are a net annual source (Fig. 5.26). The mean seasonal cycle is small near the equator, a winter sink and summer source in the Subtropics, and a small winter source and strong summer sink in the subpolar region.

The air-sea flux of CO_2 is commonly estimated by the difference of CO_2 partial pressure (pCO_2) between the ocean and atmosphere combined with the transfer velocity k, which can be derived from wind speed by various parameterisations e.g. (Nightingale et al. 2000; Wanninkhof and McGillis 1999; Wanninkhof 1992, discussed in detail in Chaps. 2 and 3). The atmospheric pCO_2 is calculated from the molar fraction of CO_2 in the atmosphere (e.g. from Globalview (2011)) and atmospheric pressure. In contrast to the well-mixed atmosphere, surface seawater pCO_2 concentration is subject to considerable variability in space and time, mainly driven by temperature and biological activity. Automated measurements of pCO_2 and related parameters onboard Voluntary Observing Ships (VOS) have provided a valuable monitoring network in the North Atlantic for more than a decade. The pCO_2 of seawater is commonly determined by equilibrating a volume of air with seawater and measuring the CO_2 concentration in the gas phase (Pierrot et al. 2009). Alternatively, membrane-based systems are used, where CO_2 equilibrates (by diffusion) through a membrane and is measured within the sensor using an infra-red detector (Hales et al. 2004). An international effort to rigorously quality control such measurements has led to the creation of a global sea surface pCO_2 data set, the Surface Ocean CO_2 Atlas, SOCAT (see Sect. 5.1.4.4 of this chapter, http://www.socat.info/ and Pfeil et al. 2013). Additionally, pCO_2 can be calculated from dissolved

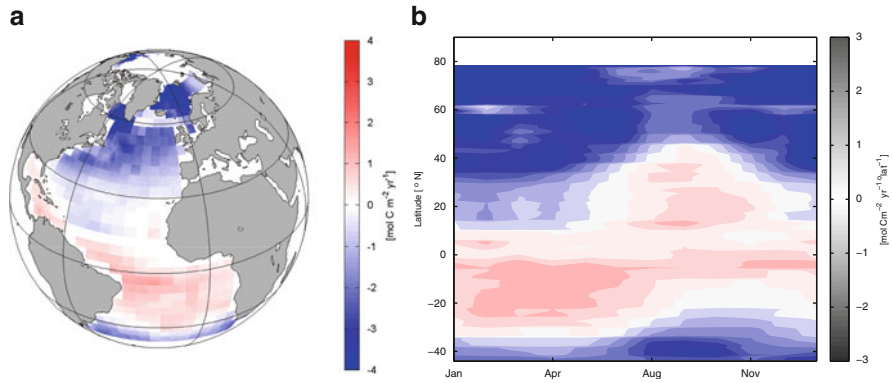

Fig. 5.26 (**a**) Geographical distribution of the mean air-sea CO_2 flux and (**b**) the zonal mean seasonal cycle of the flux in the North Atlantic (Adapted from Schuster et al. 2012)

inorganic carbon (DIC), total alkalinity (TA), temperature, salinity, and sea-surface pressure. This opens up the possibility of computing or estimating pCO_2 from parameters that can be monitored on a basin- or near basin-scale. Sea surface temperature (SST) is remotely-sensed by satellites (see Sect. 5.1.2.1) and measured by floats. Sea surface salinity (SSS) is monitored by floats and satellite data will be available soon through the Aquarius (Le Vine et al. 2007, http://aquarius.nasa.gov/) and SMOS projects (see Sect. 5.1.2.2). DIC and TA cannot yet be remotely-sensed. But for any individual ocean basin, TA can be estimated from SSS using a non-linear fit (Eden and Oschlies 2006). In addition, the SeaWiFS project provides satellite-derived estimates of the chlorophyll *a* concentration (see Sect. 5.1.2.3).

The sea surface pCO_2 and the air-sea CO_2 flux vary over time. A synthesis study by Watson et al. (2009) presented annual CO_2 flux estimates for the North Atlantic for the years 2002–2007. It demonstrated that the CO_2 uptake is subject to large interannual variability. Bates (2007) reported high observed variability of CO_2 fluxes due to increased wind speed over a 20 year period (1984–2005) at the Bermuda Atlantic Time Series (BATS) site. The occurrence of hurricanes in this region accounts for up to 29 % of the variability of summertime CO_2 fluxes (Bates 2007) and the increased frequency of hurricanes can potentially impact by approximately 16 % the interannual variability of CO_2 fluxes in the North Atlantic Ocean. In this context the North Atlantic Oscillation (NAO) is also a driver of variable wind speeds as it drives large scale climate variability over the North Atlantic (Hurrell 1995) and increasing values of NAO index correspond to increased CO_2 fluxes in the northern part of the North Atlantic (Olsen et al. 2003). However, Schuster et al. (2009) and Thomas et al. (2008) reported a link between the variability of NAO and CO_2 fluxes for the rest of the North Atlantic, although the heterogeneity makes the nature of the linkage difficult to identify. Modelling studies (Le Quéré et al. 2003; McKinley et al. 2004; Friedrich et al. 2006) show that SST is the primary control of North Atlantic subtropical surface pCO_2.

On a basin-scale, however, CO_2 fluxes simulated in the above model studies are not significantly correlated with the NAO index. Chemical buffering of changes in the CO_2 concentrations by the large pool of carbonate and bicarbonate ions (Broecker and Peng 1974) has been suggested as one reason for this decoupling.

Seawater pCO_2 itself is driven by sea surface temperature (SST), mixing (advective and convective) and biology (production/respiration). In the tropical North Atlantic NA, the seasonal pCO_2 cycle is strongly coupled to the SST variability. These oligotrophic waters do not support strong biological productivity due to the lack of nutrients (Longhurst 2007). The subtropical regions demonstrate low biological productivity and the seasonal cycle of pCO_2 is dominated by temperature changes. The annual amplitude of approximately 40 µatm peaks during the summer months, which corresponds to the temperature peak (Takahashi et al. 2009; Telszewski et al. 2009) but is reduced to a certain extent by low primary production. The pCO_2 in the subpolar NA is driven by high temperature variability (ΔSST ~ 8 °C) and high biological productivity. Here the biological productivity during spring and summer has a strong counteracting effect on the temperature driven pCO_2 increase during this period (Körtzinger et al. 2008; Lüger et al. 2004).

Steinhoff et al. (2010) have shown that the interannual variability of convective mixing of the surface layer may influence the wintertime budget of carbon and nutrients which directly impacts the observed seawater pCO_2 and thus the ΔpCO_2. Furthermore, advective mixing in the northwest Atlantic has a strong influence. The Labrador Current transports nutrient rich, colder, and fresher water with a different CO_2 signature into the North Atlantic Drift region. On a decadal timescale, increased SST and thus increased primary production may explain the observed long-term changes of seawater pCO_2 (Corbière et al. 2007; Takahashi et al. 2009).

The North Atlantic air-sea CO_2 flux is, however, not constant over time. Based on observations and sinusoidal curve fitting, Schuster et al. (2009) found that between 45°N and 65°N, pCO_2 in the sea surface increased faster than that in the atmosphere between 1990 and 2006 (3 and 1.8 µatm year^{-1}, respectively), resulting in a decreasing sink from 0.20 to 0.09 Pg C year^{-1}, whilst winter-time observations in the Subpolar North Atlantic showed that surface pCO2 in winter increased even faster at 3.7 µatm year^{-1} between 1993 and 2003 (Corbière et al. 2007).

Several problems arise when using related parameters to gain an insight into basin-wide surface pCO_2. First of all, a direct calculation is not possible with the data currently available. One needs to estimate surface pCO_2 from e.g. remote sensing data using empirical fitting functions. Thus, errors in the initial observations and data gaps will impair the accuracy of the pCO_2 estimate or result in missing data. The search for a fitting function can be challenging. For example, Watson et al. (1991) and Lefèvre and Taylor (2002) reported robust linear relationships between SST and pCO_2 in the subpolar and subtropical North Atlantic, respectively. The regression coefficients in both studies were similar in magnitude, yet of opposite sign. The study by Watson et al. (1991) also documented a promising covariation of chl *a* and pCO_2. On the other hand, Lüger et al. (2004) found no significant correlation between chl *a* and pCO_2 based on measurements covering an entire seasonal cycle in the midlatitude North Atlantic.

The pioneering study by Lefèvre et al. (2005) was the first to derive maps of North Atlantic in situ pCO_2. Using mainly VOS data of the years 1995–1997, multiple regression techniques and self-organising maps (Kohonen 1982), monthly mean surface pCO_2 fields were constructed from temperature and position in time and space on a 1° × 1° grid between 50°N and 70°N. The authors determined the Subpolar Gyre uptake to be 0.13–0.15 Pg C year^{-1} based on their pCO_2 estimates and NCEP monthly wind speed. For the year 2000, the climatological mean North Atlantic sink was approximately 0.44 Pg C year^{-1} (equator to 80°N, Takahashi et al. 2009), whilst an ocean inversion model showed the mean uptake to be 0.41 Pg C year^{-1} (equator to 90°N, Gruber et al. 2009). A recent study of the air-sea CO_2 fluxes in the Atlantic gives a best estimate of the long-term mean flux for the North Atlantic of 0.46 Pg C year^{-1} for the time period of 1990–2009 (Schuster et al. 2012); this study is based on observations, atmospheric inversions, ocean inversions, and ocean biogeochemical models. The availability of satellite-derived chl *a* and mixed layer depth (MLD) allowed for an improvement of regression techniques as demonstrated by Jamet et al. (2007). The strongly enhanced VOS coverage achieved by the CAVASSOO and CARBOOCEAN projects and their US-American partners enabled Telszewski et al. (2009) to provide seasonal pCO_2 estimates for the years 2004–2006 in the North Atlantic between 10°N and 70°N.

The accuracy of pCO_2 mapping is a major source of uncertainty to this day. Common techniques such as a validation against the data used for deriving the mapping function or against an independent data set (e.g. additional VOS data) were used in the studies mentioned above. To what degree, however, errors derived from individual VOS were representative of the basin-wide mapping error remains unclear. The study by Friedrich and Oschlies (2009a) addressed this challenge through combining observational and modelling approaches. The authors simulated the procedure of VOS monitoring and remote sensing in an eddy-resolving biogeochemical ocean model. Subsequently, the modelled pCO_2 output was used as a ground truth to analyse the accuracy of the pCO_2 maps generated from simulated SST and chlorophyll *a* fields. One major finding of this study was that the conventional validation techniques underestimate the basin-scale mapping error significantly, raising questions about the reliability of error estimates in earlier studies. However, it was also shown that despite large mapping errors in some regions, the basin-wide CO_2 uptake can be determined with promising precision and that the accuracy can be improved when ARGO float data are used (Friedrich and Oschlies 2009b).

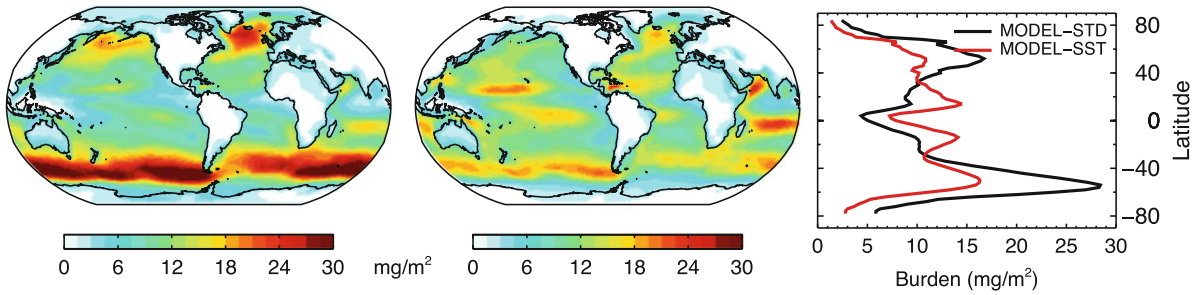

Fig. 5.27 Global burden of SSA (in mg m^{-2}) calculated with the GEOS-Chem CTM for the year 2008. *Left panel*: SSA burden calculated using the Gong (2003) source function (*MODEL-STD*). *Central panel*: SSA burden with the empirically derived source function including a sea surface temperature dependence (*MODEL-SST*). *Right panel*: Zonal average of SSA burden over the oceans (Adapted from Jaeglé et al. (2011))

In summary, the network of Voluntary Observing Ships is an efficient way to monitor the evolution of surface pCO_2 in the North Atlantic and elsewhere. Provided that sufficient coverage is maintained, VOS measurements can be combined with data from satellites and ARGO floats to generate basin-scale maps of surface pCO_2 and to estimate air-sea carbon fluxes with good precision. Future instrumentation such as floats that measure pCO_2 will be a significant asset and will help increase the accuracy of such estimates.

5.2.4 Global Distribution of Sea Salt Aerosols

The global distribution of sea salt aerosols (SSA) is generally estimated using chemical transport models (CTMs) or General Circulation Models (GCMs). Emissions are calculated by integrating a size-dependent source function of SSA at each time step over several size bins. Simultaneously, transport and depositional loss of SSA are also calculated. Models then solve the continuity equation for mass conservation in each size bin.

The resulting global distribution of SSA is highly dependent not only on the assumed sea-salt source function (see reviews by Lewis and Schwartz 2004; O'Dowd and de Leeuw 2007; de Leeuw et al. 2011b) but also on the upper size range of particles, and meteorological fields, as demonstrated in the model intercomparison study of Textor et al. (2006). These authors found a large inter-model range of 3–18 Tg for the global SSA burdens calculated in 16 different CTMs.

Calculated SSA concentrations can differ by factors of 2–3 when different source functions are used in the same CTM (e.g. Guelle et al. 2001; Pierce and Adams 2006). Most source functions are a function of whitecap coverage, with the frequently used 10 m wind speed dependence of $u_{10}{}^{3.41}$ (Mohanan and O'Muircheartaigh 1980). Thus, small biases in calculated wind speeds are amplified in the resulting SSA emissions. Even when SSA emissions are specified, differences in transport and deposition can result in a factor of 2 variation in predicted global SSA burdens for different models (Liu et al. 2007; Textor et al. 2007).

Despite these significant differences in the absolute concentrations of SSA, models generally display similar features in the global distribution of SSA following the spatial and seasonal distribution of surface wind speed: year-round very high SSA concentrations over the Southern Ocean, winter maximum over the Northern mid latitude storm tracks, and a minimum in the tropics and subtropics (Fig. 5.27, left panel).

This view has been challenged by three independent studies using satellite and in situ observations as top-down constraints on the global distribution of SSA. Haywood et al. (1999) examined the clear-sky solar irradiance measured by the CERES satellite and found a strong signature of SSA over the oceans away from pollution-influenced regions. The geographical pattern of SSA reflectance displayed maxima over both the Southern Ocean and the tropical oceans in the 10–20° latitude band. Satellite measurements of brightness temperature have been used to infer a first estimate of global whitecap coverage (Anguelova and Webster 2006). The resulting whitecap coverage showed a fairly uniform distribution with latitude, contrary to the expectation of strong enhancements over high latitude regions with high wind speeds and very low concentrations in the tropics.

Jaeglé et al. (2011) analysed cruise observations of supermicron SSA mass concentrations (1–10 μm diameter) from six Pacific Marine Environmental Laboratory (PMEL) cruises (Quinn and Bates 2005) with a CTM. They inferred that in addition to the well-known wind speed dependence, SSA emissions appear to depend on sea surface temperature. This is consistent with laboratory experiments reporting increased production of SSA with increasing water temperature for coarse SSA particles (Bowyer 1984, 1990; Woolf et al. 1987; Mårtensson et al. 2003). The temperature dependence leads to a decrease in the predicted SSA burden over the cold high latitude oceans, but enhanced SSA burden over the warm tropical oceans, especially in the trade wind regions. Implementing an empirical temperature- and wind speed-dependent SSA source function in the CTM leads to a more uniform global distribution of SSA (Fig. 5.27 central and right panels) and also improves agreement with in situ SSA observations and remotely sensing aerosol optical depth observations (Jaeglé et al. 2011).

These recent studies illustrate that one way to reduce the very high uncertainties associated with SSA source functions determined from laboratory and field measurements is via integrative studies that combine these source functions in CTMs and GCMs and use top-down constraints based on in situ and satellite observations. Compilations of aerosol observations such as the SOLAS aerosol database (Sect. 5.1.4.5), with a wide distribution over most of the ocean basins are extremely useful in this endeavour.

5.3 Perspectives for the Future

In this chapter we have summarised some of the major integrative SOLAS activities carried over the past decade. While there is a remarkable diversity in the scope, goals, approach, and tools associated with these efforts, they all fall into one or more of the following broad categories:

1. *Understanding biogeochemical cycles*: Compilation of geospatial data sets for the purpose of understanding biogeochemical cycles and discovering the physical and chemical controls on biogeochemistry. Such data sets permit hypothesis testing and provide a common basis for comparison of global models.
2. *Establishing current climatologies*: Establishing a baseline describing the current physical and biogeochemical state of the oceans and atmosphere. For most parameters we are far from an adequate description of the modern Earth, and as a result, we are ill prepared to detect changes.
3. *Closing global budgets:* Time series measurements of the composition of the atmosphere, such as the Mauna Loa CO_2 record, provide a unique integrated view of the global accumulation of greenhouse gases and other pollutants. Detecting change in the oceanic inventory of anthropogenic emissions is an equally critical step towards closing global budgets, but is considerably more logistically challenging.

The SOLAS integrative studies are examples of activities that could contribute to an Earth Observing System. Such a system spans a wide range of activities including process-scale laboratory and expeditionary research, development of new observational capabilities, and operational data streams from satellites, buoys, drifters and models. To be successful, an Earth Observing system will require contributions from many nations and a workforce of highly skilled Earth Scientists and engineers who operate as a global community. One of the most important and exciting aspects of the integrated SOLAS science described here is the extent to which it reflects the work of young scientists from many nations, and the development of a common vision for future priorities in global environmental science.

With this in mind, the International SOLAS Steering Committee identified five unresolved issues of significance to the global climate system that required improved international cooperation and networking (Law et al. 2013). These novel cross-cutting areas, or Mid Term Strategy Initiatives (http://www.solas-int.org/about/mid-term-strategy.html), i.e. Upwellings and associated Oxygen Minimum Zones, Sea ice biogeochemistry, Marine Aerosols, Atmospheric nutrient inputs to the oceans, and Ship Emissions, will benefit from enhanced community engagement to deliver major advances.

Looking forward, societal needs for large-scale integrated data and models are increasing. The human biogeochemical footprint on the planet is now

so large that the future quality and sustainability of environmental resources will be determined by societal choices rather than natural variability. At the same time, it is critical to understand how natural Earth systems will respond to this forcing. Large scale Earth Observations and Earth System models will be essential tools underpinning societal decision-making. The future challenges include:

1. *Discovery and detection:* The pace of environmental change is increasing rapidly as a result of increasing industrialisation, population growth, and technological development. The ability to detect large-scale changes in the environment at an early stage is essential in order to allow society adequate time to avoid or mitigate the deterioration of environmental resources and services.
2. *Attribution:* When environmental changes occur, it is critical to understand the underlying causes and the extent to which they can be attributed to natural or anthropogenic causes.
3. *Prediction and uncertainties:* Prediction of future environmental change is an essential tool for the development of effective environmental policy. Almost every aspect of human society and its infrastructure is sensitive to climate and other environmental conditions. Science-based models are the principle tool used to assess the likely outcomes of current trends, the effectiveness of proposed policy options and/or geoengineering strategies, and the environmental impacts of new technologies. Quantitative assessment of uncertainties inherent in predictions of future environmental change is one of the most important products of Earth System Science models. These uncertainties contribute greatly to risk assessments of policy options.

There is enormous potential benefit to society in understanding the environmental consequences of societal trends and policies. These benefits include long term planning to take advantage of new opportunities (e.g. the melting of sea ice and the opening of the Arctic Ocean to exploration and navigation), or to avoid potential costs (i.e. minimising sea level sea level rise by mitigating greenhouse gas emissions). For the SOLAS realm, providing the types of information needed for decision-making will require improved process-level understanding of biogeochemistry, and much better observational capability for remote regions of the atmosphere and oceans. Significant investment will be required in order to maintain existing observing systems, develop and deploy new sensors for in situ and remote observations, and improve infrastructure for the archiving and distribution of data for both research and operational products.

The importance of the SOLAS realm to the future trajectory of Earth's climate and habitability is very clear. Our ability to manage and improve the quality of both natural and human systems will ultimately depend on our understanding of these interactions. The coastal zone is heavily populated and most people are well aware of the impact that coastal water quality can have on their lives and local economy. Although the open oceans cover most of Earth's surface, they are largely uninhabited, and there is a tendency for the average person to see them as remote, unchanging, and disconnected from their daily lives. The reality is far from that, and societal decision-making must take into account the myriad interactions that link us with the surface ocean and lower atmosphere. The challenges are to identify and understand these linkages, to inform the public about them, and to develop tools for integrating scientific knowledge into societal decision-making. The research summarised in this volume demonstrates the remarkable progress of SOLAS science over the past decade, and shows the capacity of the SOLAS scientific community to meet the broader challenges ahead.

References

Adornato L, Cardenas-Valencia A, Kaltenbacher E, Byrne RH, Daly K, Larkin K, Hartman S, Mowlem M, Prien RD, Garçon VC (2010) In situ nutrient sensors for ocean observing systems. In: Hall J, Harrison DE, Stammer D (eds) Proceedings of the OceanObs'09: sustained ocean observations and information for society conference, vol 2. ESA Publication, Venice, 21–25 Sept 2009, WPP-306

Alvain S, Moulin C, Danndonneau Y, Breon FM (2005) Remote sensing of phytoplankton groups on case 1 waters from global SeaWiFS imagery. Deep-Sea Res I 52:1989–2004

Alvain S, Moulin C, Danndonneau Y, Loisel H (2008) Seasonal distribution and succession of dominant phytoplankton

groups in the global ocean: a satellite view. Glob Biogeochem Cycles 22, GB3001

Anderson TR (2005) Plankton functional type modelling: running before we can walk? J Plankton Res 27. doi:10.1093/plankt/fbi076

Anderson TR, Spall SA, Yool A, Cipollini P, Challenor PG, Fasham MJR (2001) Global fields of sea surface dimethylsulfide predicted from chlorophyll, nutrients and light. J Mar Syst 30(1–2):1–20. doi:10.1016/S0924-7963(01)00028-8

Andreae TW, Andreae MO, Ichoku C, Maenhaut W, Cafmeyer J, Karnieli A, Orlovsky L (2002) Light scattering by dust and anthropogenic aerosol at a remote site in the Negev desert, Israel. J Geophys Res 107(D2):4008. doi:10.1029/2001JD900252

Anguelova MD, Webster F (2006) Whitecap coverage from satellite measurements: a first step toward modeling the variability of oceanic whitecaps. J Geophys Res 111: C03017. doi:10.1029/2005JC003158

Arnold SR, Spracklen DV, Williams J, Yassaa N, Sciare J, Bonsang B, Gros V, Peeken I, Lewis AC, Alvain S, Moulin C (2009) Evaluation of the global oceanic isoprene source and its impacts on marine organic carbon aerosol. Atmos Chem Phys 9(4):1253–1262. http://www.atmos-chem-phys.net/9/1253/2009/acp-9-1253-2009.html

Arnold SR, Spracklen DV, Gebhardt S, Custer T, Williams J, Peeken I, Alvain S (2010) Relationships between atmospheric organic compounds and air-mass exposure to marine biology. Environ Chem 7(3):232–241. doi:10.1071/EN09144

Ayers GP, Gras JL (1991) Seasonal relationship between cloud condensation nuclei and aerosol methanesulphonate in marine air. Nature 353:334–835

Ayers GP, Penkett SA, Gillett R, Bandy B, Galbally IE, Meyer CP, Elsworth CM, Bentley ST, Forgan BW (1992) Evidence for photochemical control of ozone concentrations in unpolluted marine air. Nature 360:446–449. doi:10.1038/360446a0

Ayers GP, Cainey JM, Gillett RW, Ivey JP (1997) Atmospheric sulphur and cloud condensation nuclei in marine air in the southern hemisphere. Phil Trans R Soc Lond B 352:203–211

Bahurel P, MERCATOR Project Team (2006) Chapter 14: MERCATOR ocean global to regional ocean monitoring and forecasting. In: Chassignet EP, Verron J (eds) Ocean weather forecasting. Springer, New York, pp 381–395

Baker DF, Bousquet P, Bruhwiler L, Chen YH, Ciais P, Denning AS, Fung IY, Gurney KR, Heimann M, John J, Law RM, Maki T, Maksyutov S, Masarie K, Pak BC, Peylin P, Prather M, Rayner PJ, Taguchi S, Zhu ZX (2006) TransCom 3 inversion intercomparison: impact of transport model errors on the interannual variability of regional CO_2 fluxes, 1988–2003. Glob Biogeochem Cycles 20:GB1002. doi:10.1029/2004GB002439

Baker AR, Lesworth T, Adams C, Jickells TD, Ganzeveld L (2010) Estimation of atmospheric nutrient inputs to the Atlantic Ocean from 50°N to 50°S based on large-scale field sampling: fixed nitrogen and dry deposition of phosphorus. Glob Biogeochem Cycles 24:GB3006. doi:10.1029/2009GB003634

Balch WM, Kilpatrick K, Holligan PM, Harbour D, Fernandez E (1996) The 1991 coccolithophore bloom in the central north Atlantic. II. Relating optics to coccolith concentration. Limnol Oceanogr 41:1684–1696

Balch WM, Gordon HR, Bowler BC, Drapeau DT, Booth ES (2005) Calcium carbonate measurements in the surface global ocean based on moderate-resolution imaging spectroradiometer data. J Geophys Res 110:C07001. doi:10.1029/2004JC002560

Balch WM, Drapeau DT, Bowler BC, Lyczskowski E, Booth ES, Alley D (2011) The contribution of coccolithophores to the optical and inorganic carbon budgets during the Southern Ocean Gas Exchange Experiment: new evidence in support of the "Great Calcite Belt" hypothesis. J Geophys Res 116: C00F06. doi:10.1029/2011JC006941

Bange HW, Bell TG, Cornejo M, Freing A, Uher G, Upstill-Goddard RC, Zhang G (2009) MEMENTO: a proposal to develop a database of marine nitrous oxide and methane measurements. Environ Chem 6:195–197. doi:10.1071/EN09033

Bates NR (2001) Interannual variability of oceanic CO_2 and biogeochemical properties in the Western North Atlantic subtropical gyre. Deep-Sea Res II 48:1507–1528. doi:10.1016/S0967-0645(00)00151-X

Bates NR (2007) Interannual variability of the oceanic CO_2 sink in the subtropical gyre of the North Atlantic Ocean over the last two decades. J Geophys Res 112(C9):C09013. doi:10.1029/2006JC003759

Bates NR, Michaels AF, Knap AH (1996) Seasonal and interannual variability of the oceanic carbon dioxide system at the U.S JGOFS Bermuda Atlantic Time series site. Deep-Sea Res II 43(2–3):347–383. doi:10.1016/0967-0645(95)00093-3

Bates NR, Knap AH, Michaels AF (1998) Contribution of hurricanes to local and global estimates of air-sea exchange of CO_2. Nature 395:58–61. doi:10.1038/25703

Beale R, Dixon JL, Arnold SR, Liss PS, Nightingale PD (2013) Methanol, acetaldehyde and acetone in the surface waters of the Atlantic Ocean, (accepted)

Beirle S, Platt U, von Glasow R, Wenig M, Wagner T (2004) Estimate of nitrogen oxide emissions from shipping by satellite remote sensing. Geophys Res Lett 31:L18102. doi:10.1029/2004GL020312

Bell TG, Malin G, Lee GA, Stefels J, Archer S, Steinke M, Matrai P (2011) Global oceanic DMS data intercomparability. Biogeochemistry. doi:10.1007/s10533-011-9662-3

Belviso S, Moulin C, Bopp L, Stefels J (2004a) Assessment of a global climatology of oceanic dimethylsulfide (DMS) concentrations based on SeaWiFS imagery (1998–2001). Can J Fish Aquat Sci 61:804–816. doi:10.1139/F04-001

Belviso S, Bopp L, Moulin C, Orr JC, Anderson TR, Aumont O, Chu S, Elliott S, Maltrud ME, Simó R (2004b) Comparison of global climatological maps of sea surface dimethyl sulphide. Glob Biogeochem Cycles 18:GB3013. doi:10.1029/2003GB002193

Bolin B, Keeling CD (1963) Large-scale atmospheric mixing as deduced from the seasonal and meridional variations of carbon dioxide. J Geophys Res 68:3899–3920

Bonsang B, Gros V, Peeken I, Yassaa N, Bluhm K, Zöllner E, Sarda-Esteve R, Williams J (2010) Isoprene emission from phytoplankton monocultures: the relationship with

chlorophyll-a, cell volume and carbon content. Environ Chem 7(6):554–563. doi:10.1071/EN09156
Bopp L, Aumont O, Belviso S, Monfray P (2003) Potential impact of climate change on marine dimethyl sulfide emissions. Tellus B 55(1):11–22
Bopp L, Aumont O, Belviso S, Blain S (2008) Modeling the effect of iron fertilization on dimethylsulfide emissions in the Southern Ocean. Deep Sea Res II 55(5–7):901–912
Bourassa, M, Stoffelen A, Bonekamp H, Chang P, Chelton D, Courtney J, Edson R, Figa J, He Y, Hersbach H, Hilburn K, Jelenak Z, Kelly K, Knabb R, Lee T, Lindstrom E, Liu W, Long D, Perrie W, Portabella M, Powell M, Rodriguez E, Smith D, Swail V, Wentz F (2010) Remotely sensed winds and wind stresses for marine forecasting and ocean modeling. In: Hall J, Harrison DE, Stammer D (eds) Proceedings of OceanObs'09: sustained ocean observations and information for society, vol 2. Venice, 21–25 Sept 2009
Bousquet P, Peylin P, Ciais P, Le Quéré C, Friedlingstein P, Tans P (2000) Regional changes in carbon dioxide fluxes of land and oceans since 1980. Science 290:1342–1346
Boutin J, Martin N, Reverdin G, Yin X, Gaillard F (2012) Sea surface freshening inferred from SMOS and ARGO salinity: impact of rain. Ocean Sci Discuss 9:3331–3357. doi:10.5194/osd-9-3331-2012
Bovensmann H, Burrows JP, Buchwitz M, Frerick J, Noël S, Rozanov VV, Chance KV, Goede APH (1999) SCIAMACHY- mission objectives and measurement modes, conference on global measurement systems for atmospheric composition, May 1997, Toronto. J Atmos Sci 56(2):127–150
Bowyer PA (1984) Aerosol production in the whitecap simulation tank as a function of water temperature (Appendix E). In: Monahan ED, Spillane MC, Bowyer PA, Higgins MR, Stabeno PJ (eds) Whitecap and the marine atmosphere, vol 7, Report. University College, Galway, pp 95–103
Bowyer PA, Woolf DK, Monahan EC (1990) Temperature dependence of the charge and aerosol production associated with a breaking wave in a whitecap simulations tank. J Geophys Res 95:5313–5319
Boyd P (2008) Implications of large-scale iron fertilization of the oceans. Mar Ecol Prog Ser 364:213–218. doi:10.3354/meps07541
Boyd P, Harrison PJ (1999) Phytoplankton dynamics in the NE subarctic Pacific. Deep-Sea Res II 46:2405–2432
Boyd PW, Muggli DL, Varela DE, Goldblatt RH, Chretien R, Orians KJ, Harrison PJ (1996) In vitro iron enrichment experiments in the NE subarctic Pacific. Mar Ecol Prog Ser 136:179–193
Boyd PW, Jickells T, Law CS, Blain S, Boyle EA, Buesseler KO, Coale KH, Cullen JJ, de Baar HJW, Follows M, Harvey M, Lancelot C, Levasseur M, Owens NPJ, Pollard R, Rivkin RB, Sarmiento J, Schoemann V, Smetacek V, Takeda S, Tsuda A, Turner S, Watson AJ (2007) Mesoscale iron enrichment experiments 1993–2005: synthesis and future directions. Science 315(5812):612–617
Bracher A, Vountas M, Dinter T, Burrows JP, Röttgers R, Peeken I (2009) Quantitative observation of cyanobacteria and diatoms from space using PhytoDOAS on SCIAMACHY data. Biogeosciences 6:751–764
Brasseur P, Gruber N, Barciela R, Brander K, Doron M, El Moussaoui A, Hobday AJ, Huret M, Kremeur A-S, Lehodey P, Matear R, Moulin C, Murtugudde R, Senina I, Svendsen E (2009) Integrating biogeochemistry and ecology into ocean data assimilation systems. Oceanography 22(3):206–215
Brewin RJW, Lavender SJ, Hardman-Mountford NJ, Hirata T (2010a) A spectral response approach for detecting dominant phytoplankton size class from satellite remote sensing. Acta Oceanol Sin 29:14–32
Brewin RJW, Sathyendranath S, Hirata T, Lavender SJ, Barciela R, Hardman-Mountford NJ (2010b) A three-component model of phytoplankton size class for the Atlantic Ocean. Ecol Model 221:1472–1483
Brewin RJW, Hardman-Mountford NJ, Lavender SJ, Raitsos DE, Hirata T, Uitz J, Devred E, Bricaud A, Ciotti A, Gentili B (2011) An intercomparison of bio-optical techniques for detecting phytoplankton size class from satellite remote sensing. Remote Sens Environ 115:325–339
Broecker WS, Peng TH (1974) Gas exchange rates between air and sea. Tellus 26:21–35
Brown CW, Yoder JA (1994) Coccolithophorid blooms in the global ocean. J Geophys Res 99:7467–7482
Burrows J, Hölzle PE, Goede APH, Visser H, Fricke W (1995) SCIAMACHY – scanning imaging absorption spectrometer for atmospheric chartography. Acta Astronaut 35(7):445–451
Butler JH, Bell TG, Hall BD, Quack B, Carpenter LJ, Williams J (2010) Technical note: ensuring consistent, global measurements of very short-lived halocarbon gases in the ocean and atmosphere. Atmos Chem Phys 10:10327–10330
Carpenter LJ, Monks PS, Galbally IE, Meyer CP, Bandy BJ, Penkett SA (1997) A study of peroxy radicals and ozone photochemistry at coastal sites in the northern and southern hemispheres. J Geophys Res 102:417–427
Carpenter LJ, Lewis AC, Hopkins JR, Read KA, Longley ID, Gallagher MW (2004) Uptake of methanol to the North Atlantic Ocean surface. Glob Biogeochem Cycles 18:GB4027
Carpenter LJ, Fleming Z, Read KA, Lee JD, Moller SJ, Hopkins JR, Purvis RM, Lewis AC, Müller K, Heinold B, Herrmann H, Fomba KW, van Pinxteren D, Müller C, Tegen I, Wiedensohler A, Müller T, Niedermeier N, Achterberg EP, Patey MD, Kozlova EA, Heimann M, Heard DE, Plane JMC, Mahajan A, Oetjen H, Ingham T, Stone D, Whalley LK, Evans MJ, Pilling MJ, Leigh RJ, Monks PS, Karunaharan A, Vaughan S, Arnold SR, Tschitter J, Pohler D, Friess U, Holla R, Mendes LM, Lopez H, Faria B, Manning AJ, Wallace DWR (2010) Seasonal characteristics of tropical marine boundary layer air measured at the Cape Verde Atmospheric Observatory. Atmos Environ 67(2–3):87–140. doi:10.1007/s10874-011-9206-1
Carpenter LJ, MacDonald SM, Shaw MD, Kumar R, Saunders RW, Parthipan R, Wilson J, Plane JMC (2013) Atmospheric iodine levels influenced by sea surface emissions of inorganic iodine. Nat Geosci 6:108–111. doi:10.1038/ngeo1687
Chance K (1998) Analysis of BrO measurements from the Global Ozone Monitoring Experiment. Geophys Res Lett 25(17):3335–3338. doi:10.1029/98GL52359
Chassignet EP, Hurlburt HE, Smedstad OM, Halliwell GR, Hogan PJ, Wallcraft AJ, Baraille R, Bleck R (2007) The HYCOM (HYbrid Coordinate Ocean Model) data assimilative system. J Mar Syst 65(1–4):60–83
Chelton DB, Schlax MG, Freilich MH, Milliff RF (2004) Satellite measurements reveal persistent small-scale features in ocean winds. Science 303:978–983

Ciotti AM, Bricaud A (2006) Retrievals of a size parameter for phytoplankton and spectral light absorption by coloured detrital matter from water-leaving radiances at SeaWiFS channels in a continental shelf off Brazil. Limnol Oceanogr Methods 4:237–253

Clarizia MP, Gommenginger CP, Gleason ST, Srokosz MA, Galdi C, Di Bisceglie M (2009) Analysis of GNSS-R delay-Doppler maps from the UK-DMC satellite over the ocean. Geophys Res Lett 36:L02608. doi:10.1029/2008GL036292

Clarke L, Edmonds J, Jacoby H, Pitcher H, Reilly J, Richels R (2007) Scenarios of greenhouse gas emissions and atmospheric concentrations, sub-report 2.1A of synthesis and assessment product 2.1 by the US Climate Change Science Program and the Subcommittee on Global Change Research. Department of Energy, Office of Biological und Environmental Research, Washington, DC, p 154

Clausi DA, Qin AK, Chowdhury MS, Yu P, Maillard P (2010) MAGIC: MAp-guided ice classification system. Can J Remote Sens 36(S1):S13–S25

Claustre H, Antoine D, Boehme L, Boss E, D'Ortenzio F, Fanton D'Andon O, Guinet C, Gruber N, Handegard NO, Hood M, Johnson K, Körtzinger A, Lampitt R, Le Traon P-Y, Lequéré C, Lewis M, Perry MJ, Platt T, Roemmich D, Sathyendranath S, Testor P, Send U, Yoder J (2010) Guidelines towards an integrated ocean observation system for ecosystems and biogeochemical cycles. In: Hall J, Harrison DE, Stammer D (eds) Proceedings of the OceanObs'09: sustained ocean observations and information for society conference, vol 1. ESA Publication, Venice, 21–25 Sept 2009, WPP-306

Collins WD et al (2006) The community climate system model version 3 (CCSM3). J Climate 19:2122–2143. doi:10.1175/JCLI3761.1

Corbière A, Metzl N, Reverdin G, Brunet C, Takahashi T (2007) Interannual and decadal variability of the oceanic carbon sink in the North Atlantic subpolar gyre. Tellus B 59 (2):168–178. doi:10.1111/j.1600-0889.2006.00232

Crisp D, Atlas RM, Breon FM, Brown LR, Burrows JP, Ciais P, Connor BJ, Doney SC, Fung IY, Jacob DJ, Miller CE, O'Brien D, Pawson S, Randerson JT, Rayner P, Salawitch RJ, Sander SP, Sen B, Stephens GL, Tans PP, Toon GC, Wennberg PO, Wofsy SC, Yung YL, Kuang ZM, Chudasama B, Sprague G, Weiss B, Pollock R, Kenyon D, Schroll S (2004) The orbiting carbon observatory (OCO) mission. In: Burrows JP, Thompson AM (eds) Trace constituents in the troposphere and lower stratosphere. Adv Space Res 34(4):700–709

Dacey JW, Howse FA, Michaels AF, Wakeham SG (1998) Temporal variability of dimethylsulfide and dimethylsulfoniopropionate in the Sargasso Sea. Deep-Sea Res I 45:2085–2099. doi:10.1016/S0967-0637(98)00048-X

Dalsøren SB, Eide MS, Myhre G, Endresen Ø, Isaksen ISA, Fuglestved JS (2010) Impacts of the large increase in international ship traffic 2000–2007 on tropospheric ozone and methane. Environ Sci Technol 44:2482–2489

de Leeuw G, Kinne S, Leon JF, Pelon J, Rosenfeld D, Schaap M, Veefkind PJ, Veihelmann B, Winker DM, von Hoyningen-Huene W (2011a) Retrieval of aerosol properties. In: Burrows JP, Platt U, Borrell P (eds) The remote sensing of tropospheric composition from space, 536 pp. Springer, Berlin/Heidelberg, pp 359–313. doi:10.1007/978-3-642-14791-3. ISBN 978-3-642-14790-6

de Leeuw G, Andreas EL, Anguelova MD, Fairall CW, Lewis ER, O'Dowd C, Schulz M, Schwartz SE (2011b) Production flux of sea spray aerosol. Rev Geophys 49:RG2001. doi:10.1029/2010RG000349

del Moral R (2010) The importance of long-term studies of ecosystem reassembly after the eruption of the Kasatochi Island Volcano. Arct Antarct Alp Res 42:335–341

Denman KL, Brasseur G, Chidthaisong A, Ciais P, Cox PM, Dickinson RE, Hauglustaine D, Heinze C, Holland E, Jacob D, Lohmann U, Ramachandran S, da Silva Dias PL, Wofsy SC, Zhang X (2007) Couplings between changes in the climate system and biogeochemistry. In: Solomon S, Qin D, Manning M, Chen Z, Marquis M, Averyt KB, Tignor M, Miller HL (eds) Climate change 2007: the physical science basis. Contribution of working group I to the fourth assessment report of the intergovernmental panel on climate change. Cambridge University Press, Cambridge/New York, pp 499–587

Derwent RG, Simmonds PG, Manning AJ, Spain TG (2007) Trends over a 20-year period from 1987 to 2007 in surface ozone at the atmospheric research station, Mace Head, Ireland. Atmos Environ 41:9091–9098

Devred E, Sathyendranath S, Stuart V, Maas H, Ulloa O, Platt T (2006) A two-component model of phytoplankton absorption in the open ocean: Theory and applications. J Geophys Res 111:C03011. doi:03010.01029/02005JC002880

Devred E, Sathyendranath S, Stuart S, Platt T (2011) Absorption-derived phytoplankton cell size: application to satellite ocean-colour data in the Northwest Atlantic. Remote Sens Environ 115:2255–2266

Dickey T, Bates N, Byrne R, Chang G, Chavez F, Feely R, Hanson A, Karl D, Manov D, Moore C, Sabine C, Wanninkhof R (2009) The NOPP O-SCOPE and MOSEAN projects: advanced sensing for ocean observing systems. Oceanography 22(2):168–181

Dickson RR (2009) The integrated Arctic Ocean Observing System (iAOOS) in 2008, Report of the Arctic Ocean Sciences Board

Donlon C et al (2007) The Global Ocean Data Assimilation Experiment high-resolution sea surface temperature pilot project. Bull Am Meteorol Soc 88:1197–1213. doi:http://dx.doi.org/10.1175/BAMS-88-8-1197

Dore JE, Lukas R, Sadler DW, Church MJ, Karl DM (2009) Physical and biogeochemical modulation of ocean acidification in the central North Pacific. Proc Natl Acad Sci 106:12235–12240. doi:10.1073/pnas.0906044106

Draper DW, Long DG (2004) Evaluating the effect of rain on SeaWinds data. IEEE Trans Geosci Remote Sens 42:1411–1423

Drew GS, Dragoo GS, Renner M, Piatt JF (2010) At-sea observations of marine birds and their habitats before and after the 2008 eruption of Kasatochi Volcano, Alaska. Arct Antarct Alp Res 42:325–334

Duforêt-Gaurier L, Loisel H, Dessailly D, Nordkvist K, Alvain S (2010) Estimates of particulate organic carbon over the euphotic depth from in situ measurements. Application to satellite data over the global ocean. Deep-Sea Research I 57:351–367. doi:10.1016/j.dsr.2009.12.007

Duggen S, Croot P, Schacht U, Hoffmann L (2007) Subduction zone volcanic ash can fertilize the surface ocean and stimulate phytoplankton growth: evidence from biogeochemical experiments and satellite data. Geophys Res Lett 34: L01612

Duggen S, Olgun N, Croot P, Hoffmann L, Dietze H, Teschner C (2010) The role of airborne volcanic ash for the surface ocean biogeochemical iron-cycle: a review. Biogeosciences 7:827–844. doi:10.5194/bg-7-827-2010

Eden C, Oschlies A (2006) Adiabatic reduction of circulation-related CO_2 air-sea flux biases in a North Atlantic carbon-cycle model. Glob Biogeochem Cycles 20:GB2008. doi:10.1029/2005GB002521

Eicher GJ, Rousefell GA (1957) Effects of lake fertilization by volcanic activity on abundance of salmon. Adv Sci Limnol Oceanogr 2:70–76

Eicken H, Gradinger R, Salganek M, Shirasawa K, Perovich D, Leppäranta M (eds) (2009) Field techniques for sea ice research. University of Alaska Press, Fairbanks, p 566

Fairall C, Barnier B, Berry B, Bourassa F, Bradley F, Clayon C, de Leeuw G, Drennan W, Gille S, Gulev S, Kent E, McGillis W, Ryabinin V, Smith S, Weller R, Yelland M, Zhang H-M (2010) Observations to quantify air-sea fluxes and their role in climate variability and predictability. In: Hall J, Harrison DE, Stammer D (eds) Proceedings of OceanObs'09: sustained ocean observations and information for society, vol 2. Venice, 21–25 Sept 2009

Fennel K, Wilkin J (2009) Quantifying biological carbon export for the northwest North Atlantic continental shelves. Geophys Res Lett 36:L18605. doi:10.1029/2009GL039818

Fennel K, Wilkin J, Previdi M, Najjar R (2008) Denitrification effects on air-sea CO_2 flux in the coastal ocean: simulations for the Northwest North Atlantic. Geophys Res Lett 35: L24608. doi:10.1029/2008GL036147

Font J, Boutin J, Reul N, Spurgeon P, Ballabrera-Poy J, Chuprin A, Gabarró C, Gourrion J, Guimbard S, Hénocq C, Lavender S, Martin N, Martínez J, McCulloch M, Meirold-Mautner I, Mugérin C, Petitcolin F, Portabella M, Sabia R, Talone M, Tenerelli J, Turiel A, Vergely JL, Waldteufel P, Yin X, Zine S, Delwart S (2012) SMOS first data analysis for sea surface salinity determination. Int J Remote Sens 34:9–10. doi:10.1080/01431161.2012.716541

Franke K, Richter A, Bovensmann H, Eyring V, Jöckel P, Hoor P, Burrows JP (2009) Ship emitted NO_2 in the Indian Ocean: comparison of model results with satellite data. Atmos Chem Phys 9:7289–7301

Freeland HJ, Roemmich D, Garzoli SL, Le Traon PY, Ravichandran M, Riser S, Thierry V, Wijffels S, Belbéoch M, Gould J, Grant F, Ignazewski M, King B, Klein B, Mork KA, Owens B, Pouliquen S, Sterl A, Suga T, Suk MS, Sutton P, Troisi A, Vélez-Belchi PJ, Xu J (2010) Argo – a decade of progress in proceedings of the OceanObs'09. In: Monahan ED, Spillane MC, Bowyer PA, Higgins MR, Stabeno PJ (eds)/Hall J, Harrison DE, Stammer D (eds) Sustained ocean observations and information for society conference, vol 2. ESA Publication, Venice, 21–25 Sept 2009, WPP-306

Friedlingstein P et al (2006) Climate–carbon cycle feedback analysis: results from the C4MIP model intercomparison. J Clim 19:3337–3353

Friedrich T, Oschlies A (2009a) Basin-scale pCO_2 maps estimated from ARGO float data – a model study. J Geophys Res 114:C10012. doi:10.1029/2009JC005322

Friedrich T, Oschlies A (2009b) Neural network-based estimates of North Atlantic surface pCO_2 from satellite data: a methodological study. J Geophys Res 114:C03020. doi:10.1029/2007JC004646

Friedrich T, Oschlies A, Eden C (2006) Role of wind stress and heat fluxes in the interannual-to-decadal variability of air-sea CO_2 and O_2 fluxes in the North Atlantic. Geophys Res Lett 33:L21S04. doi:10.1029/2006GL026538

Frogner P, Gislason SR, Óskarsson N (2001) Fertilizing potential of volcanic ash in ocean surface water. Geology 29:487–490

Fu LL, Cazenave A (2001) Satellite altimetry and earth sciences, a handbook of techniques and applications, vol 69, International geophysics series. Academic, London

Gabric AJ, Simó R, Cropp RA, Hirst AC, Dachs J (2004) Modeling estimates of the global emission of dimethyl-sulfide under enhanced greenhouse conditions. Glob Biogeochem Cycles 18:GB3016. doi:10.1029/2004GB 002337

Gantt B, Meskhidze N, Kamykowski D (2009) A new physically-based quantification of marine isoprene and primary organic aerosol emissions. Atmos Chem Phys 9:4915. doi:10.5194/ACP-9-49152009

Gardner WD, Mishonov AV, Richardson MJ (2006) Global POC concentrations from in-situ and satellite data. Deep-Sea Res II 53(5–7):718–740. doi:10.1016/j.dsr2.2006.01.029

GCOS (2009) Progress report on the implementation of the global observing system for climate in support of the UNFCCC 2004–2008, GCOS-129 (WMO-TD/No. 1489, GOOS-173, GTOS-70). http://gosic.org/ios/GCOS-main-page.htm

GCOS (2010) Implementation plan for the global observing system for climate in support of the UNFCCC (2010 Update) GCOS-138, (GOOS-184, GTOS-76, WMO-TD/No. 1523). http://gosic.org/ios/GCOS-main-page.htm

Gent PR, Danabasoglu G, Donner LJ, Holland MM, Hunke EC, Jayne SR, Lawrence DM, Neale RB, Rasch PJ, Vertenstein M, Worley PH, Yang Z-L, Zhang M (2012) The community climate system model version 4. J Clim 24(19):4973–4991

Gerilowski K, Tretner A, Krings T, Buchwitz M, Bertagnolio PP, Belemezov F, Erzinger J, Burrows JP, Bovensmann H (2011) MAMAP – a new spectrometer system for column-averaged methane and carbon dioxide observations from aircraft: instrument description and performance analysis. Atmos Meas Tech 4(2):215–243. doi:10.5194/amt-4-215-2011

Glantz P, Nilsson EN, Hoyningen-Huene W (2009) Estimating a relationship between aerosol optical thickness and surface wind speed over the ocean. Atmos Res 92:58–68

GlobalView-CO_2 (2011) Cooperative atmospheric data integration project – carbon dioxide. CD-ROM, NOAA ESRL, Boulder, ftp.Cmdl.Noaa.Gov, path: Ccg/co2/globalview

Gloor M, Gruber N, Hughes TMC, Sarmiento JL (2001) Estimating net air-sea fluxes from ocean bulk data: methodology and application to the heat cycle. Glob Biogechem Cycles 15:767–782. doi:10.1029/2000GB001301

Gloor M, Gruber N, Sarmiento J, Sabine CL, Feely RA, Rödenbeck C (2003) A first estimate of present and preindustrial air-sea CO_2 flux patterns based on ocean

interior carbon measurements and models. Geophys Res Lett 30:1010. doi:10.1029/2002GL015594

Gong SL (2003) A parameterization of sea-salt aerosol source function for sub- and super-micron particles. Glob Biogeochem Cycles 17(4):1097. doi:10.1029/2003GB002079

González-Dávila M, Santana-Casiano JM, Rueda MJ, Llinás O (2010) The water column distribution of carbonate system variables at the ESTOC site from 1995 to 2004. Biogeosciences 7:3067–3081. doi:10.5194/bg-7-3067-2010

Gordon HR, Boynton GC, Balch WM, Groom SB, Harbour DS, Smyth TJ (2001) Retrieval of coccolithophore calcite concentration from SeaWiFS imagery. Geophys Res Lett 28 (8):1587–1590

Gruber N, Doney SC (2008) Ocean biogeochemical and ecological modeling. Encycl Ocean Sci 89–104

Gruber N, Sarmiento JL, Stocker TF (1996) An improved method for detecting anthropogenic CO_2 in the oceans. Glob Biogeochem Cycles 10(4):809–837

Gruber N, Gloor M, Fan S-M, Sarmiento JL (2001) Air-sea flux of oxygen estimated from bulk data: implications for the marine and atmospheric oxygen cycle. Glob Biogeochem Cycles 15(4):783–803

Gruber N, Friedlingstein P, Field CB, Valentini R, Heimann M, Richey JE, Romero-Lankao P, Schulze D, Chen C-TA (2004) The vulnerability of the carbon cycle in the 21st century: an assessment of carbon-climate-human interactions. In: Field CB, Raupach MR (eds) The global carbon cycle: integrating humans, climate, and the natural world. Island Press, Washington, DC, pp 45–76

Gruber N, Gloor M, Mikaloff Fletcher SE, Doney SC, Dutkiewicz S, Follows M, Gerber M, Jacobson AR, Joos F, Lindsay K, Menemenlis D, Mouchet A, Mueller SA, Sarmiento JL, Takahashi T (2009) Oceanic sources, sinks, and transport of atmospheric CO_2. Glob Biogeochem Cycles 23:GB1005. doi:10.1029/2008GB003349

Gruber N, Lachkar Z, Frenzel H, Marchesiello P, Munnich M, McWilliams JC, Nagai T, Plattner G-K (2011) Eddy-induced reduction of biological production in eastern boundary upwelling systems. Nat Geosci 4(11):787–792

Guelle W, Schulz M, Balkanski Y (2001) Influence of the source formulation on modeling the atmospheric global distribution of sea salt aerosol. J Geophys Res 106:27509–27524

Gurney K, Law RM, Denning AS, Rayner PJ, Baker D, Bousquet P, Bruhwiler L, Chen YH, Ciais P, Fan S, Fung IY, Gloor M, Heimann M, Higuchi K, John J, Maki T, Maksyutov S, Masarie K, Peylin P, Prather M, Pak BC, Randerson J, Sarmiento J, Taguchi S, Takahashi T, Yuen CW (2002) Towards robust regional estimates of CO_2 sources and sinks using atmospheric transport models. Nature 415:626–630

Hales B, Chipman D, Takahashi T (2004) High-frequency measurement of partial pressure and total concentration of carbon dioxide in seawater using microporous hydrophobic membrane contactors. Limnol Oceanogr Methods 2 (2):356–364

Hales B, Takahashi T, Bandstra L (2005) Atmospheric CO_2 uptake by a coastal upwelling system. Glob Biogeochem Cycles 19:1–11. doi:10.1029/2004GB002295

Halloran PR, Bell TG, Totterdell IJ (2010) Can we trust empirical marine DMS parameterisations within projections of future climate? Biogeosciences 7:1645–1656. doi:10.5194/bg-7-1645-2010

Hamazaki T, Kuze A, Kondo K (2004) Sensor system for greenhouse gas observing satellite (GOSAT). In: Strojnik M (ed) Infrared spaceborne remote sensing XII, proceedings of the society of photo-optical instrumentation engineers (SPIE) 5543:275–282. doi:10.1117/12.560589

Hamme RC, Webley PW, Crawford WR, Whitney FA, DeGrandpre MD, Emerson SR, Eriksen CC, Giesbrecht KE, Gower JFR, Kavanaugh MT, Angelica PM, Sabine CL, Batten SD, Coogan LA, Grundle DS, Lockwood D (2010) Volcanic ash fuels anomalous plankton bloom in subarctic northeast Pacific. Geophys Res Lett 37. doi:10.1029/2010GL044629

Haywood J, Ramaswamy V, Soden B (1999) Tropospheric aerosol climate forcing in clear sky satellite observation over the oceans. Science 283:1299–1303

Heikes BG, Chang WN, Pilson MEQ, Swift E, Singh HB, Guenther A, Jacob DJ, Field BD, Fall R, Riemer D, Brand L (2002) Atmospheric methanol budget and ocean implication. Glob Biogeochem Cycles 16:1133

Heue KP, Brenninkmeijer CAM, Wagner T, Mies K, Dix B, Frieß U, Martinsson BG, Slemr F, van Velthoven PFJ (2010) Observations of the 2008 Kasatochi volcanic SO_2 plume by CARIBIC aircraft DOAS and the GOME-2 satellite. Atmos Chem Phys 10:4699–4713

Hill PG, Zubkov MV, Purdie DA (2010) Differential responses of Prochlorococcus and SAR11-dominated bacterioplankton groups to atmospheric dust inputs in the tropical Northeast Atlantic Ocean. FEMS Microbiol Lett 306(1):82–89. doi:10.1111/j.1574-6968.2010.01940.x

Hill PG, Haywood JL, Holland RJ, Purdie DA, Fuchs BM, Zubkov MV (2012) Internal and external influences on near-surface microbial community structure in the vicinity of the Cape Verde Islands. Microb Ecol 63(1):139–148. doi:10.1007/s00248-011-9952-2

Hirata T, Aiken J, Hardman-Mountford NJ, Smyth TJ, Barlow RG (2008) An absorption model to derive phytoplankton size classes from satellite ocean colour. Remote Sens Environ 112:3153–3159

Hirata T, Hardman-Mountford NJ, Brewin RJW, Aiken J, Barlow R, Suzuki K, Isada T, Howell E, Hashioka T, Noguchi-Aita M, Yamanaka Y (2011) Synoptic relationships between surface Chlorophyll-a and diagnostic pigments specific to phytoplankton functional types. Biogeosciences 8:311–327

Hoffmann LJ, Peeken I, Lochte K, Assmy P, Veldhuis M (2006) Different reactions of Southern Ocean phytoplankton size classes to iron fertilization. Limnol Oceanogr 51:1217–1229. doi:10.4319/lo.2006.51.3.1217

Huang H, Thomas GE, Grainger RG (2010) Relationship between wind speed and aerosol optical depth over remote ocean. Atmos Chem Phys 10:5943–5950. doi:10.5194/acp-10-5943-2010

Hurrell JW (1995) Decadal trends in the North Atlantic oscillation: regional temperatures and precipitation. Science 269 (5224):676–679

IOCCP (2007) Surface ocean CO_2 variability and vulnerabilities workshop. IOCCP Report 7. UNESCO, Paris, 11–14 Apr 2007. http://www.ioccp.org/

Jacob DJ, Field BD, Li QB, Blake DR, de Gouw J, Warneke C, Hansel A, Wisthaler A, Singh HB, Guenther A (2005) Global budget of methanol: constraints from atmospheric observations. J Geophys Res 110:D08303

Jacobson AR, Mikaloff Fletcher SE, Gruber N, Sarmiento JL, Gloor M (2007) A joint atmosphere–ocean inversion for surface fluxes of carbon dioxide, I: methods and global-scale fluxes. Glob Biogeochem Cycles 21. doi:10.1029/2005GB002556

Jaeglé L, Steinberger L, Martin RV, Chance K (2005) Global partitioning of NOx sources using satellite observations: relative roles of fossil fuel combustion, biomass burning and soil emissions. Faraday Discuss 130:407–423

Jaeglé L, Quinn PK, Bates TS, Alexander B, Lin J-T (2011) Global distribution of sea salt aerosols: new constraints from in situ and remote sensing observations. Atmos Chem Phys 11:3137–3157. doi:10.5194/acp-11-3137-2011

Jamet C, Moulin C, Lefèvre N (2007) Estimation of the oceanic pCO2 in the North Atlantic from VOS lines in-situ measurements: parameters needed to generate seasonally mean maps. Ann Geophys 25:2247–2257

Jammoul A, Dumas S, D'Anna B, George C (2009) Photoinduced oxidation of sea salt halides by aromatic ketones: a source of halogenated radicals. Atmos Chem Phys 9 (13):4229–4237

Jickells TS, An ZA, Baker AR, Bergametti G, Brooks N, Boyd PW, Duce RA, Hunter KA, Junji C, Kawahata H, Kubilay N, Anderson KK, la Roche J, Liss PS, Mahowald N, Prospero JM, Ridgwell AJ, Tegan I, Torres R (2005) Global iron connections between desert dust, ocean biogeochemistry and climate. Science 308:67–71

Johnson KS, Berelson WM, Boss ES, Chase Z, Claustre H, Emerson SR, Gruber N, Körtzinger A, Perry MJ, Riser SC (2009) Observing biogeochemical cycles at global scales with profiling floats and gliders, prospects for a global array. Oceanography 22(3):216–225

Jones N (2010) Sparks fly over theory that volcano caused salmon boom. Nat News. doi:10.1038/news.2010.572

Jones MT, Gislason SR (2008) Rapid releases of metal salts and nutrients following the deposition of volcanic ash into aqueous environments. Geochim Cosmochim Acta 72:3661–3680

Jones CE, Hornsby KE, Sommariva R, Dunk RM, von Glasow R, McFiggans G, Carpenter LJ (2010) Quantifying the contribution of marine organic gases to atmospheric iodine. Geophys Res Lett 37:L18804. doi:10.1029/2010GL043990

Jones CE, Andrews SJ, Carpenter LJ et al (2011) Results from the first national UK inter-laboratory calibration for very short-lived halocarbons. Atmos Meas Tech 4:865–874. doi:10.5194/amt-4-865-2011

Joos F, Plattner G-K, Stocker TF, Marchal O, Schmittner A (1999) Global warming and marine carbon cycle feedbacks on future atmospheric CO_2. Science 284:464–467

Kahn RA, Nelson DL, Garay MJ, Levy RC, Bull MA, Diner DJ, Martonchik MJ, Paradise SR, Hansen EG, Remer LA (2009) MISR aerosol product attributes and statistical comparisons with MODIS. IEEE Trans Geosci Remote Sens 47:4095–4114

Kaleschke L, Heygster G (2004) Towards multisensor microwave remote sensing of frost flowers on sea ice. Ann Glaciol 39:219–222

Keene WC, Long MS, Pszenny AAP, Sander R, Maben JR, Wall AJ, O'Halloran TL, Kerkweg A, Fischer EV, Schrems O (2009) Latitudinal variation in the multiphase chemical processing of inorganic halogens and related species over the eastern North and South Atlantic Oceans. Atmos Chem Phys 9:7361–7385

Kettle AJ, Andreae MO (2000) Flux of dimethylsulfide from the oceans: a comparison of updated data seas and flux models. J Geophys Res 105(D22):26793–26808

Kettle AJ, Andreae MO, Amouroux D et al (1999) A global database of sea surface dimethylsulfide (DMS) measurements and a procedure to predict sea surface DMS as a function of latitude, longitude, and month. Glob Biogeochem Cycles 13 (2):399–444. doi:10.1029/1999GB900004

Kieber RJ, Mopper K (1990) Determination of picomolar concentrations of carbonyl-compounds in natural-waters, including seawater, by liquid-chromatography. Environ Sci Technol 24:1477–1481

Kiliyanpilakkil VP, Meskhidze N (2011) Deriving the effect of wind speed on clean marine aerosol optical properties using the A-Train satellites. Atmos Chem Phys 11:11401–11413. doi:10.5194/acp-11-11401-2011

Kloster S, Six KD, Feichter J, Maier-Reimer E, Roeckner E, Wetzel P, Stier P, Esch M (2007) Response of dimethylsulfide (DMS) in the ocean and atmosphere to global warming. J Geophys Res 112:G03005. doi:10.1029/2006JG000224

Knepp TN, Bottenheim J, Carlsen M, Carlson D, Donohoue D, Friederich G, Matrai PA, Netcheva S, Perovich DK, Santini R, Shepson PB, Simpson W, Stehle R, Valentic T, Williams C, Wyss PJ (2010) Development of an autonomous sea ice tethered buoy for the study of ocean–atmosphere-sea ice-snow pack interactions: the O-buoy. Atmos Meas Tech 3:249–261

Kohonen T (1982) Self-organized formation of topologically correct feature maps. Biol Cybern 43:59–69

Kokhanovsky AA, de Leeuw G (eds) (2009) Satellite aerosol remote sensing over land. Springer-Praxis, Berlin, p 388. ISBN 978-3-540-69396-3

Korhonen H, Carslaw KS, Spracklen DV, Mann GW, Woodhouse MT (2008) Influence of oceanic dimethyl sulfide emissions on cloud condensation nuclei concentrations and seasonality over the remote Southern Hemisphere oceans: a global model study. J Geophys Res 113:D15204

Körtzinger A, Send U, Lampitt RS, Hartman S, Wallace DWR, Karstensen J, Villagarcia MG, Llinás O, DeGrandpre MD (2008) The seasonal pCO_2 cycle at 49°N/16.5°W in the northeastern Atlantic Ocean and what it tells us about biological productivity. J Geophys Res 113:C04020

Kostadinov TS, Siegel DA, Maritorena S (2010) Global variability of phytoplankton functional types from space: assessment via the particle size distribution. Biogeosciences Discuss 7:4295–4340. doi:10.5194/bg-7-3239-2010

Krishfield R, Toole J, Proshutinsky A, Timmermans M-L (2008) Automated ice-tethered profilers for seawater observations under pack ice in all seasons. J Atmos Ocean Technol 25 (11):2091–2105

Krueger AJ (1983) Sighting of El Chichón sulfur dioxide clouds with the Nimbus 7 total ozone mapping spectrometer. Science 220(4604):1377–1379

Kühn W, Pätsch J, Thomas H, Borges AV, Schiettecatte L-S, Bozec Y, Prowe AEF (2010) Nitrogen and carbon cycling in

the North Sea and exchange with the North Atlantic – a model study, Part II: carbon budget and fluxes. Cont Shelf Res 30:1701–1716. doi:10.1016/j.csr.2010.07.001

Kwok R (2010) Satellite remote sensing of sea-ice thickness and kinematics: a review. J Glaciol 56(200):1129–1140

Lachkar Z, Gruber N (2013) Response of biological production and air-sea CO_2 fluxes to upwelling intensification in the California and Canary Current Systems. J Mar Syst 109–110:149–160. doi:10.1016/j.jmarsys.2012.04.003

Lagerloef G, Swift C, LeVine D (1995) Sea surface salinity: the next remote sensing challenge. Oceanography 8:44–50

Lagerloef G, Boutin J, Chao Y, Delcroix T, Font J, Niiler P, Reul N, Riser S, Schmitt R, Stammer D, Wentz F (2010) Resolving the global surface salinity field and variations by blending satellite and in situ observations. In: Hall J, Harrison DE, Stammer D (eds) Proceedings of OceanObs'09: sustained ocean observations and information for society, vol 2. ESA Publication, Venice, 21–25 Sept 2009, WPP-306. doi:10.5270/OceanObs09.cwp.51

Lana A, Bell TG, Simó R, Vallina SM, Ballabrera-Poy J, Kettle AJ, Dachs J, Bopp L, Saltzman ES, Stefels J, Johnson JE, Liss PS (2011) An updated climatology of surface dimethlysulfide concentrations and emission fluxes in the global ocean. Glob Biogeochem Cycles 25(1):GB1004. doi:10.1029/2010GB003850

Langmann B, Zaksek K, Hort M, Duggen S (2010) Volcanic ash as fertiliser for the surface ocean. Atmos Chem Phys 10:3891–3899

Lapina K, Heald CL, Spracklen DV, Arnold SR, Allan JD, Coe H, McFiggans G, Zorn SR, Drewnick F, Bates TS, Hawkins LN, Russell LM, Smirnov A, O'Dowd C, Hind AJ (2011) Investigating organic aerosol loading in the remote marine environment. Atmos Chem Phys 11:8847–8860. doi:10.5194/acp-11-8847-2011

Law CS, Brévière E, de Leeuw G, Guieu C, Garçon VC, Kieber DJ, Kontradowitz S, Paulmier A, Quinn PK, Saltzman E, Stefels J, von Glasow R (2013) Evolving research directions in Surface Ocean Lower Atmosphere (SOLAS) science. Environ Chem 10:1–16, http://dx.doi.org/10.1071/EN12159

Le Clainche Y, Levasseur M, Vezina A et al (2006) Modelling analysis of the effect of iron enrichment on DMS dynamics in the NE Pacific (SERIES experiment). J Geophys Res 111. doi:10.1029/2005JC002947

Le Clainche Y et al (2010) A first appraisal of prognostic ocean DMS models and prospects for their use in climate models. Glob Biogeochem Cycles 24:GB3021. doi:10.1029/2009GB003721

Le Quéré C, Aumont O, Monfray P, Orr J (2003) Propagation of climatic events on ocean stratification, marine biology and CO_2: case studies over the 1979–1999 period. J Geophys Res 108. doi:10.1029/2001JC000920

Le Quéré CL, Harrison SP, Prentice C, Buitenhuis ET, Aumont O, Bopp L, Claustre H, Cotrim Da Cunha L, Geider R, Giraud X, Klaas C, Kohfeld KE, Legendre L, Manizza M, Platt T, Rivkin RB, Sathyendranath S, Uitz J, Watson AJ, Wolf-Gladrow D (2005) Ecosystem dynamics based on plankton functional types for global ocean biogeochemistry models. Glob Change Biol 11:2016–2040. doi:10.1111/j.1365-2486.2005.1004.x

Le Quéré C, Rödenbeck C, Buitenhuis ET, Conway TJ, Langenfelds R, Gomez A, Labuschagne C, Ramonet M, Nakazawa T, Metzl N, Gillett N, Heimann M (2007) Saturation of the Southern Ocean CO_2 sink due to recent climate change. Science 316:1735–1738

Le Vine DML, Lagerloef GSE, Colomb FR, Yueh SH, Member S, Pellerano FA, Member S (2007) Aquarius: an instrument to monitor sea surface salinity from space IEEET. Geosci Remote 45(7):2040–2050

Lee JD, Moller SJ, Read KA, Lewis AC, Mendes L, Carpenter LJ (2009a) Year-round measurements of nitrogen oxides and ozone in the tropical North Atlantic marine boundary layer. J Geophys Res 114:D21302. doi:10.1029/2009JD011878

Lee KH, Li Z, Kim YJ, Kokhanovsky AA (2009b) Atmospheric aerosol monitoring from satellite observations: a history of three decades. In: Kim YJ, Platt U, Gu MB, Iwahashi H (eds) Atmospheric and biological environmental monitoring. Springer, Berlin

Lefèvre N, Taylor A (2002) Estimating pCO_2 from sea surface temperatures in the Atlantic gyres. Deep-Sea Res I 49 (3):539–554

Lefèvre N, Watson AJ, Watson AR (2005) A comparison of multiple regression and neural network techniques for mapping in situ pCO_2 data. Tellus 57B:375–384

Lehahn Y, Koren I, Boss E, Ben-Ami Y, Altaratz O (2010) Estimating the maritime component of aerosol optical depth and its dependency on surface wind speed using satellite data. Atmos Chem Phys 10:6711–6720. doi:10.5194/acp-10-6711-2010

Lelieveld J, van Aardenne J, Fischer H, de Reus M, Williams J, Winkler P (2004) Increasing ozone over the Atlantic Ocean. Science 304:1483–1487

Lerot C, Stavrakou T, De Smedt I, Müller J-F, Van Roozendael M (2010) Glyoxal vertical columns from GOME-2 backscattered light measurements and comparisons with a global model. Atmos Chem Phys 10:12059–12072

Lewis ER, Schwartz SE (2004) Sea salt aerosol production: mechanisms, methods, measurements, and models: a critical review. American Geophysical Union, Washington, DC

Li X, Maring H, Savoie D, Voss K, Prospero JM (1996) Dominance of mineral dust in aerosol light-scattering in the North Atlantic trade winds. Nature 380(6573):416–419. doi:10.1038/380416a0

Lin II, Hu C, Li YH, Ho TY, Fischer TP, Wong GTF, Wu J, Huang CW, Chu DA, Ko DS, Chen JP (2011) Fertilization potential of volcanic dust in the low-nutrient low-chlorophyll western North Pacific subtropical gyre: satellite evidence and laboratory study. Glob Biogeochem Cycles 25:GB1006

Lindenthal A (2011) Phytoplankton growth in the NE Pacific. Diploma thesis, Institute of Geophysics, University of Hamburg, Germany (written in German)

Liss PS, Hatton AD, Malin G, Nightingale PD, Turner SM (1997) Marine sulphur emissions. Philos Trans R Soc Lond B Biol Sci 352:159. doi:10.1098/RSTB.1997.0011

Liu WT (2002) Progress in scatterometer application. J Oceanogr 58:121–136

Liu X, Penner JE, Das B, Bergmann D, Rodriguez JM, Strahan S, Wang M, Feng Y (2007) Uncertainties in global aerosol simulations, assessment using three meteorological data sets. J Geophys Res 112:D11212. doi:10.1029/2006JD008216

Liu WT, Tang W, Xie X, Navalgund R, Xu K (2008) Power density of ocean surface wind-stress from international

scatterometer tandem missions. Int J Remote Sens 29:6109–6116
Loisel H, Bosc E, Stramski D, Oubelkheir K, Deschamps PY (2001) Seasonal variability of the backscattering coefficient in the Mediterranean Sea based on Satellite SeaWiFS imagery. J Geophys Res Lett 28(22):4203–4206
Loisel H, Nicolas JM, Deschamps PY, Frouin R (2002) Seasonal and inter- annual variability of particulate organic matter in the global ocean. Geophys Res Lett 29(49):2196. doi:10.1029/2002GL015948
Longhurst AR (2007) Ecological geography of the sea, 2nd edn. Academic, Burlington/Boston
Lüger H, Wallace DWR, Körtzinger A, Nojiri Y (2004) The pCO_2 varability in the midlatitude North Atlantic Ocean during a full annual cycle. Glob Biogeochem Cycles 18: GB3023. doi:10.1029/2003GB002200
Mahajan AS, Plane JMC, Oetjen H, Mendes L, Saunders RW, Saiz-Lopez A, Jones CE, Carpenter LJ, McFiggans GB (2010) Measurement and modelling of tropospheric reactive halogen species over the tropical Atlantic Ocean. Atmos Chem Phys 10:4611–4624
Marbach T, Beirle S, Platt U, Hoor P, Wittrock F, Richter A, Vrekoussis M, Grzegorski M, Burrows JP, Wagner T (2009) Satellite measurements of formaldehyde linked to shipping emissions. Atmos Chem Phys 9:8223–8234
Maritorena S, d'Andon OHF, Mangin A, Siegel DA (2010) Merged satellite ocean color data products using a bio-optical model: characteristics, benefits and issues. Remote Sens Environ 114(8):1791–1804
Mårtensson EM, Nilsson ED, de Leeuw G, Cohen LH, Hansson H-C (2003) Laboratory simulations and parameterizations of the primary marine aerosol productions. J Geophys Res 108:4297
Martin JH, Fitzwater SE (1988) Iron deficiency limits phytoplankton growth in the north-east Pacific subarctic. Nature 331:341–343
Martin M, Dash P, Ignatov A, Banzon V, Beggs H, Brasnett B, Cayula J-F, Cummings J, Donlon C, Gentemann C, Grumbine R, Ishizaki S, Maturi E, Raynolds RW, Roberts-Jones J (2012) Group for High Resolution Sea Surface temperature (GHRSST) analysis fields inter-comparisons. Part 1: a GHRSST multi-product ensemble (GMPE). Deep-Sea Res II. http://dx.doi.org/10.1016/j.dsr2.2012.04.013
Martino M, Mills GP, Woeltjen J, Liss PS (2009) A new source of volatile organoiodine compounds in surface seawater. Geophys Res Lett 36:L01609. doi:10.1029/2008GL036334
Massom RA (2009) Principal uses of remote sensing in sea ice field research. In: Eicken H, Gradinger R, Salganek M, Shirasawa K, Perovich D, Leppäranta M (eds) Field techniques for sea ice research. University of Alaska Press, Fairbanks, pp 405–466
McDonald D, Pedersen TF (1999) Multiple late Quaternary episodes of exceptional diatom production in the Gulf of Alaska. Deep-Sea Res II 46:2993–3017
McGillicuddy DJ, Johnson RJ, Siegel DA, Michaels AF, Bates NR, Knap AH (1999) Mesoscale variations of biogeochemical properties in the Sargasso Sea. J Geophys Res 104:13381–13394
McGillicuddy DJ, Anderson LA, Bates NR, Bibby T, Buesseler KO, Carlson CA, Davis CS, Ewart C, Falkowski PG, Goldthwait SA, Hansell DA, Jenkins WJ, Johnson R, Kosnyrev VK, Ledwell JR, Li QP, Siegel DA, Steinberg DK (2007) Eddy/wind interactions stimulate extraordinary mid-ocean plankton blooms. Science 316(5827):1016–1021. doi:10.1126/science.1136256
McKinley GA, Follows MJ, Marshall J (2004) Mechanisms of air-sea CO_2 flux variability in the equatorial Pacific and the North Atlantic. Glob Biogeochem Cycles 18:GB2011. doi:10.1029/2003GB002179
Meissner T, Wentz FJ (2009) Wind-vector retrievals under rain with passive satellite microwave radiometers. IEEE Trans Geosci Remote Sens 47(9):3065–3083. doi:10.1109/TGRS.2009.2027012
Mikaloff Fletcher SE, Gruber N, Jacobson AR, Doney SC, Dutkiewicz S, Gerber M, Gloor M, Follows M, Joos F, Lindsay K, Menemenlis D, Mouchet A, Müller SA, Sarmiento JL (2007) Inverse estimates of the oceanic sources and sinks of natural CO_2 and the implied oceanic transport. Glob Biogeochem Cycles 21:GB1010. doi:10.1029/2006GB002751
Mikaloff-Fletcher SE, Gruber N, Jacobson AR, Doney SC, Dutkiewicz S, Gerber M, Follows M, Joos F, Lindsay K, Menemenlis D, Mouchet A, Mueller SA, Sarmiento JL (2006) Inverse estimates of anthropogenic CO_2 uptake, transport, and storage by the ocean. Glob Biogeochem Cycles 20:GB2002. doi:10.1029/2005GB002530
Mills MM, Ridame C, Davey M, La Roche J, Geider RJ (2004) Iron and phosphorous co-limit nitrogen fixation in the eastern tropical North Atlantic. Nature 429:292–294
Mohanan EC, O'Muircheartaigh IG (1980) Optimal power-law description of oceanic whitecap coverage dependence on wind speed. J Phys Ocean 10:2094–2099
Montzka SA, Reimann S (2011) Ozone depleting substances (ODS's) and related chemicals, Chapter 1 in: scientific assessment of ozone depletion: 2010. Global Ozone Research and Monitoring Project, Report No. 52, 373 pp
Moore CM, Mills MM, Achterberg EP, Geider RJ, La Roche J, Lucas MI, McDonagh EL, Pan X, Poulton AJ, Rijkenberg MJA, Suggett DJ, Ussher SJ, Woodward MJ (2009) Large-scale distribution of Atlantic nitrogen fixation controlled by iron availability. Nat Geosci. doi:10.1038/ngeo667
Mouw CB, Yoder JA (2010) Optical determination of phytoplankton size composition from global SeaWiFS imagery. J Geophys Res 115:C12018. doi:10.1029/2010JC006337
Mulcahy JP, O'Dowd CD, Jennings SG, Ceburnis D (2008) Significant enhancement of aerosol optical depth in marine air under high wind conditions. Geophys Res Lett 35: L16810. doi:10.1029/2008GL034303
Müller C, Iinuma Y, Karstensen J, van Pinxteren D, Lehmann S, Gnauk T, Herrmann H (2009) Seasonal variation of aliphatic amines in marine sub-micrometer particles at the Cape Verde islands. Atmos Chem Phys 9(24):9587–9597
Myhre G, Stordal F, Johnsrud M, Ignatov A, Mishchenko MI, Geogdzhayev IV, Tanré D, Deuzé JL, Goloub P, Nakajima T, Higurashi A, Torres O, Holben BN (2004) Intercomparison of satellite retrieved aerosol optical depth over ocean. J Atmos Sci 61:499–513
Myhre G, Stordal F, Johnsrud M, Diner DJ, Geogdzhayev IV, Haywood JM, Holben BN, Holzer-Popp T, Ignatov A, Kahn RA, Kaufman YJ, Loeb N, Martonchik JV, Mishchenko MI, Nalli NR, Remer LA, Schroedter-

Homscheidt M, Tanré D, Torres O, Wang M (2005) Intercomparison of satellite retrieved aerosol optical depth over ocean during the period September 1997 to December 2000. Atmos Chem Phys 5:1697–1719

Newsam GN, Enting IG (1988) Inverse problems in atmospheric constituent studies: I. Determination of surface sources under a diffusive transport approximation. Inverse Probl 4:1037–1054

Nie C, Long DG (2008) A C-band scatterometer simultaneous wind/rain retrieval method. IEEE Trans Geosci Remote Sens 46:3618–3632

Nightingale PD, Malin G, Law CS, Watson AJ, Liss PS, Liddicoat MI, Boutin J, Upstill-Goddard RC (2000) In situ evaluation of air-sea gas exchange parameterizations using novel conservative and volatile tracers. Glob Biogeochem Cycles 14(1):373–387

Nowlan CR, Liu X, Chance K, Cai Z, Kurosu TP, Lee C, Martin RV (2011) Retrievals of sulfur dioxide from the Global Ozone Monitoring Experiment 2 (GOME-2) using an optimal estimation approach: algorithm and initial validation. J Geophys Res 116:D18301. doi:10.1029/2011JD015808

O'Dowd CD, de Leeuw G (2007) Marine aerosol production: a review of the current knowledge. Philos Trans R Soc A 365:1753–1774. doi:10.1098/rsta.2007.2043

O'Dowd CD, Facchini MC, Cavalli F, Ceburnis D, Mircea M, Decesari S, Fuzzi S, Yoon YL, Putaud JP (2004) Biogenically driven organic contribution to marine aerosol. Nature 431:676. doi:10.1038/NATURE02959

O'Dowd C, Scannell C, Mulcahy J, Jennings SG (2010) Wind speed influences on marine aerosol optical depth. Adv Meteorol 2010:830846. doi:10.1155/2010/830846

Okin GS, Baker AR, Tegen I, Mahowald NM, Dentener FJ, Duce RA, Galloway JN, Hunter K, Kanakidou M, Kubilay N, Prospero JM, Sarin M, Surapipith V, Uematsu M, Zhu T (2011) Impacts of atmospheric nutrient deposition on marine productivity: roles of nitrogen, phosphorus, and iron. Glob Biogeochem Cycles 25:GB2022. doi:10.1029/2010GB003858

Olgun N, Duggen S, Croot P, Dietze H, Schacht U, Oskarsson N, Siebe C, Auer A (2011) Surface ocean iron fertilization: the role of subduction zone and hotspot volcanic ash and fluxes into the Pacific Ocean. Glob Biogeochem Cycles 25. doi:10.1029/2009GB003761

Olgun N, Duggen S, Langmann B, Hort M, Waythomas CF, Hoffmann L, Croot P (2013) Geochemical evidence for oceanic iron fertilization from the Kasatochi volcanic eruption and evaluation of the potential impacts on sockeye salmon population. Mar Ecol Prog Ser (in press)

Olsen A, Bellerby RGJ, Johannesseen T, Omar AM, Skjelvan I (2003) Interannual variability in the wintertime air-sea flux of carbon dioxide in the northern North Atlantic, 1981–2001. Deep-Sea Res I 50:1323–1338

Ono S, Ennyu A, Najjar RG, Bates NR et al (2001) Shallow remineralisation in the Sargasso Sea estimated from seasonal variations in oxygen, dissolved inorganic carbon and nitrate. Deep-Sea Res II 48(8–9):1567–1582. doi:10.1016/S0967-0645(00)00154-5

Parsons TR, Whitney FA (2012) Did volcanic ash from Mt. Kasatochi in 2008 contribute to a phenomenal increase in Fraser River sockeye salmon (Oncorhynchus nerka) in 2010? Fish Oceanogr 21:374–377. doi:10.1111/j.1365-2419.2012.00630.x

Perovich D (2009) Automatic measurement stations. In: Eicken H, Gradinger R, Salganek M, Shirasawa K, Perovich D, Leppäranta M (eds) Field techniques for sea ice research. University of Alaska Press, Fairbanks, pp 383–394

Perovich DK, Eicken H, Meier W (2012) International coordination to improve studies of changes in Arctic sea ice cover. Eos 93(12):128

Pfeil B, Olsen A, Bakker DCE, Hankin S, Koyuk H, Kozyr A, Malczyk J, Manke A, Metzl N, Sabine CL, Akl J, Alin SR, Bates N, Bellerby RGJ, Borges A, Boutin J, Brown PJ, Cai W-J, Chavez FP, Chen A, Cosca C, Fassbender AJ, Feely RA, González-Dávila M, Goyet C, Hales B, Hardman-Mountford N, Heinze C, Hood M, Hoppema M, Hunt CW, Hydes D, Ishii M, Johannessen T, Jones SD, Key RM, Körtzinger A, Landschützer P, Lauvset SK, Lefèvre N, Lenton A, Lourantou A, Merlivat L, Midorikawa T, Mintrop L, Miyazaki C, Murata A, Nakadate A, Nakano Y, Nakaoka S, Nojiri Y, Omar AM, Padin XA, Park G-H, Paterson K, Perez FF, Pierrot D, Poisson A, Ríos AF, Salisbury J, Santana-Casiano JM, Sarma VVSS, Schlitzer R, Schneider B, Schuster U, Sieger R, Skjelvan I, Steinhoff T, Suzuki T, Takahashi T, Tedesco K, Telszewski M, Thomas H, Tilbrook B, Tjiputra J, Vandemark D, Veness T, Wanninkhof R, Watson AJ, Weiss R, Wong CS, Yoshikawa-Inoue H (2013) A uniform, quality controlled Surface Ocean CO_2 Atlas (SOCAT). Earth Syst Sci Data 5:125–143. doi:10.5194/essd-5-125-2013

Pierce JR, Adams PJ (2006) Global evaluation of CCN formation by direct emission of sea salt and growth of ultrafine sea salt. J Geophys Res 111:D06203. doi:10.1029/2005JD006186

Pierrot D, Neill C, Sullivan K, Castle R, Wanninkhof R, Lüger H, Johannessen T, Olsen A, Feely RA, Cosca CE (2009) Recommendations for autonomous underway pCO_2 measuring systems and data reduction routines. Deep-Sea Res II 56:512–522. doi:10.1016/j.dsr2.2008.12.005

Plass-Dülmer C, Koppmann R, Ratte M, Rudolph J (1995) Light nonmethane hydrocarbons in seawater. Glob Biogeochem Cycles 9:79. doi:10.1029/94GB02416

Powell CF, Baker AR, Jickells TD, Bange HW (in preparation) Estimation of the atmospheric flux of iron, nitrogen and phosphate to the eastern tropical North Atlantic

Previdi M, Fennel K, Wilkin J, Haidvogel DB (2009) Interannual variability in atmospheric CO_2 uptake on the Northeast US Continental Shelf. J Geophys Res 114:G04003. doi:10.1029/2008JG000881

Prinn RG, Weiss RF, Fraser PJ et al (2000) A history of chemically and radiatively important gases in air deduced from ALE/GAGE/AGAGE. J Geophys Res 105:17751–17792. doi:10.1029/2000JD900141

Prospero JM, Lamb PJ (2003) African droughts and dust transport to the Caribbean: climate change implications. Science 302:1024–1027

Prospero JM, Nees RT (1986) Impact of the North African drought and El Nino on mineral dust in the Barbados trade winds. Nature 320(6064):735–738. doi:10.1038/320735a0

Prowe AEF, Thomas H, Pätsch J, Kühn W, Bozec Y, Schiettecatte L-S, Borges AV, de Baar HJW (2009) Mechanisms controlling the air-sea CO_2 flux in the North Sea. Cont Shelf Res 29:1801–1808. doi:10.1016/j.csr.2009.06.003

Qin AK, Clausi DA (2010) Multivariate image segmentation using semantic region growing with adaptive edge penalty. IEEE Trans Image Proc 19:2157–2170

Quack B, Atlas E, Petrick G, Schauffler S, Wallace D (2004) Oceanic bromoform sources for the tropical atmosphere. Geophys Res Lett. doi:10.1029/2004GL020597

Quack B, Peeken I, Petrick G, Nachtigall K (2007) Oceanic distribution and sources of bromoform and dibromomethane in the Mauritanian upwelling. J Geophys Res 112:C10006. doi:10.1029/2006JC003803

Quilfen Y, Vandemark D, Chapron B, Feng H, Sienkiewicz J (2011) Estimating gale to hurricane force winds using the satellite altimeter. J Atmos Ocean Technol 28:453–458. doi:10.1175/JTECH-D-10-05000.1

Quinn PK, Bates TS (2005) Regional aerosol properties: comparisons of boundary layer measurements from ACE 1, ACE 2, Aerosols99, INDOEX, ACE Asia, TARFOX, and NEAQS. J Geophys Res 110(D14):D14202

Raitsos DE, Lavender SJ, Maravelias CD, Haralambous J, Richardson AJ, Reid PC (2008) Identifying four phytoplankton functional types from space: an ecological approach. Limnol Oceanogr 53(2):605–613

Read KA, Mahajan AS, Carpenter LJ, Evans MJ, Faria BE, Heard DE, Hopkins JR, Lee JD, Moller SJ, Lewis AC, Mendes L, McQuaid JB, Oetjen H, Saiz-Lopez A, Pilling MJ, Plane JMC (2008) Extensive halogen-mediated ozone destruction over the tropical Atlantic Ocean. Nature 453:1232–1235. doi:10.1038/nature07035

Read KA, Carpenter LJ, Arnold SR, Beale R, Nightingale PD, Hopkins JR, Lewis AC, Mendes L, Fleming ZL (2012) Time-series and atmospheric budgets of acetone, methanol and acetaldehyde in remote marine air at the Cape Verde Atmospheric Observatory. Environ Sci Technol 46 (20):11028–11039. doi:10.1021/es302082p

Remer LA et al (2008) Global aerosol climatology from the MODIS satellite sensors. J Geophys Res 113:D14S07. doi:10.1029/2007JD009661

Reul N, Tenerelli J, Boutin J, Chapron B, Paul F, Brion E, Gaillard F, Archer O (2012a) Overview of the first SMOS sea surface salinity products. Part I: quality assessment for the second half of 2010. IEEE Trans Geosci Remote Sens 99:1–12, http://dx.doi.org/10.1109/TGRS.2012.2188408

Reul N, Tenerelli J, Chapron B, Vandemark D, Quilfen Y, Kerr Y (2012b) SMOS satellite L-band radiometer: a new capability for ocean surface remote sensing in hurricanes. J Geophys Res 117:C02006. doi:10.1029/2011JC007474

Richter A, Wittrock F, Eisinger M, Burrows JP (1998) GOME observations of tropospheric BrO in Northern Hemispheric spring and summer 1997. Geophys Res Lett 25:2683–2686

Richter A, Eyring V, Burrows JP, Bovensmann H, Lauer A, Sierk B, Crutzen PJ (2004) Satellite measurements of NO_2 from international shipping emissions. Geophys Res Lett 31: L23110. doi:10.1029/2004GL020822

Rijkenberg MJA, Langlois RJ, Mills MM, Patey MD, Hill PG, Nielsdottir MC, Compton TJ, La Roche J, Achterberg EP (2011) Environmental forcings of nitrogen fixation in the eastern (sub-) tropical North Atlantic Ocean. PlosOne 6 (12):e28989

Rintoul SR, Sparrow M, Meredith MP, Wadley V, Speer K, Hofmann E, Summerhayes C, Urban E, Bellerby R (eds) (2012) The Southern Ocean observing system: initial science and implementation strategy. SOOS International Project Office, Hobart. ISBN 978-0-948277-27-6

Rödenbeck C, Houweling S, Gloor M, Heimann M (2003) CO_2 Flux History 1982–2001 Inferred from atmospheric data using a global inversion of atmospheric transport. Atmos Chem Phys 3:1919–1964

Rödenbeck C, Le Quéré C, Heimann M, Keeling R (2008) Interannual variability in oceanic biogeochemical processes inferred by inversion of atmospheric O_2/N_2 and CO_2 data. Tellus 60B:685

Roeckner E et al (2006) Sensitivity of simulated climate to horizontal and vertical resolution in the ECHAM5 atmosphere model. J Clim 19:3771–3791. doi:10.1175/JCLI3824.1

Roemmich D et al (2009) Argo: the challenge of continuing 10 years of progress. Oceanography 2(30):46–55. http://www.knmi.nl/publications/fulltexts/roemmich_et_al.oceanography_godae_09.pdf. Accessed 25 Jan 2012

Röhrs J, Kaleschke L, Bröhan D, Siligam PK (2012) An algorithm to detect sea ice leads by using AMSR-E passive microwave imagery. The Cryosphere 6(2):343–352

Roy T, Bopp L, Gehlen M, Schneider B, Cadule P, Frölicher TL, Segschneider J, Tjiputra J, Heinze C, Joos F (2011) Regional impacts of climate change and atmospheric CO_2 on future ocean carbon uptake: a multi-model linear feedback analysis. J Clim 24:2300–2318

Sabine CL, Feely RA, Gruber N, Key RM, Lee K, Bullister JL, Wanninkhof R, Wong CS, Wallace DWR, Tilbrook B, Millero FJ, Peng T-H, Kozyr A, Ono T, Ríos AF (2004) The oceanic sink for anthropogenic CO_2. Science 305:367–371

Sabine CL, Hankin S, Koyuk H, Bakker DCE, Pfeil B, Olsen A, Metzl N, Kozyr A, Fassbender A, Manke A, Malczyk J, Akl J, Alin SR, Bellerby RGJ, Borges A, Boutin J, Brown PJ, Cai W-J, Chavez FP, Chen A, Cosca C, Feely RA, González-Dávila M, Goyet C, Hardman-Mountford N, Heinze C, Hoppema M, Hunt CW, Hydes D, Ishii M, Johannessen T, Key RM, Körtzinger A, Landschützer P, Lauvset SK, Lefèvre N, Lenton A, Lourantou A, Merlivat L, Midorikawa T, Mintrop L, Miyazaki C, Murata A, Nakadate A, Nakano Y, Nakaoka S, Nojiri Y, Omar AM, Padin XA, Park G-H, Paterson K, Perez FF, Pierrot D, Poisson A, Ríos AF, Salisbury J, Santana Casiano JM, Sarma VVSS, Schlitzer R, Schneider B, Schuster U, Sieger R, Skjelvan I, Steinhoff T, Suzuki T, Takahashi T, Tedesco K, Telszewski M, Thomas H, Tilbrook B, Vandemark D, Veness T, Watson AJ, Weiss R, Wong CS, Yoshikawa-Inoue H (2013) Gridding of the Surface Ocean CO_2 Atlas (SOCAT) gridded data products. Earth Syst Sci Data 5:145–153. doi:10.5194/essd-5-145-2013

Sadeghi A, Dinter T, Vountas M, Taylor B, Peeken I, Bracher A (2011) Improvements to the PhytoDOAS method for the identification of major Phytoplankton groups using high spectrally resolved satellite data. Ocean Sci Discuss 8:2271–2311. doi:10.5194/osd-8-2271-2011

Sadeghi A, Dinter T, Vountas M, Taylor B, Altenburg-Soppa M, Bracher A (2012) Remote sensing of coccolithophore blooms in selected oceanic regions using the PhytoDOAS method applied to hyper-spectral satellite data. Biogeosciences 9:2127–2143. doi:10.5194/bg-9-2127-2012

Saiz-lopez A, Chance K, Liu X, Kurosu TP, Sander S (2007) First observations of iodine oxide from space. Geophys Res Lett 34:L12812. doi:10.1029/2007GL030111

Sander R, Crutzen PJ (1996) Model study indicating halogen activation and ozone destruction in polluted air masses transported to the sea. J Geophys Res 101:9121–9138

Sarmiento JL, Hughes TMC, Stouffer RJ, Manabe S (1998) Simulated response of the ocean carbon cycle to anthropogenic climate warming. Nature 393:245–249

Sathyendranath S, Watts L, Devred E, Platt T, Caverhill C, Maass H (2004) Discrimination of diatoms from other phytoplankton using ocean-colour data. Mar Ecol Prog Ser 272:59–68

Schönhardt A, Richter A, Wittrock F, Kirk H, Oetjen H, Roscoe HK, Burrows JP (2008) Observations of iodine monoxide columns from satellite. Atmos Chem Phys 8:637–653

Schuster U et al (2009) Trends in North Atlantic sea-surface fCO_2 from 1990 to 2006. Deep-Sea Res II 56 (8–10):620–629. doi:10.1016/j.dsr2.2008.12.011

Schuster U, McKinley GA, Bates N, Chevallier F, Doney SC, Fay AR, González-Dávila M, Gruber N, Jones S, Krijnen J, Landschützer P, Lefèvre N, Manizza M, Mathis J, Metzl N, Olsen A, Rios AF, Rödenbeck C, Santana-Casiano JM, Takahashi T, Wanninkhof R, Watson AJ (2012) Atlantic and Arctic sea-air CO_2 Fluxes, 1990–2009. Biogeosciences Discuss 9:10669–10724

Siegel DA, Peterson P, McGillicuddy DJ, Maritorena S, Nelson NB (2011) Bio-optical footprints created by mesoscale eddies in the Sargasso Sea. Geophys Res Lett 38:L13608. doi:10.1029/2011GL047660

Simó R, Dachs J (2002) Global ocean emission of dimethylsulfide predicted from biogeophysical data. Glob Biogeochem Cycles 16(4):1018. doi:10.1029/2001GB001829

Simó R, Pedrós-Alio C (1999) Role of vertical mixing in controlling the oceanic production of dimethyl sulphide. Nature 402:396–399

Singh HB, Kanakidou M, Crutzen PJ, Jacob DJ (1995) High concentrations and photochemical fate of oxygenated hydrocarbons in the global troposphere. Nature 378:50–54

Singh HB, Tabazadeh A, Evans MJ, Field BD, Jacob DJ, Sachse G, Crawford JH, Shetter R, Brune WH (2003) Oxygenated volatile organic chemicals in the oceans: interferences and implications based on atmospheric observations and air–sea flux exchange models. Geophys Res Lett 30:1862. doi:10.1029/2003GL017933

Small R, deSzoeke SP, Xie SP, O'Neill LO, Seo H, Song Q, Cornillon P, Spall M, Minobe S (2008) Air-sea interaction over ocean fronts and eddies. Dyn Atmos Ocean 45:274–319

Smirnov A, Holben BN, Giles DM, Slutsker I, O'Neill NT, Eck TF, Macke A, Croot P, Courcoux Y, Sakerin SM, Smyth TJ, Zielinski T, Zibordi G, Goes JI, Harvey MJ, Quinn PK, Nelson NB, Radionov VF, Duarte CM, Losno R, Sciare J, Voss KJ, Kinne S, Nalli NR, Joseph E, Krishna Moorthy K, Covert DS, Gulev SK, Milinevsky G, Larouche P, Belanger S, Horne E, Chin M, Remer LA, Kahn RA, Reid JS, Schulz M, Heald CL, Zhang J, Lapina K, Kleidman RG, Griesfeller J, Gaitley BJ, Tan Q, Diehl TL (2011) Maritime aerosol network as a component of AERONET – first results and comparison with global aerosol models and satellite retrievals. Atmos Meas Tech 4:583–597. doi:10.5194/amt-4-583-2011

Smirnov A, Sayer AM, Holben BN, Hsu NC, Sakerin SM, Macke A, Nelson NB, Courcoux Y, Smyth TJ, Croot P, Quinn PK, Sciare J, Gulev SK, Piketh S, Losno R, Kinne S, Radionov VF (2012) Effect of wind speed on aerosol optical depth over remote oceans, based on data from the Maritime Aerosol Network. Atmos Meas Tech 5:377–388. doi:10.5194/amt-5-377-2012

Smith RC, Baker KS (1978) The bio-optical state of ocean waters and remote sensing. Limnol Oceanogr 23:247–259

Smith MA, White M (1985) Observations on lakes near Mount St. Helens: phytoplankton. J Arch Hydrobiol 104:345–363

Sofiev M, Soares J, Prank M, de Leeuw G, Kukkonen J (2011) A regional-to-global model of emission and transport of sea salt particles in the atmosphere. J Geophys Res 116:D21302. doi:10.1029/2010JD014713

Soh L-K, Tsatsoulis C, Gineris D, Bertoia C (2004) ARKTOS: an intelligent system for SAR sea ice image classification. IEEE Trans Geosci Remote Sens 42:229–248

Steinberg DK, Carlson CA, Bates NR, Johnson RJ, Michaels AF, Knap AH (2001) Overview of the US JGOFS Bermuda Atlantic Time-series Study (BATS): a decade-scale look at ocean biology and biogeochemistry. Deep-Sea Res II 48 (8–9):1405–1447. doi:10.1016/S0967-0645(00)00148-X

Steinhoff T, Friedrich T, Hartman SE, Oschlies A, Wallace DWR, Körtzinger A (2010) Estimating mixed layer nitrate in the North Atlantic Ocean. Biogeosciences 7:795–807

Stewart DJ, Taylor CM, Reeves CE, McQuaid JB (2008) Biogenic nitrogen oxide emissions from soils: impact on NOx and ozone over west Africa during AMMA (African Monsoon Multidisciplinary Analysis): observational study. Atmos Chem Phys 8:2285–2297. doi:10.5194/acp-8-2285-2008

Stramski D (1999) Refractive index of planktonic cells as a measure of cellular carbon and chlorophyll a content. Deep-Sea Res I 46:335–351

Stramski D, Reynolds RA, Babin M, Kaczmarek S, Lewis MR, Röttgers R, Sciandra A, Stramska M, Twardowski MS, Claustre H (2008) Relationship between the surface concentration of particulate organic carbon and optical properties in the eastern South Pacific and eastern Atlantic Oceans. Biogeosciences 5:171–201

Takahashi T et al (2009) Climatological mean and decadal change in surface ocean pCO_2, and net sea-air CO_2 flux over the global oceans. Deep-Sea Res II 56(8–10):554–577. doi:10.1016/j.dsr2.2008.12.009

Tebaldi C, Knutti R (2007) The use of the multi-model ensemble in probabilistic climate projections. Phil Trans R Soc A 365:2053–2075

Telszewski M et al (2009) Estimating the monthly pCO_2 distribution in the North Atlantic using a self-organizing neural network. Biogeosciences 6:1405–1421

Textor C et al (2006) Analysis and quantification of the diversities of aerosol life cycles within AeroCom. Atmos Chem Phys 6:1777–1813

Textor C et al (2007) The effect of harmonized emissions on aerosol properties in global models – an AeroCom experiment. Atmos Chem Phys 7:4489–4501

Thomas H, Prowe F, Lima ID, Doney SC, Wanninkhof R, Greatbatch RJ, Schuster U, Corbière A (2008) Changes in the North Atlantic Oscillation influence CO_2 uptake in the North Atlantic over the past 2 decades. Glob Biogeochem Cycles 22(4):1–13. doi:10.1029/2007GB003167

Tie X, Guenther A, Holland E (2003) Biogenic methanol and its impacts on tropospheric oxidants. Geophys Res Lett 30:1881

Toole DA, Siegel DA, Doney SC (2008) A light-driven, one-dimensional dimethylsulfide biogeochemical cycling

model for the Sargasso Sea. J Geophys Res 113:G02009. doi:10.1029/2007JG000426

Trapp JM, Millero FJ, Prospero JM (2010) Temporal variability of the elemental composition of African dust measured in trade wind aerosols at Barbados and Miami. Mar Chem 20:71–82

Turi G, Lachkar Z, Gruber N (2013) Spatiotemporal variability of air-sea CO_2 fluxes and pCO_2 in the California current system: an eddy-resolving modeling study. J Geophys Res (in press)

Turner SM, Harvey MJ, Law CS, Nightingale PD, Liss PS (2004) Iron-induced changes in oceanic sulfur biogeochemistry. Geophys Res Lett 31. doi:10.1029/2004GL020296

Uematsu M, Toratani M, Narita Y, Senga Y, Kimoto T (2004) Enhancement of primary productivity in the western North Pacific caused by the eruption of the Miyake-jima volcano. Geophys Res Lett 31:1–4

Uitz J, Claustre H, Morel A, Hooker SB (2006) Vertical distribution of phytoplankton communities in open ocean: an assessment based on surface chlorophyll. J Geophys Res 111:CO8005. doi:10.1029/2005JC003207

Valsala V, Maksyutov S (2010) Simulation and assimilation of global ocean pCO2 and air–sea CO2 fluxes using ship observations of surface ocean pCO2 in a simplified biogeochemical offline model. Tellus 62B:821–840. doi:10.1111/j.1600-0889.2010.00495.x

Vogt R, Crutzen PJ, Sander R (1996) A mechanism for halogen release from sea-salt aerosol in the remote marine boundary layer. Nature 383:327–330

von Glasow R, Sander R, Bott A, Crutzen PJ (2002a) Modeling halogen chemistry in the marine boundary layer – 1. Cloud-free MBL. J Geophys Res 107:4341. doi:10.1029/2001JD000942

von Glasow R, Sander R, Bott A, Crutzen PJ (2002b) Modeling halogen chemistry in the marine boundary layer – 2. Interactions with sulfur and the cloud-covered MBL. J Geophys Res 107:4323

von Glasow R, von Kuhlmann R, Lawrence MG, Platt U, Crutzen PJ (2004) Impact of reactive bromine chemistry in the troposphere. Atmos Chem Phys 4:2481–2497

Vrekoussis M, Wittrock F, Richter A, Burrows JP (2009) Temporal and spatial variability of glyoxal as observed from space. Atmos Chem Phys 9:4485–4504

Wagner T, Platt U (1998) Satellite mapping of enhanced BrO concentrations in the troposphere. Nature 395:486–490

Wanninkhof R (1992) Relationship between wind speed and gas exchange over the ocean. J Geophys Res 97 (C5):7373–7382

Wanninkhof R, McGillis WR (1999) A cubic relationship between air-sea CO_2 gas exchange and wind speed. Geophys Res Lett 26:1889–1892

Watson AJ, Robinson C, Robinson JE, Williams PJB, Fasham MJR (1991) Spatial variability in the sink for atmospheric carbon dioxide in the North Atlantic. Nature 350:50–53

Watson AJ et al (2009) Tracking the variable North Atlantic sink for atmospheric CO_2. Science 326(5958):1391–1393. doi:10.1126/science.1177394

Weissman DE, Bourassa MA, Tongue J (2002) Effects of rain rate and wind magnitude on Sea Winds scatterometer wind speed errors. J Atmos Ocean Technol 19:738–746

Whalley LK, Furneaux KL, Goddard A, Lee JD, Mahajan A, Oetjen H, Read KA, Kaaden N, Carpenter LJ, Lewis AC, Plane JMC, Saltzman ES, Wiedensohler A, Heard DE (2010) The chemistry of OH and HO_2 radicals in the boundary layer over the tropical Atlantic Ocean. Atmos Chem Phys 10(4):1555–1576

Whitney FA, Crawford DW, Yoshimura T (2005) The uptake and export of Si and N in HNLC waters of the NE Pacific. Deep-Sea Res II 52:1055–1067

Williams JE, Holzinger R, Gros V, Xu X, Atlas E, Wallace DWR (2004) Measurements of organic species in air and seawater from the tropical Atlantic. Geophys Res Lett 31:L23S06

Williams JC, Drummond BA, Buxton RT (2010) Initial effects of the August 2008 volcanic eruption on breeding birds and marine mammals at Kasatochi Island, Alaska. Arct Antarct Alp Res 42:306–314

Wingenter OW, Elliott SM, Blake DR (2007) New directions: enhancing the natural sulfur cycle to slow global warming. Atmos Environ. doi:10.1016/j.atmosenv.2007.07.021

Wong CS, Matear RJ (1999) Sporadic silicate limitation of phytoplankton productivity in the subarctic NE Pacific. Deep-Sea Res II 46:2539–2555

Woolf DK, Bowyer PA, Monahan EC (1987) Discriminating between the film drops and jet drops produced by a simulated whitecap. J Geophys Res 92:5142–5150

Wunsch C, Heimbach P (2007) Practical global oceanic state estimation. Physica D 230:197–208. doi:10.1016/j.physd.2006.09.040

Yassaa N, Peeken I, Zöllner E, Bluhm K, Arnold S, Spracklen D, Williams J (2008) Evidence for marine production of monoterpenes. Environ Chem 5:391–401. doi:10.1071/EN08047

Young RW, Carder KL, Betzer PR, Costello DK, Duce RA, DiTuio GR, Tindale NW, Laws EA, Uematsu M, Merril JT, Feely RA (1991) Atmospheric iron inputs and primary productivity: phytoplankton responses in the North Pacific. Glob Biogeochem Cycles 5:119–134

Ziska F, Quack B, Abrahamsson K, Archer SD, Atlas E, Bell T, Butler JH, Carpenter LJ, Jones CE, Harris NRP, Hepach H, Heumann KG, Hughes C, Kuss J, Krüger K, Liss P, Moore RM, Orlikowska A, Raimund S, Reeves CE, Reifenhaeuser W, Robinson AD, Schall C, Tanhua T, Tegtmeier S, Turner S, Wang L, Wallace D, Williams J, Yamamoto H, Yvon-Lewis S, Yokouchi Y (2013) Global sea-to-air flux climatology for bromoform, dibromomethane and methyl iodide. Atmos. Chem. Phys. Discuss., 13:5601–5648, 2013 www.atmos-chem-phys-discuss.net/13/5601/2013/ doi:10.5194/acpd-13-5601-2013